A Report on

Design and Analysis of Field Oriented Control of Permanent Magnet Brushless DC Motor

By

MD. ASHRAFUL ISLAM
Roll: 1403552

A project report submitted in partial fulfillment of the requirements for the degree of Master of Science in Engineering in the Department of Electrical and Electronic Engineering.

Department of Electrical and Electronic Engineering

Khulna University of Engineering & Technology

Khulna – 9203, Bangladesh

May 2017

DECLARATION

This is to certify that the project work entitled, "**Design and Analysis of Field Oriented Control of Permanent Magnet Brushless DC Motor**," has been carried out by **Md. Ashraful Islam,** Roll: 1403552, in the Department of **Electrical and Electronic Engineering**, Khulna University of Engineering & Technology, Khulna, Bangladesh. The above research work or any part of this work has not been submitted anywhere for the award of any degree or diploma.

Signature of Supervisor

Signature of Candidate

APPROVAL

This is to certify that the research work submitted by **Md. Ashraful Islam,** entitled, "**Design and Analysis of Field Oriented Control of Permanent Magnet Brushless DC Motor,**" has been approved by the board of examiners for the partial fulfillment of the requirements for the degree of **M.Sc. Engineering** in the Department of **Electrical and Electronic Engineering**, Khulna University of Engineering & Technology, Khulna, Bangladesh in May 2017.

BOARD OF EXAMINERS

1. _____ Chairman
   Dr. Bashudeb Chandra Ghosh (Supervisor)
   Professor
   Department of Electrical and Electronic Engineering
   Khulna University of Engineering & Technology

2. _____ Member
   Dr. Md. Shahjahan
   Professor and Head
   Department of Electrical and Electronic Engineering
   Khulna University of Engineering & Technology

3. _____ Member
   Dr. Md. Abdur Rafiq
   Professor
   Department of Electrical and Electronic Engineering
   Khulna University of Engineering & Technology

4. _____ Member
   Dr. Naruttam Kumar Roy
   Assistant Professor
   Department of Electrical and Electronic Engineering
   Khulna University of Engineering & Technology

5. _____ Member
   Dr. Md. Abdul Goffer Khan (External)
   Professor
   Department of Electrical and Electronic Engineering
   Rajshahi University of Engineering & Technology

ACKNOWLEDGEMENT

All approvals belong to the Almighty Creator Allah, the most kind and bounteous to all His creatures and their actions. I humbly praise and grateful to Him, Who permits me to live and accomplish tasks including the research work being presented in this report.

The author gratefully express his deepest sense of gratitude and profound indebtedness to his project supervisor, **Dr. Bashudeb Chandra Ghosh**, Professor, Dept. of Electrical and Electronic Engineering (EEE), Khulna University of Engineering & Technology (KUET), Bangladesh, for his continuous supervision, encouragements, precious guidance, advices, helps, constructive criticisms and keen interests throughout the progress of the work. The author believes that work with him is a grand opportunity and would be a never-ending memory.

The author also extends his appreciation to Dr. Naruttam Kumar Roy, Assistant professor, Dept. of EEE, KUET, Bangladesh. I learned from him that a qualified researcher should keep open mind and pay continuous effort. The author is also thankful to Dr. Md. Abdur Rafiq, Professor, Dept. of EEE, KUET, Bangladesh, for his valuable discussion.

The author is grateful and expresses special thanks to Protik Chandra Biswas, Lecturer, Dept. of EEE, KUET, Bangladesh, for his adorable attitude, precious mental support and lend a hand to make successful this project. Without his valuable guidance and help, any success in this project work will never be possible.

The author gratefully acknowledges Prof. Dr. Md. Shahjahan, Head, Dept. of EEE, KUET, Bangladesh, for providing all sorts of facilities to finish this work in time. The author is also indebted to all the teachers in the Dept. of EEE for their valuable counseling and constructive criticisms at every stages of the work, which helped him a lot to complete this study in time.

Last but not least, the author solemnly acknowledges his parents and all the family members, who gave him the utmost mental and financial supports throughout his whole student life and make a way to build up his career in the field of EEE.

May, 2017

Md. Ashraful Islam
Roll: 1403552

ABSTRACT

Design and Analysis of Field Oriented Control of Permanent Magnet Brushless DC Motor

By Md. Ashraful Islam

This research project is about Field Oriented Control strategies for Permanent Magnet Brushless DC (PMBLDC) Motor. In PMBLDC Motor for Field Oriented Control direct axis reference current $I_{d\ ref}$ is considered zero, therefore forces the current space vector in the quadrature direction. Since only the quadrature axis current produces useful torque, this maximizes the torque efficiency of the system. Three PMBLDC Motor Control systems are designed, namely (1) Sinusoidal Current Regulated Pulse Width Modulation (CRPWM) Control, (2) Square Wave Current Regulated Pulse Width Modulation Control and (3) Voltage Regulated Space Vector Pulse Width Modulation Control. A state space model consisting three phase currents, three phase voltages, speed and position is developed. For testing, C++ simulation programs are designed for these three control strategies. The performance of the proposed control methods are studied for starting condition, load torque changes, speed variation, stator resistance changes and initial rotor angle mismatch condition. We have observed that Field Orientation Control methods have good performance and speed response. But speed response in Space Vector Pulse Width Modulation Control is better. Overall performance of all three control methods are proved satisfactory for speed control.

A simple experiment is also done in the laboratory with a prototype design by using customized software in an electronic control board with integrated inverter. There is a built in position sensor embedded on the motor. The system was run in open loop and found to work satisfactorily.

Dedicated

To

My Creator and My Beloved Parents

&

Respected Teachers

CONTENTS

LIST OF FIGURES

LIST OF TABLES

LIST OF ABBREVIATIONS

ADC	Analog to Digital Converter
BEMF	Back EMF
BLDC	Brushless DC
BLDCM	BLDC Motor
CC-VSI	Current Controlled Voltage Source Inverter
CNC	Computer and Numerical Control
CRPWM	Current Regulated Pulse Width Modulation
CT	Current Transducer
DAC	Digital to Analog Converter
DSP	Digital Signal Processor
DTC	Direct Torque Control
d-q	Direct – Quadrature Axis
FLC	Fuzzy Logic Controller
FOC	Field Oriented Control
ICD	In-circuit Debugger
IFLC	Integrated Fuzzy Logic Controller
IGBT	Insulated Gate Bipolar Junction Transistor
IPM	Intelligent Power Module
PI	Proportional - Integral
PM	Permanent Magnet
PID	Proportional Integral Derivative

PMBLDCM	Permanent Magnet Brushless DC Motor
PMSM	Permanent Magnet Synchronous Motor
PWM	Pulse Width Modulation
RKG	Runge-Kutta-Gill
SDK	System Development Kit
SPM	Synchronous Permanent Magnet
SPWM	Sinusoidal Pulse Width Modulation
SVM	Space Vector Modulation
SVPWM	Space Vector Pulse Width Modulation

LIST OF SYMBOLS

B	Damping constant
$\frac{d}{dt}$	Derivative operator
e_a, e_b ,e_c	Motor phase back EMFs
e(t)	Speed error
f_{as} (θ_r),f_{bs} (θ_r), $f_{cs}(\theta_r)$	Trapezoidal unit functions
i_a, i_b, i_c	Motor phase currents
I_d	Direct axis current
I_q	Quadrature axis current
I_α	Current in alpha axis
I_β	Current in beta axis
J	Moment of inertia
K_i	Integral constant
K_p	Proportional constant
L	Stator inductance per phase
M	Mutual inductance between phases
R_S	Stator resistance per phase
T_e	Electro-magnetic torque
T_l	Load torque
v_{ab}, v_{bc}, v_{ca}	Line voltages
v_{as}, v_{bs}, v_{cs}	Stator phase voltages
V_d	Direct axis voltage
V_{dc}	DC source voltage
V_q	Quadrature axis voltage
V_{ref}	Reference voltage
V_α	Voltage in alpha axis
V_β	Voltage in beta axis
ω_m	Angular speed of the motor
θ	Angular position of the rotor
λ_m	Flux linkages

Chapter

I

INTRODUCTION

Chapter at a Glance

1.1 Background

A machine that converts DC power into mechanical power is known as DC Motor. In a DC Motor, the brushes make mechanical contact with a set of electrical contacts on the rotor called the commutator, which forms an electrical circuit between the DC electrical source and the armature coil-windings. As the armature rotates on axis, the stationary brushes come into contact with different sections of the rotating commutator. The commutator and brush together form a set of electrical switches, each firing in sequence, such that electrical-power always flows through the armature-coil closest to the stationary stator (permanent magnet).

A Synchronous Motor is a machine that operates at synchronous speed. It is a constant speed motor. It has a stator with 3 phase armature winding which receives 3 phase power supply. Rotor works as a magnet energized by DC power. The stator winding produces a rotating field, which revolves around the stator at a synchronous speed. The opposite magnetic poles of the rotating field and rotor magnetic poles attract each other producing a unidirectional torque and constant synchronous speed.

Brushless DC (BLDC) Motor is like a Synchronous Motor inside out. Armature winding gets its 3 phase power supply from an inverter fed by DC source. By using inverter with control circuit a wide range of speed control is possible in BLDC Motor [1].

In a DC Motor field is stationary but in a BLDC Motor field is rotating and armature is stationary. BLDC Motor also can be defined as commutatorless DC Motor as its torque-current is identical to the DC Motor [2]. The commutator action is provided by a solid-state electronic inverter circuit. Instead of commutating the armature current using brushes like DC Motor, Electronic commutation is used in a BLDC Motor. This eliminates the problems associated with the brush and the commutator arrangement, for example, sparking and wearing out of the commutator-brush arrangement.

A Permanent Magnet Brushless DC (PMBLDC) Motor is like a permanent magnet excited Synchronous Motor. It has permanent magnet made rotor. It has trapezoidal field. This motor requires almost no maintenance and the performance is also high [1].

BLDC Motors have become popular for many industrial applications due to their high power density, torque-to-inertia ratio and efficiency [3,4]. The motor is unique and in future

they will dominate in various applications from very low power to very high power applications and from very low speed to very high speed applications. It is better than other motors of similar type. It is mostly used as small horsepower control motor because of their high efficiency, reliability, compactness and silent operation [4]. Household devices use electrical motor like - Universal Motor, Single Phase AC Induction Motor, capacitor-start, capacitor–run type motor and Split Phase Motor. Most of the time these traditional motors operate at a constant speed and get power from main AC power source and they give very little concern about efficiency. Now there is more demand for lower energy devices and devices with better performance, low noise and convenience features. BLDC Motor can be that solution.

1.2 Motivation

BLDC Motors have many advantages over DC Motors. For example long operating life, acoustic noiseless operation, higher speed ranges, fast dynamic response, higher efficiency and more reliability [5]. But main disadvantage is comparatively high cost and there are two reasons for it.

Firstly, high cost of semiconductor switching devices. The cost of power semiconductor switching devices is decreasing day by day, so opportunity for BLDC Motor application is widening.

Secondly, it needs complex speed controller to run. Brushed DC Motor speed can be regulated by a comparatively cheap variable resistor, which is inefficient but also satisfactory for cost-sensitive applications. But for perfect speed control and efficiency, a controller circuit is necessary. Modeling of speed controller is therefore essential for cost savings, for increasing the motor efficiency and for faster speed response and control [4].

The motor power density and light weight of controller of the drive system encourage us to select the motor where sophisticated control is needed along with efficiency. But the commercial simulation packages are lacking for the proper design of controller for PMBLDC Motor drives because the high software development cost incurred is not justified for their typical low cost fractional/integral KW application areas such as CNC machine tools and robot drives [2].

So, PMBLDC Motors are becoming a promising motor for many researchers. There are some Field Oriented Control systems found in literatures and they use too much sensors. But we want to explore Field Oriented Control intensively and reduce the number of sensors for control. This project's main research area covers different current controls and vector control of the motor using minimum sensor.

1.3 Brief Literature Review

The BLDC Motor is an AC Synchronous Motor but with characteristics of a DC Motor where armature coil is stationary and permanent magnet field is rotating. It is fed from a DC source but controlled AC voltage is given for speed control by inverter. Integrated circuit chips are now available for the control of Brushless DC Motor by Pulse Width Modulation (PWM). Permanent magnets create the rotor flux and the energized stator windings create electromagnet poles. The stator field and rotor field remain stationary at all speed with respect to each other [1]. Inverter is used for electronic commutation instead of brush and commutator. So, no sparking problem occurs [2,3]. Inverter switching is controlled by logic microchip controller [2,4] for speed control of the motor. The transistor switches of the inverter which feed the stator winding are controlled by pulses generated by the controller with rotor position sensor and other sensors. In BLDC Motor back EMFs are trapezoidal shape with 120° phase differences [2,5]. The Permanent Magnet Brushless DC Motor consists of four main parts: power converter, motor, sensors and controller with control algorithm [5].

Different types of control are possible for BLDC Motor by controlling width of voltage pulses and varying switching sequence of the inverter by sensing position, speed, current and voltage magnitude. Like- Field orientation control, direct torque control, scalar current or voltage control and other vector control methods. Also combination of these control systems has created some advance control methods.

In Field Oriented Control (FOC), motor current and voltage are manipulated in the d-q reference frame of the rotor [6]. The transformation from synchronously rotating frame to stationary frame and inverse are done by Clarke, Park's transformation and inverse transformation for voltage and current [6,7]. The drives direct current component is considered zero and therefore forces the current space vector to be exclusively in the quadrature direction. Since only the quadrature axis current produces useful torque, this

maximizes the torque efficiency and dynamics of the system [6]. In Pulse Width Modulation Control, three phase reference modulating signals are compared against a common triangular carrier to generate PWM pulses for the three phases. The inverter switches are turned off or on according to a hysteresis controller [5,6].

The Space Vector PWM (SVPWM) method is an advanced, computation-intensive PWM method and it is possibly the best among all the PWM techniques for variable-frequency drive application. Because of its superior performance characteristics, it has been finding widespread application in recent years [2]. Space Vector Pulse Width Modulation has 15% more output voltage then conventional modulation, better DC-link utilization and more efficient use of DC supply voltage [8].The voltage reference is provided using a revolving reference vector [8]. This PWM technique approximates the reference voltage V_{ref} by a combination of the eight switching patterns (V_0 to V_7) [9,10].

To make a suitable control model of BLDC Motor and to increase its efficiency has created a lot of research opportunity. Recently, a good number of researchers have been working in this area, as it is indicated in large number of publications in the literature.

The paper [3] proposes a trapezoidal model for three phase back EMF of the BLDC Motor. The control method obtains the actual phase current values by using a single DC link current sensor, thus reducing the cost and the size of the drive. Also, if the current sensor is placed on the ground line, insulated systems are not necessary and a low cost resistor can be used. They claim that the undesirable imbalances in the phase currents as well as pulsating torque due to mismatch in the current sensor sensitivities, are also avoided. The simulation results indicate that, by using the proposed method, drive gives the same closed loop performance as that of the conventional method.

A technical review of position and speed sensorless method for controlling BLDC Motor drive is given in [4]. They claim that the control for BLDC Motor using position sensor, such as shaft encoder, resolvers or hall-effect probe, can be improved by means of the elimination of these sensors to further reduce cost and increase reliability. Furthermore, sensorless control is the only choice for some application where those sensors cannot function reliably due to harsh environmental condition and a higher performance is required.

S. Ramababu [5] in his M. Tech. thesis has provided a detail study of PMBLDC Motor. A trapezoidal back EMF system has been shown in his mathematical model. Fuzzy

logic controller (FLC) has been used in his research study. Very good convincing results have been presented in the study. Mathematical model of PMBLDC Motor is well described.

A Space Vector PWM based BLDC Motor modeling and simulation is provided in [6]. They use both continuous time and discrete time models in their study. Torque is calculated on the basis of back EMF, phase currents and speed. The switching to proper space vector is done using torque error and position of the field. Fuzzy logic based PI controller adjustment system is used in the control system. Simulation results show fast dynamic performance with FLC and SVPWM.

In paper [8], a detail theory of mathematical model of Space Vector PWM technique is given with switching sequence. A PSIM-MATLAB/SIMULINK simulation study of Space Vector Modulation technique of two levels inverter reveals that Space Vector Modulation technique utilizes DC bus voltage more efficiently and generates less harmonic distortion when compared with Sinusoidal PWM technique.

In paper [9], mathematical model of Space Vector PWM with sector switching sequence and respective line and phase voltage are explained. A novel Current Controlled Space Vector Pulse Width Modulation (CCSVPWM) technique for reducing torque ripple in a three-level neutral-point-clamped (NPC) inverter fed trapezoidal BLDC motor is proposed. In BLDC Motor, the different current slew rates between switching-in and switching-out phase generate current ripple, further leading to the generation of commutation torque ripple in the commutation interval. In the proposed method, the CCSVPWM method has been applied to the three-level NPC inverter fed trapezoidal BLDC Motor, therefore current ripple and commutation torque ripple are suppressed.

The paper [10] reveals comparison of the performance of Brushless DC Motor control with Sinusoidal Pulse Width Modulation (SPWM) and Space Vector Pulse Width Modulation. Using SVPWM method performance and efficiency of the drive system increases to higher level. The harmonics and switching losses are reduced, since it is switched in a vector space. A PI controller is designed to maintain the constant speed of the motor drive. SVPWM method provides much better output in comparison with SPWM. The output voltage increases to 15.5%. The DC link power utilization is also high.

Mathematical model of a Brushless DC Motor including the state space model of the motor and speed controller are explained in details in [11], including trapezoidal field and

back EMF, torque, speed, voltage and current equations with simulation. The paper also indicates that Brushless DC Motor has a permanent-magnet rotor, and the stator windings are wound such that the back electromotive force (EMF) is trapezoidal. The trapezoidal back EMF implies that the mutual inductance between the stator and rotor is non-sinusoidal. So, according to their paper, no particular advantage exists in transforming the machine equations into the two-axis equations, which is done in the case of machines with sinusoidal back EMF.

A novel approach to Field Oriented Control of a BLDC Motor to produce a significantly reduced torque ripple is proposed in [12]. A standard mathematical model of a BLDC Motor in the 'abc' reference frame which is suitable for simulation of the six-step control strategy and a mathematical model of a BLDC Motor in the 'd-q' reference frame suitable for standard and modified Field Oriented Control strategy are presented through this paper.

Mainly BLDC Motors are used as a replacement for AC motors and this holds true for innumerous applications, and these motors also reduce the overall system weight. Brief comparative study of three different control schemes i.e. Sinusoidal Field Oriented Control, Field Oriented Control and hysteresis control of a BLDC Motor primarily on the aspect of output torque ripple are given in [13].

A mathematical description of a PMBLDC Motor using two-axis variables is given in [14]. Sinusoidal variation of flux and EMF is proposed in this paper.

A technical report [15] on PMBLDC Motor with comparison of characteristics indicates that the FOC is the best method irrespective of drive performance. However, the FOC method is based on the complex transformations and sensing circuits.

The paper [16] proposes a sliding mode controller (SMC) designed for a Brushless DC Motor to achieve high-performance speed control. Based on Pulse Width Modulation technique, a PWM-based controller in the inner current loop is first developed to perform a fast current control. A sliding mode speed controller is then designed in its outer control loop to enhance the speed control. Finally, the effectiveness of the proposed integrated control scheme under the load disturbances and parameter uncertainties is verified by simulation results and comparison with proportional-integral control (PIC) approach is given. Simulation studies demonstrated that the proposed SMC controller, in comparison with the PIC

approach, can produce a better speed response for different speed commands, load disturbances and parameter uncertainties.

The paper [17] introduces a BLDC fan motor drive system using modified Sinusoidal PWM (SPWM). The driver board is assembled in the motor to minimize system size. Hall position sensor on the board is used to generate the SPWM to the power module to drive the BLDC Motor. The simulation and experimental results are presented to verify the stability of the driver system.

BLDC Motor with current control scheme is discussed in the paper [18]. BLDC drive with fixed speed and variable speed is developed using MATLAB/SMULINK and results are shown for both fixed and variable speed application and basic operation of BLDC Motor is explained with open loop and closed loop speed controls.

The paper [19] proposes Field Oriented Control for PMBLDC Motor drive with current fed inverters. BLDC Motor has a trapezoidal field pattern rather than sinusoidal, therefore to study the motor behavior with Field Oriented Control is more suitable in compare with scalar control. A hysteresis type current controller is proposed. An adaptive PI speed control based vector controlled current fed delta modulated PMBLDC Motor drive system is simulated in a C++ environment in discrete form. Transient response and loading capability of the motor are analyzed. The performance of the vector controlled drive is found to be better than the scalar controlled system considering response time, speed overshoot, settling time and load torque handling capacity of the system.

A mathematical model of Space Vector modulated PWM inverter fed PMBLDC Motor is shown in [20]. They have considered sinusoidal functions for three phase back EMF. The analytical results show that current and torque harmonics are found less in Space Vector PWM compared to Sinusoidal PWM.

A fuzzy logic based PI controller adjustment system is shown in [21]. In this paper, fuzzy PI controller for BLDC Motor considering variable sampling time is proposed. Three fuzzy logic controllers to scale speed error for the three PI controllers, are used in the paper. The paper describes BLDC Motor for (1) continuous time, (2) variable sampling time and (3) discrete time speed and variable sampling time constant estimator. The results have been presented and analyzed for different speed conditions. MATLAB /SIMULINK analysis shows that SVPWM drive results in a faster dynamic response.

In paper [22] SVPWM method with a revolving reference voltage vector is provided as voltage reference instead of three phase modulating waves. The magnitude and frequency of the fundamental component in the line side are controlled by the magnitude and frequency respectively, of the reference vector. The study of Space Vector Modulation technique reveals that Space Vector Modulation technique utilizes DC bus voltage more efficiently.

A novel back EMF sensing scheme is shown in [23] for speed-sensorless BLDC drive. In this scheme, the motor true back EMF of the floating motor winding can be detected during off time of PWM because the terminal voltage of the motor is directly proportional to the phase back EMF during this interval. Also, the back EMF voltage is referenced to ground without any common mode noise. Therefore, this back EMF sensing method is immune to switching noise and common mode voltage.

A fuzzy logic based soft-switching resonant pole inverter using transformer, which can generate DC link voltage notches during chopping which minimize the drawbacks of soft switching, is proposed in [24].

A fuzzy logic based implementation of BLDC Motor is presented in [25]. From the simulation result, it has indicated that wide range of speed control is possible by means of fuzzy controller. The results are obtained without peak overshoot and with negligible steady state error. The fuzzy logic based system does not require explicit knowledge of the motor and load characteristics. The results of adaptive fuzzy controller are better than the fuzzy controller without adaptation, are showed in this paper.

In [26] three fuzzy logics to scale speed error for the three PI controllers is proposed. The simulation result demonstrates the fuzzy logic control at different load torque. It is shown that the speed of the BLDC Motor remains constant as load torque changes.

The paper [27] introduces an integrated fuzzy logic controller (IFLC) for Brushless DC Motor drive using trapezoidal back EMF simulation model and presents a comparative study of performances of PID controller and IFLC. The results show that IFLC is better than the PID controller for all speeds. It is also found that the IFLC is robust to external load disturbances and parameter variation.

A fuzzy logic controller for PMBLDC Motor drives is proposed in [28]. The fuzzy logic controller is developed using MATLAB Fuzzy-Logic Toolbox and then inserted into the SIMULINK model. The dynamic characteristics of the Brushless DC Motor such as speed,

torque, current and voltage of the inverter components are observed and analyzed using the developed MATLAB model. They have verified the effectiveness of the controller by comparing the simulation results with TMS320F2808 DSP experimental results. The paper shows that the BLDC Motor is successfully and efficiently controlled by this fuzzy logic controller.

An efficient simulation model for fuzzy logic controlled BLDC Motor drives using MATLAB/SIMULINK is presented in [29]. Trapezoidal back EMF is considered for the model. It is shown that the BLDC Motor is efficiently controlled by fuzzy logic controller (FLC). FLC and PID based system performances have been compared by using the developed model. It is seen that the desired real speed and torque values could be reached in a short time by FLC.

A direct torque control (DTC) application for BLDC Motor with non-sinusoidal back-EMF operating in the constant torque region is presented in the paper [30]. This approach introduces a two-phase conduction mode as opposed to the conventional three-phase DTC drives. The control scheme applies only two phases to conduct at any instant of time. They demonstrate fast speed control. A look-up table is used to minimize computation time. Trapezoidal back EMF is used in modeling.

A theoretical concept is developed and the validity of the proposed DTC of BLDC Motor drive scheme with rotor position estimation is verified in [31] through the simulation results using Lab VIEW. The DTC for BLDC Motor drive using two phase conduction mode in the constant torque region with rotor position estimation has been implemented. A look-up table for the two-phase voltage vector selection is designed to provide faster torque response for both on rising and falling conditions. Compared to the three phase DTC technique, this approach eliminates the flux control and only torque is considered in the overall control system. The size of these sharp dips in speed because torque change is unpredictable.

The application of direct torque control to Brushless AC drives has been investigated in [32]. The paper highlights the essential differences in its implementation, as regards torque estimation and the representation of the inverter voltage space vectors. A two axis model for flux and current is introduced. Simulated and experimental results are presented. It is shown that, compared to conventional current control, the DTC results in reduced torque ripple and have faster dynamic response.

Performance analysis of BLDC Motor with stair step-shaped magnet poles, magnet pole width variation and by using different remanance value has been shown in [33]. The results indicate considerable reduction in cogging torque has been achieved by varying the stair step height of magnet poles. It is observed that as the stair step height is increased there is considerable reduction in average torque. As the magnet pole width is varied there is considerable reduction in cogging torque and improvement in average torque. The design with NdFeB material gives the best performance in terms average torque and cogging torque.

A mathematical model of a PMBLDC Motor has been proposed in [34] with a trapezoidal back EMF function. A comparison of the results using sensors and sensor less systems has been documented. It is shown that sensor less control is more advantageous.

A review paper on modeling and controller design of permanent magnet BLDC Motor is given in [35]. The paper considers sinusoidal back EMF and differences of current and voltages as variables. They claim the model being simplified and easy to implement for low cost vehicles.

BLDC Motor have been demanding as in-wheel motor in electric vehicles because of high efficiency, desired torque versus speed characteristics, high power density and low maintenance cost [36]. In this paper BLDC Motor with ideal back-EMF is modeled and simulated in MATLAB/SIMULINK. Simulation model of the controller and BLDC drive are also presented.

Since PMBLDC Motors are small sizes, prototype inverter controller design is an interesting topic of research. The tendency is to design microchip or application note with microcontrollers. An application report [37] presents a solution for the control of Brushless DC Motors using the TMS320F2803x microcontrollers. TMS320F280x devices are part of the C2000™ family of microcontrollers that enable the cost-effective design of intelligent controllers for three-phase motors by reducing the system components and increasing efficiency. Using these devices, it is possible to realize far more precise control algorithms. Very fast response is observed.

An application note [38] on BLDC Motor control using microchip discusses the steps of developing several controllers for brushless motors. The note covers sensored, sensorless, open loop and closed loop design. There is even a controller with independent voltage and speed control so that specific motor characteristics are selected empirically. The code of the

application note is developed with the Microchip PIC16F877 PICmicro® Microcontroller, in conjunction with the In-Circuit Debugger (ICD). This combination is chosen because the ICD is inexpensive and code can be debugged in the prototype hardware without need for an extra programmer or emulator.

The Application Note [39] describes the design of a 3-phase sensorless BLDC Motor drive with Back-EMF Zero Crossing using an analog to digital (AD) converter based on Freescale's 56F80x family dedicated for motor control application. The concept of the application is that of a speed-closed loop drive using an AD converter for Back-EMF Zero Crossing technique for position detection. It serves as an example of a sensorless BLDC Motor control system using Freescale's Digital Signal Processor (DSC) with SDK support. It also illustrates the usage of dedicated motor control on chip peripherals, software drivers and software libraries that are included in the SDK. The application note includes a description of the controller's feature, basic BLDC Motor theory, system design concept, hardware implementation and software design including the PC master software visualization tool inclusion.

The application note [40] provides a general overview of BLDC Motor, including its advantages against other commonly-used motor's structure, electromagnetic principles, and mode of operation. The document also examines the control principle using hall sensors for both single-phase and three-phase BLDC Motor. A brief introduction to sensorless control method using back EMF for a three-phase BLDC Motor is also discussed.

The application note [41] describes implementation of a Brushless DC Motor control in sensor mode using the ATmega32M1 AVR microcontroller. A short description of the ATAVRMC310 and ATAVRMC300 boards are used in this application note. Software implementation is also discussed with software control loop using a PID filter. This application note deals only with BLDC Motor control application using Hall Effect position sensor to control commutation sequence.

1.4 Objectives

Our main desire is to design Field Oriented Controllers for PMBLDC Motor with minimum number of sensors. They are (1) Sinusoidal Current Regulated PWM (CRPWM) Controller, (2) Square Wave Current Regulated PWM Controller and (3) Space Vector Pulse Width Modulation (SVPWM) Controller.

We will design two current control methods based on Field Oriented Control. We proposed sinusoidal current approach with PWM control and this technique has current and speed sensors as a feedback and an adaptive PI controller, the inverter transistor switches will be turned on or off based on a hysteresis controller. The adaptive PI controller will generate quadrature axis reference current from the speed error. The other current control method is the Square Wave Current Regulated PWM Control and this technique also has current and speed sensors as a feedback with an adaptive PI controller.

We will also design a voltage vector control method. We proposed Space Vector Pulse Width Modulation technique for Brushless DC Motor control. It is constructed with current and speed feedback and three adaptive PI controllers to generate reference voltage and current vectors.

This study is intended to design and analyze performances of the previously mentioned control methods of the PMBLDC Motor. The results obtained from different control methodologies will be compared under normal and variable parametric conditions. The ability of the control laws to work under parameter perturbed condition and response time both in steady state and dynamic conditions will be studied.

1.5 Contents of the Project Report in Brief

Contents of this project report are described in seven chapters, describing the modeling and control technique of a PMBLDC Motor. A brief of these contents are as follows-

In Chapter I, a brief literature review is given and also the objective and motivation of this project.

In Chapter II, principle of PMBLDC Motor operation with inverter by 120 degree angle operation and PWM voltage and current operation are presented. A brief description of position sensors and mathematical modeling of machine in state space form are presented.

In Chapter III, description of the Field Oriented Control is given. We have proposed the Sinusoidal Current Regulated PWM Control and Square Wave Current Regulated PWM Control for PMBLDC Motor. A detail discussion of these methods is also given.

In Chapter IV, a description of Space Vector Pulse Width Modulation Control is

given. We have proposed the Voltage Regulated Space Vector PWM Control with current feedback for PMBLDC Motor. A detail discussion of this method is given.

Chapter V describes the results of simulation of the program of above control systems for different parametric perturbed condition. Signal conditioners and overview of software development of speed control of Brushless DC Motor are given. All characteristic curves of the simulations for normal and parametric perturbed conditions are being analyzed and graphically presented.

Chapter VI describes the experimental set up, which is designed using a prototype design. A very simple program is designed for the motor and inverter system.

Chapter VII describes the conclusion of the speed control strategies of the Brushless DC Motor and further work to be carried out.

Chapter

II

MATHEMATICAL MODEL OF PERMANENT MAGNET BRUSHLESS DC MOTOR

Chapter at a Glance

2.1 Introduction

The Brushless DC Motor is a synchronous electric motor that, from a modeling perspective, looks exactly like a DC motor. It has a linear relationship between current and torque, between voltage and rpm [4]. It has an electronically controlled commutation system, instead of having a mechanical commutation, which is typical of Brushed DC Motors. In PMBLDC Motor the magnetic fields generated by both the stator and the rotor have the same frequency therefore, PMBLDC Motor does not experience the "slip" that is normally seen in Induction Motor [42]. It takes power from variable frequency inverter. The inverter is controlled by shaft position sensors and other sensors. It is an integrated system comprise of motor, sensor, inverter & controller.

2.2 Construction and Operation of PMBLDC Motor

A Brushless DC Motor is a DC motor turned inside out, so that the field is on the rotor and the armature is on the stator [2] as shown in Figure (2.1). In a PMBLDC Motor, the electromagnets do not move; instead, the permanent magnets rotate and the armature remains static. So, the commutator assembly is replaced by an intelligent electronic inverter [4].

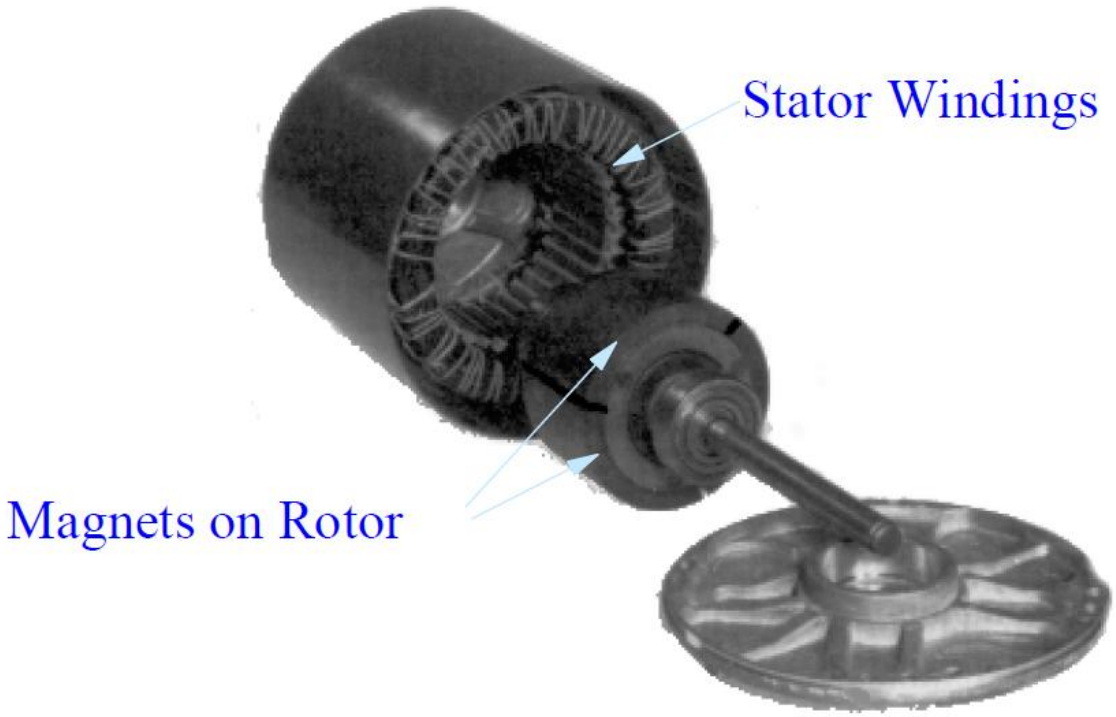

Fig.2.1: Rotor and stator of Permanent Magnet Brushless DC Motor [23].

Permanent Magnet Brushless DC Motor consists of three star connected stator windings and a rotor. The rotor is made of permanent magnet. It can vary from two to eight pole pairs with alternate north and south poles. NdFeB material is used for permanent magnet. The armature on the stator helps to conduct heat away from the windings [2]. The stator winding produces a rotating field which attracts the opposite poles of the permanent magnet rotor. The rotor creates a rotation in the direction of the rotating field.

PMBLDC Motor has trapezoidal back EMF as shown in Figure (2.4). The "commutation region" of the back EMF of a PMBLDC Motor should be as small as possible, while at the same time it should not be so narrow as to make it difficult to commutate a phase of that motor when driven by a Inverter [2]. The flat constant portion of the back EMF is120°.

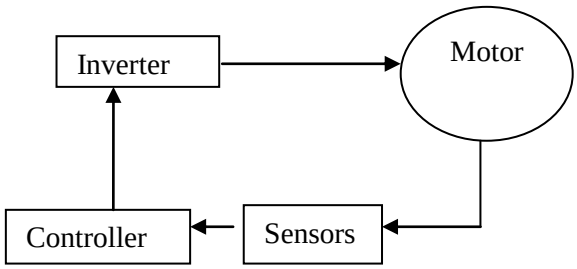

Fig.2.2: Basic block diagram of a Permanent Magnet Brushless DC Motor drive.

The basic block diagram of Brushless DC Motor drive is shown in Figure (2.2). The Permanent Magnet Brushless DC Motor consists of four main parts: inverter, motor, sensors and controller with control algorithm [5]. The proposed control drive mainly consists of adaptive PI controllers, field oriented reference current generator, Delta Modulated PWM Current Controller or SVPWM Controller, IGBT voltage source inverter, speed sensor, current sensor and PMBLDC Motor.

The position of the rotor can be sensed by using an optical position sensor with its logic. Optical position sensors consist of phototransistors (sensitive to light), revolving shutters and a light source. The output of an optical position sensor is a Logical signal [1]. The hall sensors are normally mounted on a printed circuit board and fixed to the enclosure cap on the non-driving end [4].

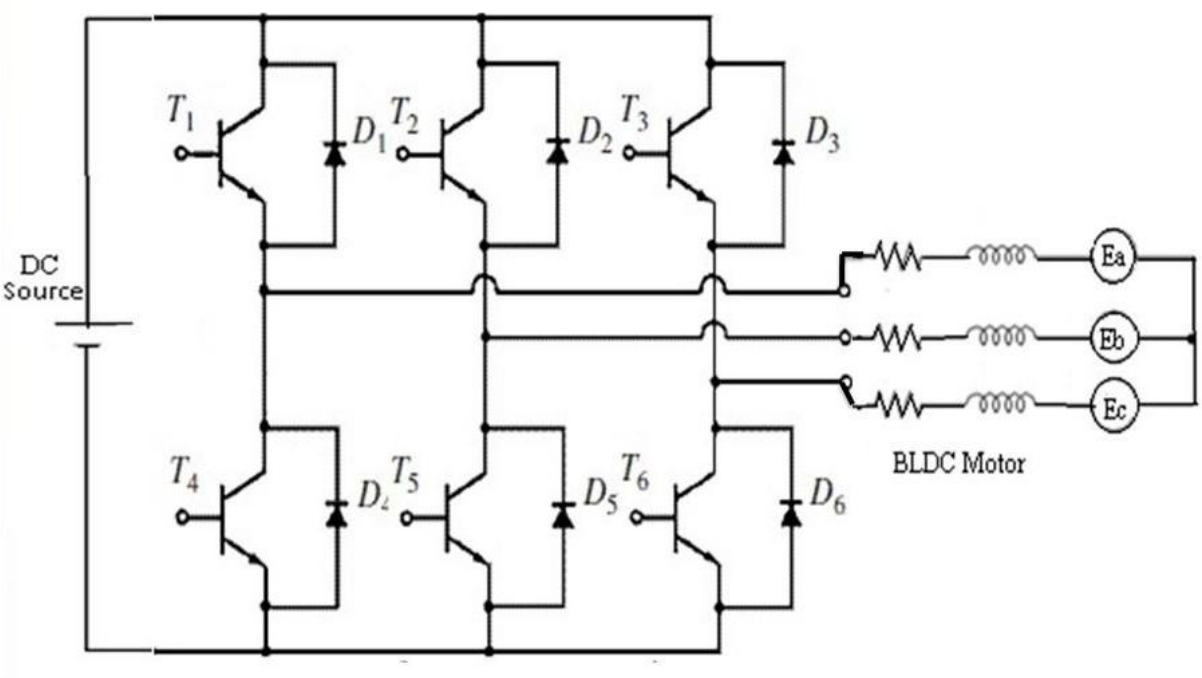

Fig.2.3: Brushless DC Motor circuit diagram.

The Brushless DC Motor is controlled by three phase inverter. The gate signals to each semiconductor switch in the power electronic converter are determined based on the rotor position and command signals which may be a torque command, voltage command, speed command and the control algorithm. Rotor position sensor is needed for starting and for providing proper commutation sequence to turn on the inverter switches based on the rotor position [5].

The inverter operates in two modes –

- $\frac{2\pi}{3}$ angle switch-on mode.
- Voltage or current controlled Pulse Width Modulation mode.

As shown in Figure (2.3), there are (T_1- T_6) six switches of inverter. In angle switch on mode [5], they operate to put the input DC current I_d symmetrical for $\frac{2\pi}{3}$ angle in the middle of each phase voltage wave. The angle α is the angle of current with respect to voltage. In any instant, two switches are on (one in the upper group and another one in the lower group). For any moment of time t_1, the T_1 and T_6 are on; then the supply voltage V_{dc} and I_d are put across the line ab (phase A, phase B in series), to make I_d positive in phase a; but negative in phase b, after $\frac{\pi}{3}$ interval (middle of phase A). After that T_6 is turned off and T_2

is turned on, but T_1 continues to conduct current during the full $\frac{2\pi}{3}$ angle. This switching commutates negative I_d from phase b to phase c while phase a is carrying positive I_d , the conduction changes for every $\frac{\pi}{3}$ angle representing the switching modes in a full cycle [5]. From the position sensor and controller, the switching and commutation sequence of the PMBLDC Motor in any instants are decided.

In Pulse Width Modulation (PWM) mode the supply voltage is chopped at a fixed frequency with a duty cycle depending on the current error [37]. Therefore, both the current and the rate of change of current can be controlled. The two phase supply duration is limited by the two phase commutation angle. The main advantage of the PWM strategy is that the chopping frequency is a fixed parameter; hence, acoustic and electromagnetic noises are relatively easy to filter [37]. We can control the switches with Pulse Width Modulation and 'Chopping' to control the voltage and current continuously at motor terminal [5]. There are two 'Chopping' modes for current controlled operation of the inverter, (1) feedback (FB) mode and (2) freewheeling mode. In these modes devices are turned 'on' and 'off' on duty cycle basis for controlling current average I_{av} and voltage average V_{av}.

2.3 Mathematical Model of the Machine

PMBLDC Motor consists of three phase stator windings and a permanent magnet rotor. Rotor induced currents in the rotor is neglected because of high resistance in both magnets and steel core [2]. Damper windings are neglected in the equation of the windings where phase variables are calculated. Resistance of all the phase windings are assumed to be equal to R_s. The phase currents of stator are considered to be balanced.

Phase voltages of stator = V_{as} , V_{bs} , V_{cs}
Stator resistance per phase = R_s
Stator currents = i_a , i_b , i_c
Self-inductance of phases= L_{aa} , L_{bb} and L_{cc}
Mutual inductances = L_{ab} , L_{bc} and L_{ca}
Phase back electromotive forces = e_a , e_b and e_c

Phase voltage-equation is similar to armature–voltage equation of DC motor. The circuit equation of the three windings in phase variables are [11,42],

$$\begin{bmatrix} V_{as} \\ V_{bs} \\ V_{cs} \end{bmatrix} = \begin{bmatrix} R_s & 0 & 0 \\ 0 & R_s & 0 \\ 0 & 0 & R_s \end{bmatrix} \begin{bmatrix} i_a \\ i_b \\ i_c \end{bmatrix} + \frac{d}{dt} \begin{bmatrix} L_{aa} & L_{ab} & L_{ac} \\ L_{ba} & L_{bb} & L_{bc} \\ L_{ca} & L_{cb} & L_{cc} \end{bmatrix} \begin{bmatrix} i_a \\ i_b \\ i_c \end{bmatrix} + \begin{bmatrix} e_a \\ e_b \\ e_c \end{bmatrix} \quad (2.1)$$

We also have assumed that if with angle, the rotor reluctance does not change due to non-salient type rotor (uniform reluctance) then [2],

$$L_{aa} = L_{bb} = L_{cc} = L \quad (2.2)$$

$$L_{ab} = L_{ba} = L_{ac} = L_{ca} = L_{bc} = L_{cb} = M \quad (2.3)$$

Substituting Equations (2.2) and (2.3) in Equation (2.1),

$$\begin{bmatrix} V_{as} \\ V_{bs} \\ V_{cs} \end{bmatrix} = \begin{bmatrix} R_s & 0 & 0 \\ 0 & R_s & 0 \\ 0 & 0 & R_s \end{bmatrix} \begin{bmatrix} i_a \\ i_b \\ i_c \end{bmatrix} + \frac{d}{dt} \begin{bmatrix} L & M & M \\ M & L & M \\ M & M & L \end{bmatrix} \begin{bmatrix} i_a \\ i_b \\ i_c \end{bmatrix} + \begin{bmatrix} e_a \\ e_b \\ e_c \end{bmatrix} \quad (2.4)$$

Line voltages,

$$V_{ab} = V_{as} - V_{bs}$$

$$V_{bc} = V_{bs} - V_{cs}$$

$$V_{ca} = V_{cs} - V_{as} \quad (2.5)$$

The phase currents of stator are considered to be balanced for no neutral connection [2],

$$i_a + i_b + i_c = 0 \quad (2.6)$$

Inductances matrix is simplified,

$$M.i_b + M.i_c = -M.i_a \quad (2.7)$$

So, the machine equation is [28,29],

$$\begin{bmatrix} V_{as} \\ V_{bs} \\ V_{cs} \end{bmatrix} = \begin{bmatrix} R_s & 0 & 0 \\ 0 & R_s & 0 \\ 0 & 0 & R_s \end{bmatrix} \begin{bmatrix} i_a \\ i_b \\ i_c \end{bmatrix} + \frac{d}{dt} \begin{bmatrix} L-M & 0 & 0 \\ 0 & L-M & 0 \\ 0 & 0 & L-M \end{bmatrix} \begin{bmatrix} i_a \\ i_b \\ i_c \end{bmatrix} + \begin{bmatrix} e_a \\ e_b \\ e_c \end{bmatrix} \quad (2.8)$$

Trapezoidal back EMF's are [3,29],

$$\begin{bmatrix} e_a \\ e_b \\ e_c \end{bmatrix} = \omega_m \lambda_m \begin{bmatrix} f_{as}(\theta_r) \\ f_{bs}(\theta_r) \\ f_{cs}(\theta_r) \end{bmatrix} \quad (2.9)$$

Angular rotor speed = ω_{m_r} (Radians per seconds)

Flux linkage = λ_m

Rotor position = θ_r (Radian)

Where, $f_{as}(\theta_r)$, $f_{bs}(\theta_r)$ and $f_{cs}(\theta_r)$ are the flux function of rotor position having the same shape as back EMF with a maximum value of ±1. The $f_{bs}(\theta_r)$ and $f_{cs}(\theta_r)$ are similar to $f_{as}(\theta_r)$ but $120°$ phase displacements have to be considered [2]. There are no sharp corners in the induced EMF due to trapezoidal nature. The flux linkages are continuous functions of the rotor position. The EMF comes from the flux linkages derivatives. The flux density function becomes smooth without sudden edges because of fringing [2]. The $f_{as}(\theta_r)$, $f_{bs}(\theta_r)$ and $f_{cs}(\theta_r)$ are unit function generator corresponding to the trapezoidal induced EMF of the PMBLDC Motor as a function of the θ_r.

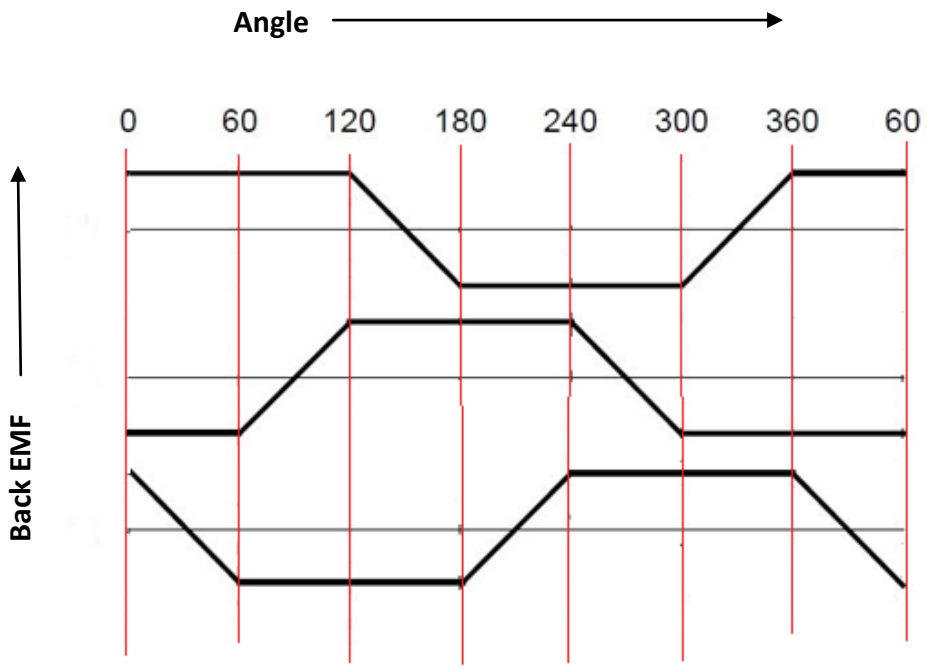

Fig.2.4: Trapezoidal back EMF of three phase PMBLDC Motor.

The back EMF functions mathematical model as [3,28,29],

$$f_{as}(\theta_r) = \begin{cases} \theta_r \frac{6}{\pi} & 0 \le \theta_r \le \frac{\pi}{6} \\ 1 & \frac{\pi}{6} \le \theta_r \le 5\frac{\pi}{6} \\ (\pi - \theta_r)\frac{6}{\pi} & 5\frac{\pi}{6} \le \theta_r \le 7\frac{\pi}{6} \\ -1 & 7\frac{\pi}{6} \le \theta_r \le 11\frac{\pi}{6} \\ (\theta_r - 2\pi)\frac{6}{\pi} & 11\frac{\pi}{6} \le \theta_r \le 2\pi \end{cases} \quad (2.10)$$

$$f_{bs}(\theta_r) = \begin{cases} -1 & 0 \le \theta_r \le \frac{\pi}{2} \\ \left(-\frac{2\pi}{2} + \theta_r\right)\frac{6}{\pi} & \frac{\pi}{2} \le \theta_r \le 5\frac{\pi}{6} \\ 1 & 5\frac{\pi}{6} \le \theta_r \le 3\frac{\pi}{2} \\ \left(-5\frac{\pi}{3} + \theta_r\right)\frac{6}{\pi} & 3\frac{\pi}{2} \le \theta_r \le 11\frac{\pi}{6} \\ -1 & 11\frac{\pi}{6} \le \theta_r \le 2\pi \end{cases} \quad (2.11)$$

$$f_{cs}(\theta_r) = \begin{cases} 1 & 0 \le \theta_r \le \frac{\pi}{6} \\ \left(\frac{\pi}{3} - \theta_r\right)\frac{6}{\pi} & \frac{\pi}{6} \le \theta_r \le \frac{\pi}{2} \\ -1 & \frac{\pi}{2} \le \theta_r \le 7\frac{\pi}{2} \\ \left(-4\frac{\pi}{3} + \theta_r\right)\frac{6}{\pi} & 7\frac{\pi}{2} \le \theta_r \le 3\frac{\pi}{2} \\ 1 & 3\frac{\pi}{2} \le \theta_r \le 2\pi \end{cases} \quad (2.12)$$

Electromagnetic developed torque (Newton-meter) [16],

$$T_e = (e_a i_a + e_b i_b + e_c i_c)/\omega_m \quad (2.13)$$

The moment of inertia,

$$J = J_m + J_l \quad (2.14)$$

Where, J is total inertia, J_m is motor inertia and J_l is load inertia.

If friction coefficient is B, and load torque is T_l then the motion system equation is [16,28,32,42],

$$J\frac{d\omega_m}{dt} + B\,\omega_m = (T_e - T_l) \quad (2.15)$$

B is the damping co-efficient, which is very small, so it is neglected. The rotor position θ_r repeats every 2π.

Mechanical Speed (ω_m) and position of electrical rotor (θ_r) is related to [16]-

$$\omega_r = \frac{d\theta_r}{dt} = \frac{P}{2}\omega_m \tag{2.16}$$

The differential equations defines the developed model in term of the variables i_a , i_b , i_c , ω_m . The θ_r and time is an independent variable.

The system in state-space form is [2],

$$\dot{x} = Ax + Bu + Ce \tag{2.17}$$

here, $x = [i_a \quad i_b \quad i_c]^t$ (2.18)

$$A = \begin{bmatrix} -\frac{R_s}{L-M} & 0 & 0 \\ 0 & -\frac{R_s}{L-M} & 0 \\ 0 & 0 & -\frac{R_s}{L-M} \end{bmatrix} \tag{2.19}$$

$$B = \begin{bmatrix} \frac{1}{L-M} & 0 & 0 \\ 0 & \frac{1}{L-M} & 0 \\ 0 & 0 & \frac{1}{L-M} \end{bmatrix} \tag{2.20}$$

$$C = \begin{bmatrix} -\frac{1}{L-M} & 0 & 0 \\ 0 & -\frac{1}{L-M} & 0 \\ 0 & 0 & -\frac{1}{L-M} \end{bmatrix} \tag{2.21}$$

$u = [v_{as} \quad v_{bs} \quad v_{cs}]^t$ (2.22)

$e = [e_a \quad e_b \quad e_c]^t$ (2.23)

The PMBLDC Motor model is represented using Equation (2.8), (2.9), (2.15) and (2.16).

2.4 Digital Simulation of the Motor

For digital simulation of the motor drive system a computer program in C++ is to be written. The state equations are solved using the Runge-Kutta-Gill (RKG) method [43,44]. The Equations (2.15), (2.16) and (2.17) are solved simultaneously. The four coefficients are evaluated according to the following rules.

The basic technique is to start with a known value of $y(t)$ and then approximate the next value $y(t+h)$ using a finite difference approximation to the derivative $\frac{dy}{dt}$.

For a first order finite difference:

$$\frac{dy}{dt} \approx \frac{y^{(n+1)}-y^n}{h} = f(y^*,t^*) \Rightarrow y^{(n+1)} = y^n + h.f(y^*,t^*) \quad (2.24)$$

Where $y^{(n)}$ refers to the value of y from the numerical scheme at the n-th time step. The trick is to find some appropriate values for h and $f(y^*,t^*)$ that lead to high accuracy & stability without requiring an unmanageable number function evaluations and time steps.

The technique is applicable to systems non linear 1st order differential equation:

$$\frac{dy_i}{dt} = f_i(y_1, y_2, \dots, y_n) \text{ , for i=1,2,...,N} \quad (2.25)$$

Or in vector notation:

$$\frac{d\mathbf{y}}{dt} = \mathbf{f}(y) \quad (2.26)$$

Where y refers to the set of variables $[y_1, y_2, \dots, y_N]^T$ and f refers to the set of defining functions $[f_1, f_2, \dots, f_N]^T$. Note that a dependency on time can always be included by defining a new variable:

$$\frac{dy_{N+1}}{dt} = 1 \quad (2.27)$$

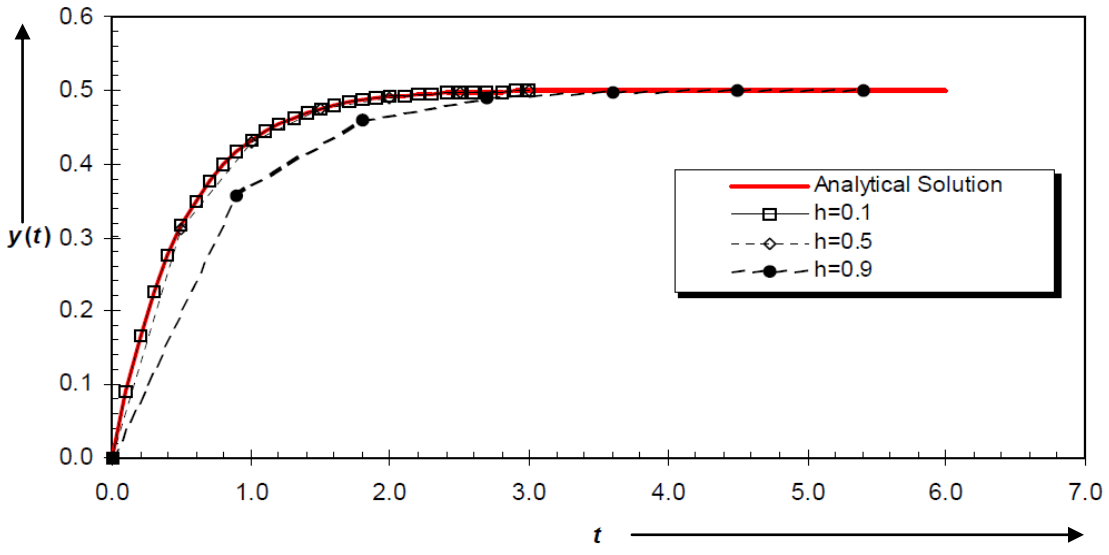

Fig 2.5: Runge-Kutta-Gill solution [43] to $y' = 1 - 2y, y(0) = 0$.

The most widely used fourth order method with constants developed by Gill. The method is [43],

$$y^{(n+1)} = y^{(n)} + \frac{1}{6}k_1 + \frac{b}{3}k_2 + \frac{d}{3}k_3 + \frac{1}{6}k_4 \tag{2.28}$$

$$k_1 = h.f(\mathrm{t}^{(n)}, \mathrm{y}^{(n)}) \tag{2.29}$$

$$k_2 = h.f(\mathrm{t}^{(n)} + \frac{1}{2}h, y^{(n)} + \frac{1}{2}k_1)\ . \tag{2.30}$$

$$k_3 = h.f\left(\mathrm{t}^{(n)} + \frac{1}{2}h, y^{(n)} + ak_1 + bk_2\right). \tag{2.31}$$

$$k_4 = h.f\left(\mathrm{t}^{(n)} + h, y^{(n)} + ck_2 + dk_3\right). \tag{2.32}$$

Where the constants are:

$$a = \frac{\sqrt{2}-1}{2},\ b = \frac{2-\sqrt{2}}{2},\ c = -\frac{\sqrt{2}}{2},\ d = \frac{2+\sqrt{2}}{2}. \tag{2.33}$$

It is reported that Runge-Kutta-Gill method is stable for $h \leq 2.8/\lambda$.

2.5 Conclusion

In this chapter construction, operation and mathematical model of a PMBLDC Motor are described. The mathematical model is simultaneous differential equations. The equations may be solved using RKG method in a digital computer environment. The time step is taken as 25 microsecond to have solution closer to analog system.

Chapter III

CONTROLLER DESIGN FOR FIELD ORIENTED CURRENT CONTROL SYSTEMS

Chapter at a Glance

3.1 Introduction

A Permanent Magnet BLDC Motor has electronic commutator that is very position sensitive. The currents injected to the phase windings need to be both position and magnitude controlled [1]. So, position sensor or estimator is needed for a PMBLDC Motor. Normally, closed loop control systems require speed feedback and speed transducer. In a vector current controlled drive current magnitude and position should be controlled. For this purpose the voltages must be switched properly. There may be two loops: the speed control loop and the current control loop.

In this chapter Field Orientated Current Control schemes are proposed for vector control system. These are: Sinusoidal Current Regulated PWM (CRPWM) Control and Square Wave Current Regulated PWM Control system. The effectiveness of the control schemes are tested using C++ program simulation environment. An Adaptive Proportional plus Integral (PI) controller is used in the speed control loop.

3.2 Field Oriented Control System

In Field Oriented Control (FOC), motor currents and voltages are manipulated in the d-q reference frame [6]. This means that measured motor currents must be mathematically transformed from the three-phase static reference frame of the stator windings to the two axis rotating d-q reference frame, prior to processing by the controllers. Similarly, the voltages to be applied to the motor are transformed from the d-q frame of the rotor to the three phase reference frame of the stator before they can be used for PWM output [6].

By Clarke, Park's transformation and inverse transformation, the reference frame transformations can be performed in a single step but they are best described as a two step process. The three phase quantities (stator current or voltage) in 'abc' 120 degree physical frame can be transformed to their equivalent two phase fixed orthogonally aligned 'αβ' frame; then 'αβ' are translated to rotating 'dq' (direct-quadrature) frame [6,7]. d and q are also orthogonally aligned; such that their inner product is zero. In synchronous motor or in PMBLDC motor 'dq' frame is rotating at synchronous speed. Park transformation transform an AC machine equation with time varying co-effieient to a equation with time non-varying coefficient.

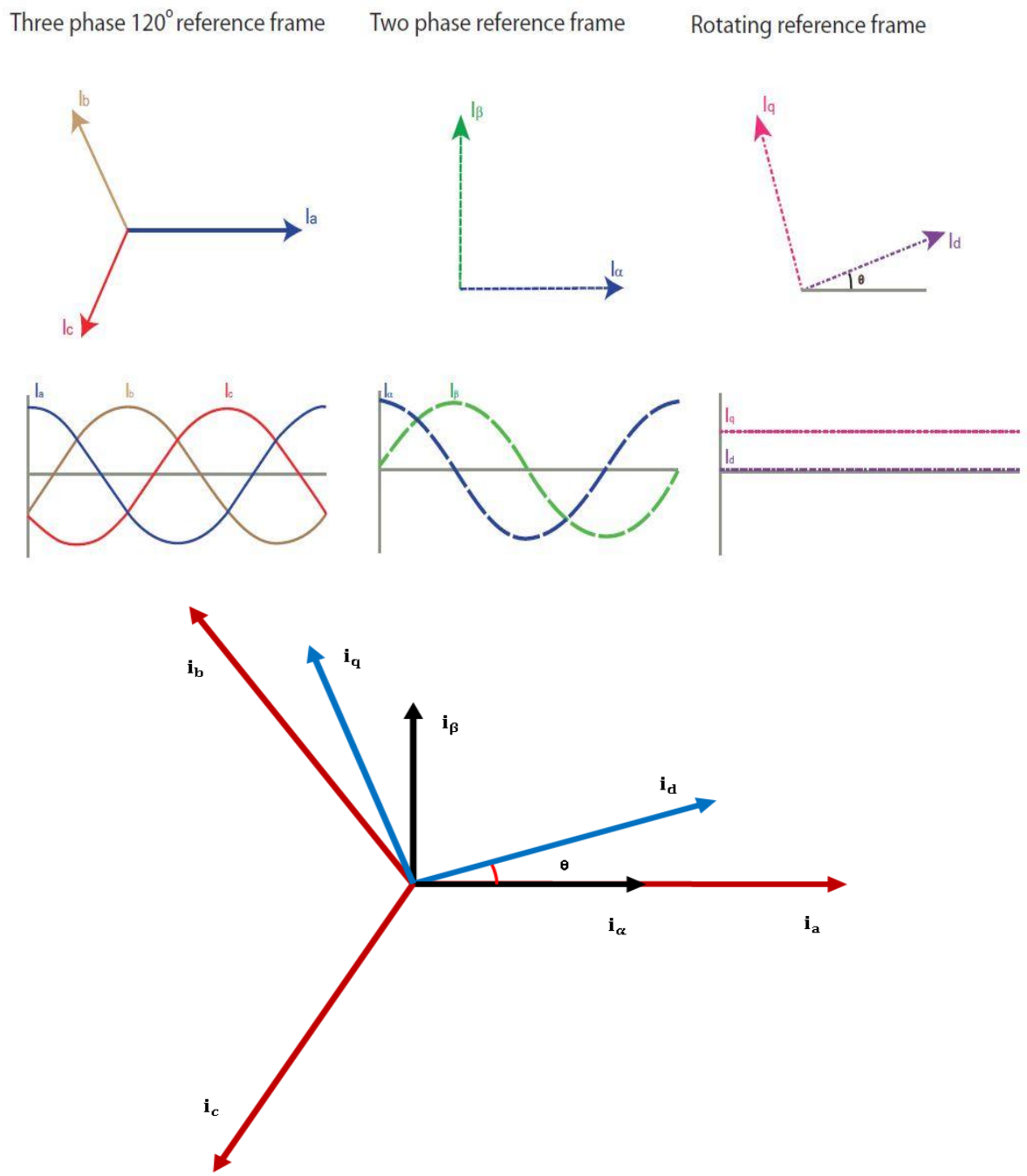

Fig.3.1: Three phase quantities transformed into their equivalent 2-phase quantity either in synchronously rotating frame (or) stationary frame.

The required transformations are given below [6]:

1. Clarke Transformation :

$$I_\alpha = I_a$$

$$I_\beta = \frac{1}{\sqrt{3}} I_a + \frac{2}{\sqrt{3}} I_b \qquad (3.1)$$

2. Park Transformation :

$$I_d = I_\alpha \cos\theta + I_\beta \sin\theta$$
$$I_q = I_\beta \cos\theta - I_\alpha \sin\theta \quad (3.2)$$

3. Inverse Park Transformation:

$$I_\alpha = I_d \cos\theta - I_q \sin\theta$$
$$I_\beta = I_d \sin\theta + I_q \cos\theta \quad (3.3)$$

4. Inverse Clarke Transformation:

$$I_a = I_\alpha$$
$$I_b = -\frac{1}{2} I_\alpha + \frac{\sqrt{3}}{2} I_\beta$$
$$I_c = -\frac{1}{2} I_\alpha - \frac{\sqrt{3}}{2} I_\beta \quad (3.4)$$

In Field Oriented Control, the direct and quadrature axis currents i_d and i_q are controlled to achieve the requested torque. Field and torque component in DC Motor can be seperately controlled by controlling respective field current and armature current. In Field Oriented Control the AC Synchronous Motor is controlled like a Sperately Excited DC Motor. FOC is a Vector Control. In FOC three phase stator current are identified as two orthogonal 'dq' component, where direct axis component defines magnetic flux and quadrature axis component defines torque. Field flux linkage and armature flux linkage created by respected field current and armature current (torque component) are orthogonally aligned, such that when torque is controlled, the field flux linkage is not affected. So, it gives dynamic torque response. FOC can generate full torque at zero speed and has faster speed response, fast acceleration and fast decceleration.

The direct axis current has no effect on torque production and it needs to be zero to reach maximum torque per ampere ratio. So, this drives direct axis reference current component is considered zero and therefore forces the current space vector in the quadrature direction. Since only the quadrature axis current produces useful torque and the direct axis current has no effect on torque production, so for Permanent Magnet BLDC Motor the direct axis referencce current is considered zero to maximize the torque efficiency of the system [6]. The torque curves will be linear in the d-q plane and the maximum torque per ampere ratio trajectory will be along the quadrature-axis. Field Oriented Control is mainly a mathematical technique utilized for achieving a separate control of the field production and the torque

production portions of the stator currents in a three-phase motor. Stator current is decomposed into magnetizing current i_d responsible for producing a magnetic field and quadrature current i_q which controls the developed torque. FOC maintains a constant stator field in quadrature axis with the rotor field by manipulating the motor current and voltage with reference to the rotor's direct and quadrature axis irrespective of any bandwidth limitation of the PI controllers [19].

3.3 Adaptive PI Controller Design

There could be three types of control loops functioning simultaneously: Torque Control Loop, Speed Control Loop and Position Control Loop. Optical encoder or synchronous resolver is used for measuring the actual speed of the motor. In some cases, same sensors are used to get relative position information. Otherwise, separate position sensors may be used to get absolute positions. Computer Numeric Controlled (CNC) machines are a good example of this.

In industry PI controller is widely used due to its simple structure and easy to design. A PI controller is a proportional integral control loop feedback system. The main aim of any modulation technique is to obtain variable output having a maximum fundamental component with minimum harmonics. A PI controller tries to correct the error between a measured process variable and a desired reference point by calculating and giving corrective action to adjust the process as desired [5]. A limiter is put on the speed controller output depending on permissible maximum winding currents to prevent overshoot.

The calculation of adaptive PI controller constants is done in two separate modes the proportional mode and the integral mode. The proportional mode minimizes the settling time to gain reference speed. The integral mode reduces system oscillation. The proportional mode determines the analysis of current error and the integral mode determines the analysis based on recent error. Sum of these two modes output, gives corrective action into control section. We can implement algorithm of PI controller as [3],

$$\text{Output, } e_o(t) = K_p e_i(t) + K_I \int_o^t e_i(t)dt \qquad (3.5)$$

Where, K_p and K_I are the proportional and integral gains of the PI controller respectively.

$e_i(t)$ = Desired set reference value – actual calculated value.

$$I_{q\,ref} = {}^{T_{ref}}/_{K_t} \quad (3.6)$$

Where, T_{ref} is the reference torque and K_t is the torque constant. Since only the quadrature current produces useful torque. The P-I controller operates on quadrature current and takes the requested torque as input. This causes the quadrature current to track the requested torque, as desired. So, the actual speed of the PMBLDC Motor is compared with its reference speed and the speed error is processed through PI controller to estimate reference quadrature axis current $I_{q\,ref}$ [5]. Where, the gains of PI speed controller are K_P and K_I.

$$e(t) = \omega_{merror}\,(t) = \omega_{mref} - \omega_m\,(t) \quad (3.7)$$

$$I_{q\,ref}\,(t) = I_{q\,ref}\,(t-1) + K_P\,[e(t) - e(t-1)] + K_I\,e(t)\,dt \quad (3.8)$$

From simulation studies it has been observed that the speed error base PI controller reduces the effectiveness of the PI controller and becomes slower due to the nonadjustable nature of gain constants. In this control systems K_P and K_I gain constants are made adjustable with speed by using Equation (3.9-3.10). Where, K_{P0} and K_{I0} are initial gain constants of the system, K_1 and K_2 are the constant of the tuner of the proportional and integral gain constants with speed respectively. K_{P0} =0.21, K_{I0} =0.01, K_1 =0.025, K_2 = 0.004 are selected for the simulation of PMBLDC Motor drives. Thus an Adaptive PI controller is designed, so that speed and current overshoot in system is prevented and settling time to gain reference speed can be minimized.

$$K_P = K_{P0} + K_1 * \omega_m \quad (3.9)$$

$$K_I = K_{I0} + K_2 * \omega_m \quad (3.10)$$

3.4 Sinusoidal Current Regulated PWM Control

The block diagram of the proposed Field Oriented Sinusoidal Current Regulated PWM (CRPWM) Control for the PMBLDC Motor drive is shown in Figure (3.2). The proposed system has the following elements: PMBLDC Motor, position sensor, adaptive PI speed controller, sinusoidal reference current generator, Delta Modulated PWM Current Controller and IGBT based current controlled voltage source inverter (CC-VSI). In this system, the current vector is adjusted by generating the reference current vector from torque component of current from speed error and rotor position information. The reference phase currents are assumed to be sinusoidal and obtained from Clarke and Park inverse

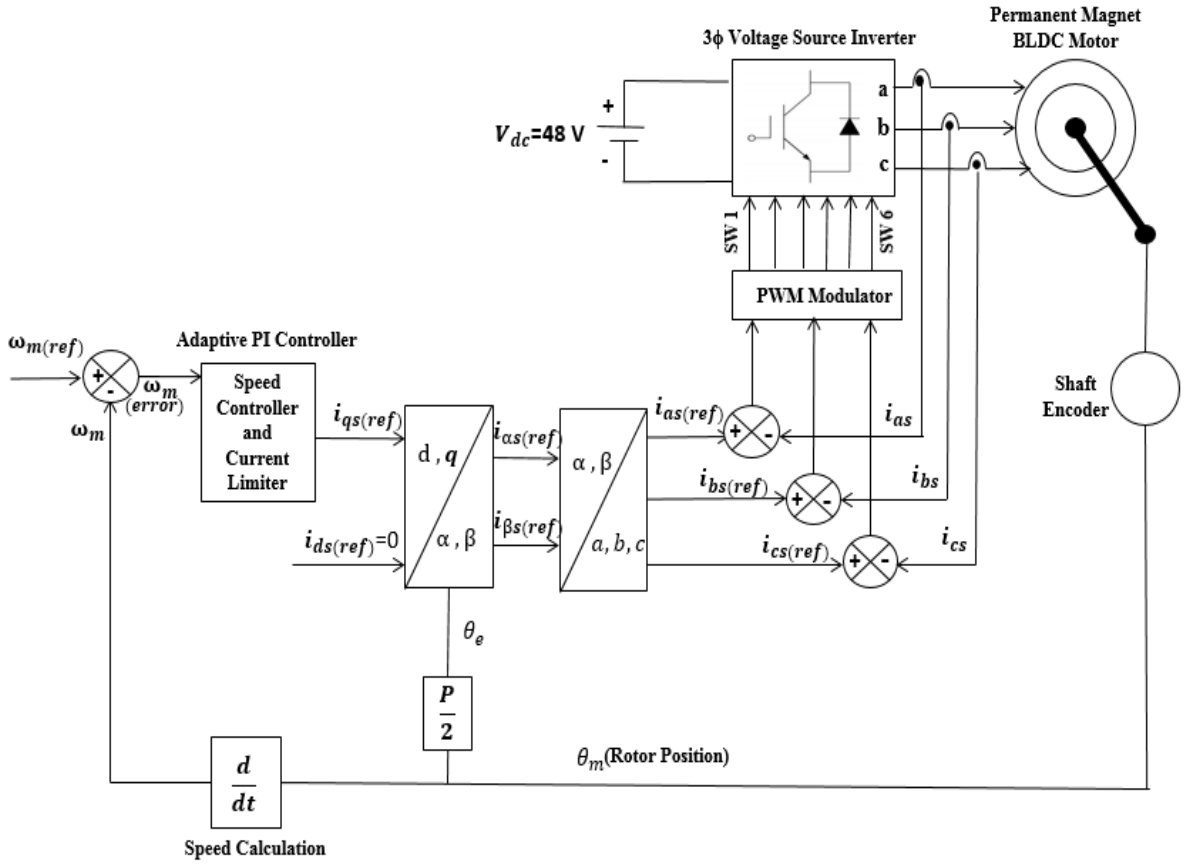

Fig. 3.2: Block diagram of the proposed field oriented current fed Sinusoidal CRPWM Controller of PMBLDC Motor.

transformations. The back EMFs are trapezoidal in nature. Reference three phase currents are compared with the actual currents for voltage vector generation using delta modulation and the inverter switches are turned off or on according to a hysteresis controller.

In proposed control systems, three phase reference currents are generated by considering reference direct axis current $i_{d\ ref}$ = 0 and by calculating the value of reference quadrature axis current $i_{q\ ref}$ according to the requested load torque through the adaptive PI controller from speed error using Equation (3.8). At first, the currents in rotating d-q reference frame are transformed to two-axis orthogonal stationary α-β reference frame by using Inverse Park transformation using Equation (3.3). Then Inverse Clarke transformation is applied to generate three phase reference current in 'abc' frame using using Equation (3.4).

In delta modulation, a triangular wave is allowed to oscillate within a defined window. It is also known as hysteresis modulation [45]. In the hysteresis-type current regulator, the power transistors are switched off and on according to whether the current is greater or less than a reference current within the defined window [37]. The error is used directly to control

the states of the power transistors. The hysteresis controller is used to limit the phase current within a preset hysteresis band. As the supply voltage is fixed, the result is that the switching frequency varies as the current error varies. Since the width of the tolerance band is a design parameter, this mode allows current control to be as precise as desired, but acoustic and electromagnetic noise are difficult to filter because of the varying switching frequency [37].

In Delta modulated current control, the PWM is used for the switching of voltage source inverter. This hysteresis-band PWM is basically an instantaneous feedback current control method of PWM where the actual current continually tracks the reference current. When the current exceeds upper band limit, then the upper switch has to be off and lower switch has to be on. Similarly when the current exceeds lower band limit, upper switch is on and lower switch is off. Switch 1,3,5 are considered upper switches and Switch 4,6,2 are considered lower switches respectively of the inverter.

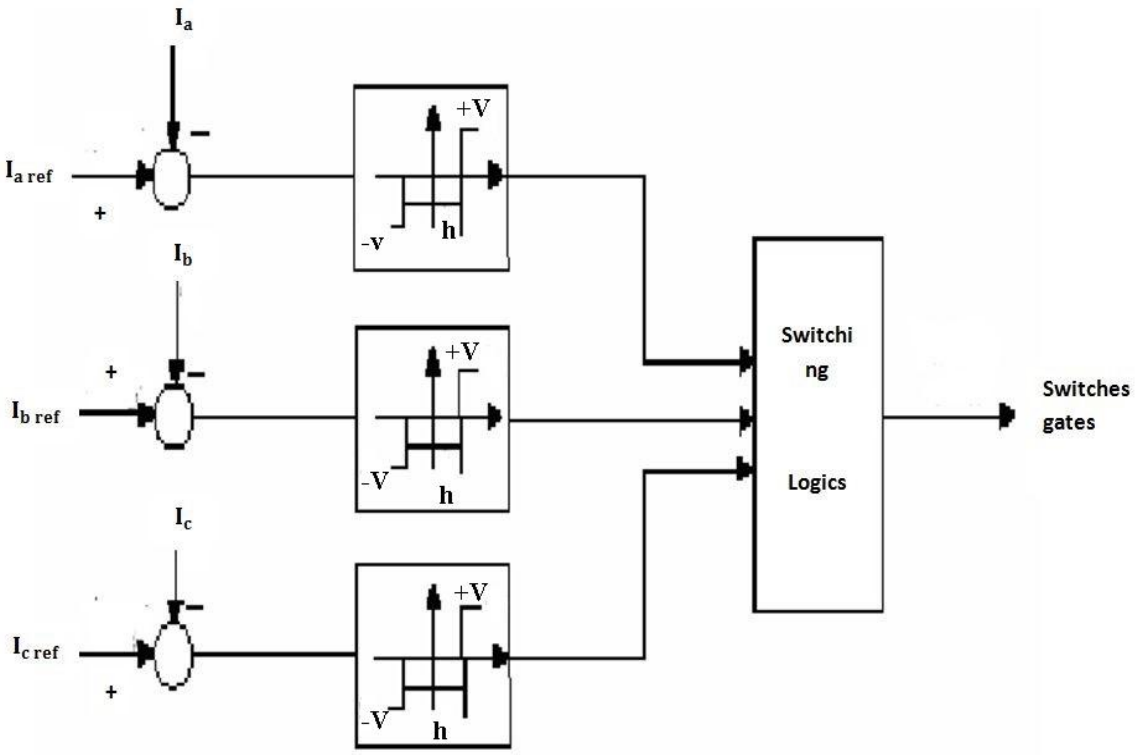

Fig.3.3: The structure of PWM hysteresis current controller.

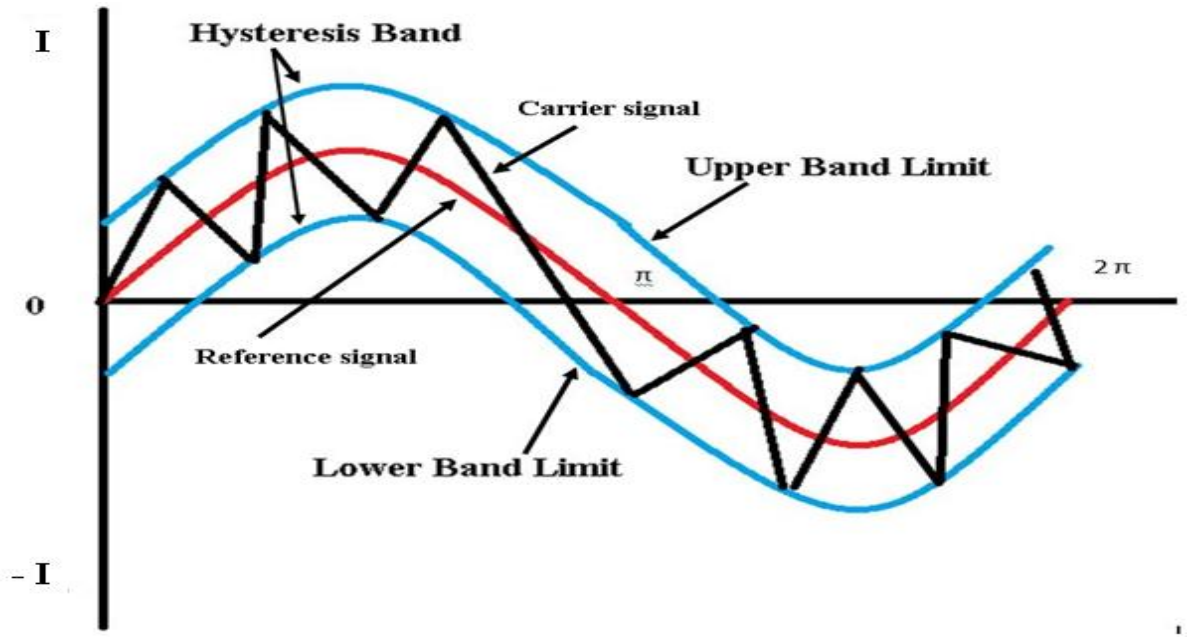

Fig. 3.4: Delta modulation for sinusoidal PWM.

The switching logic which is used in this control drive is given below [5],

If $i_a < (i_{a\,ref} - h_b)$ (3.11)

Then switch 1 is ON and switch 4 is OFF (S_A = 1)

If $i_a > (i_{a\,ref} + h_b)$ (3.12)

Then switch 1 is OFF and switch 4 is ON (S_A = 0)

If $i_b < (i_{b\,ref} - h_b)$ (3.13)

Then switch 3 is ON and switch is 6 OFF (S_B = 1)

If $i_b > (i_{b\,ref} + h_b)$ (3.14)

Then switch 3 is OFF and switch 6 is ON (S_B = 0)

If $i_c < (i_{c\,ref} - h_b)$ (3.15)

Then switch 5 is ON and switch 2 is OFF (S_C = 1)

If $i_c > (i_{c\,ref} + h_b)$ (3.16)

Then switch 5 is OFF and switch 2 is ON (S_C = 0)

Here, h_b is the hysteresis band around reference current. The inverter output voltage according to the above switching conditions are given [5] below,

$$V_a = {}^1/_3 [2S_A - S_B - S_C] \quad (3.17)$$

$$V_b = {}^1/_3 [-S_A + 2S_B - S_C] \quad (3.18)$$

$$V_c = {}^1/_3 [-S_A - S_B + 2S_C] \quad (3.19)$$

Simulation result:

A C++ program code is written for Field Oriented Sinusoidal CRPWM Control of PMBLDC Motor. The effectiveness of the drive system is studied through simulation. The Motor parameters are given in Appendix A.

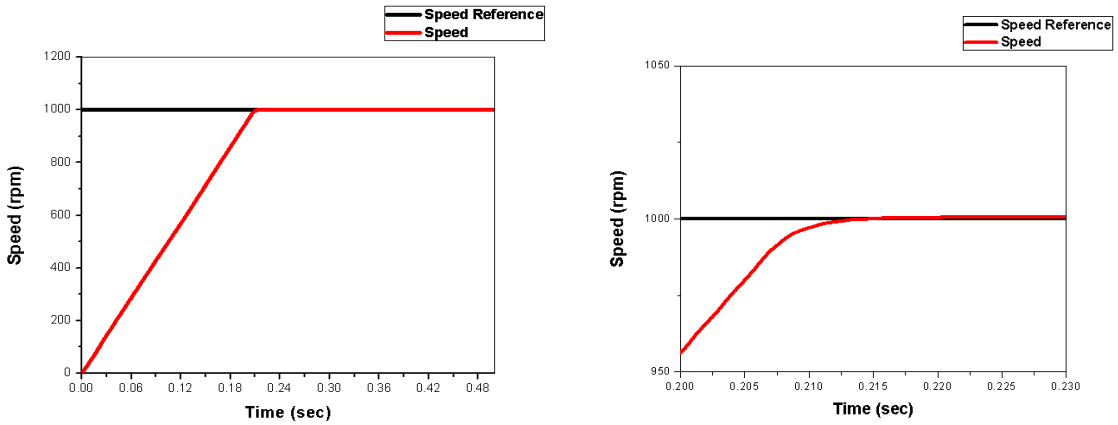

Fig 3.5: Speed characteristic of PMBLDC Motor for Sinusoidal CRPWM Control.

The speed curve indicates that the motor reaches full speed within 0.22 second for 104.72 radian/second or 1000 rpm without any overshoot.

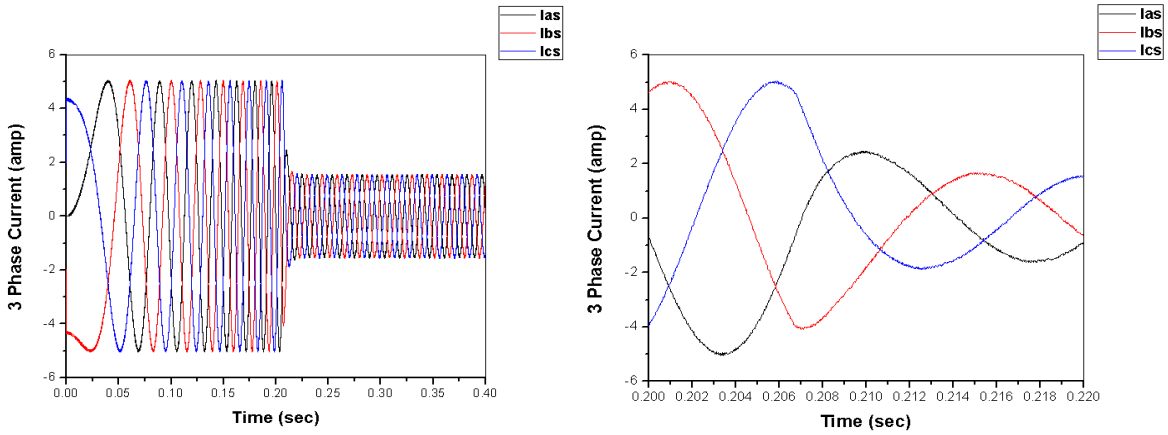

Fig 3.6: Three-phase current with transient condition for Sinusoidal CRPWM Control.

During transient time when speed is rising a very high current flows, due to Current Limiter current does not exceed 5 amp. After 0.22 second when motor reaches the desired speed, level of current decreases like shown in Figure (3.7). Pulsating harmonics are showing hysteresis control characteristics.

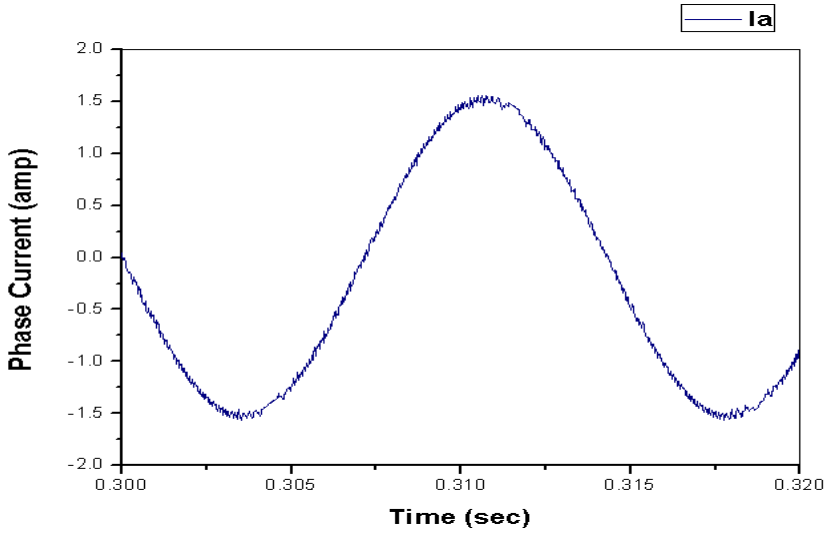

Fig 3.7: Steady state phase current in PMBLDC Motor for Sinusoidal CRPWM Control.

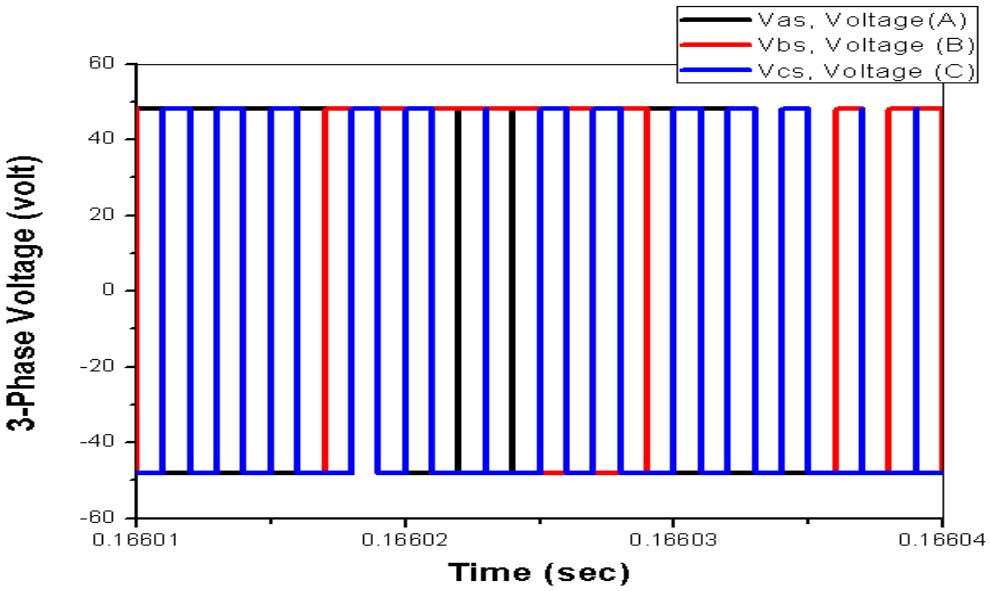

Fig.3.8: 3- Phase voltage for Sinusoidal CRPWM Control.

Inverter output 3-phase voltages are put into 3 phase windings of PMBLDC Motor. As we can see in Figure (3.8) voltages are rectangular shape.

The fluctuation of two axis (α-β) flux is shown in Figure (3.9). The developed torque is shown Figure (3.10). During starting very high torque is generated as speed reaches its desired speed torque decreases. Load torque is considered 0.8 N-m.

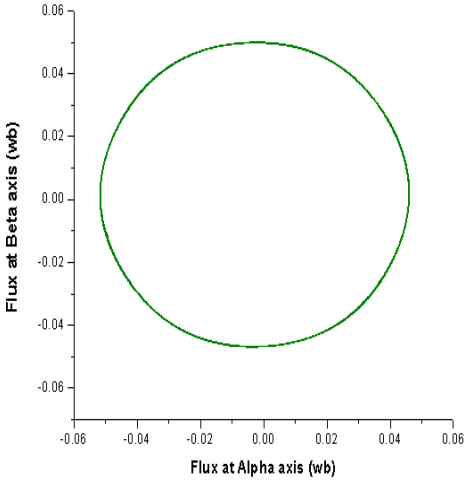

Fig 3.9: Two axis (α-β) flux.

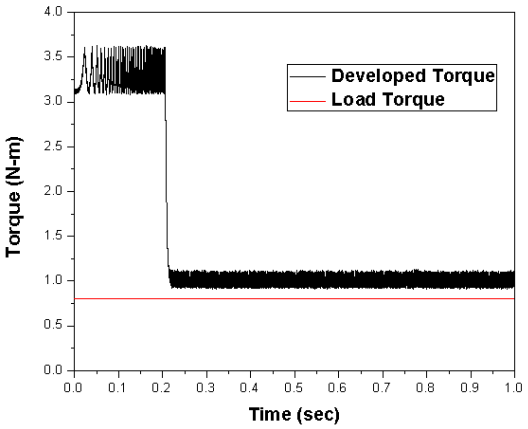

Fig 3.10: Developed torque.

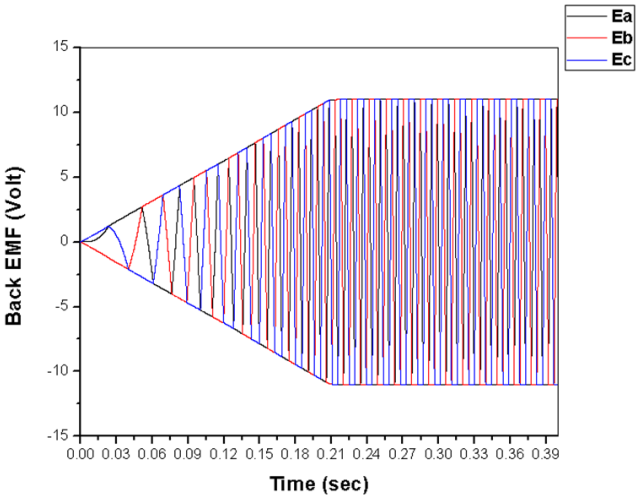

(a)

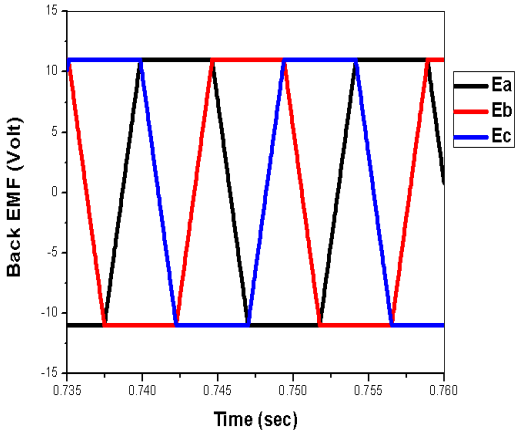

(b)

Fig 3.11: Back EMF with (a) transient condition, (b) steay state condition.

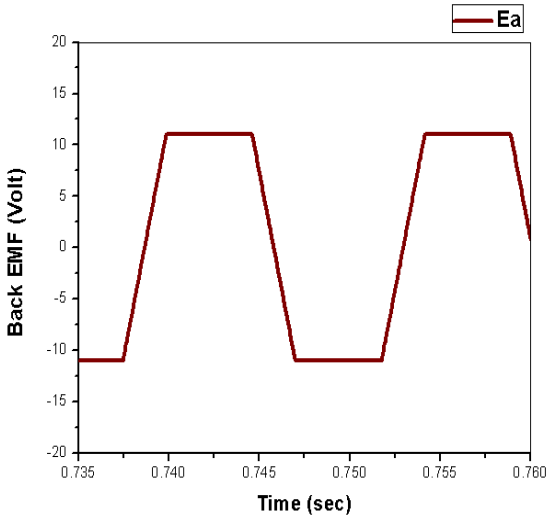

Fig.3.11: (c) Steady state single phase back EMF.

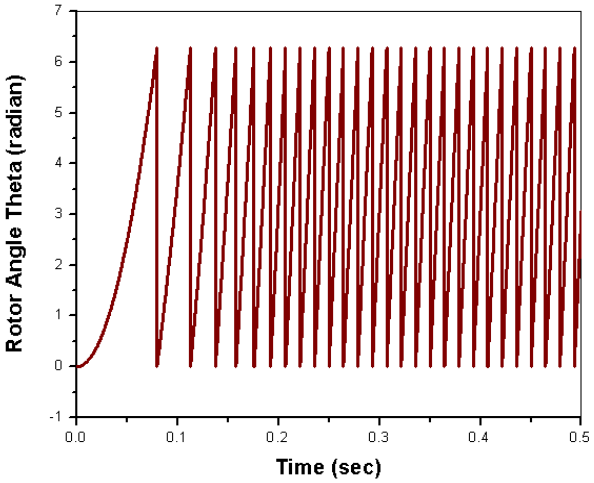

Fig 3.12: Rotor angle variation plot.

Figure (3.11)(a) shows trapezoidal back EMF with transient period. Steady state back EMF plot is shown in Figure (3.11)(b,c). Back EMF starts from zero and when motor reach the desire speed, then back EMF is a constant trapezoidal shape voltage.

Rotor angle plot in Figure (3.12) is showing unidirectional 360 degree rotation of the rotor.

3.5 Square Wave Current Regulated PWM Control

The block diagram of the Square Wave Current Regulated PWM Control of PMBLDC Motor is shown in Figure (3.13). The proposed Permanent Magnet BLDC Motor drive have the following elements: PMBLDC Motor, delta modulated PWM current controller, optical position sensor, adaptive PI speed controller, square wave reference current generator and IGBT based current controlled voltage source inverter (CC-VSI).

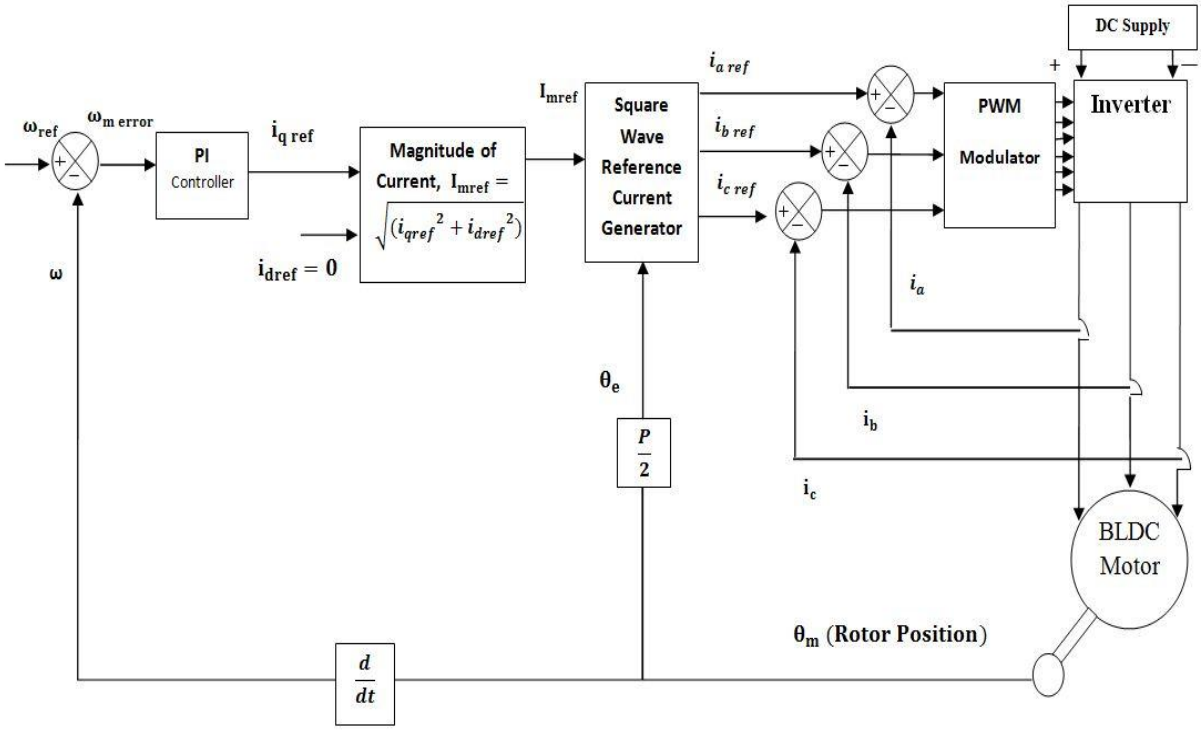

Fig 3.13: Block diagram of the Square Wave Current Regulated PWM Control of Permanent Magnet Brushless DC Motor.

In Square Wave CRPWM Control, the current vector is adjusted by generating the reference current vector from torque component of current from speed error and rotor position information. The back EMFs are trapezoidal in nature. The reference direct axis current $i_{d\ ref}$ is considered zero. The reference quadrature axis current $i_{q\ ref}$ is calculated

according to the requested load torque through the adaptive PI controller from speed error using Equation (3.8). The magnitude of reference currents are obtained using Equation (3.20). The square wave shape of reference currents are generated using Equation (3.21-3.27). Reference three phase currents are compared with the actual currents for voltage vector generation using delta modulation and the inverter switches are turned off or on according to a hysteresis controller. The construction and operation of hysteresis controller are discussed before in Sinusoidal CRPWM Control.

The magnitude of reference currents are given as,

$$I_{m\ ref} = \sqrt{{i_{q\ ref}}^2 + {i_{d\ ref}}^2} \tag{3.20}$$

Reference currents are given below [5],

$$0 < \theta < \frac{\pi}{6} \begin{cases} I_{aref} = 0 \\ I_{bref} = -I_m \\ I_{cref} = I_m \end{cases} \tag{3.21}$$

$$\frac{\pi}{6} < \theta < \frac{\pi}{2} \begin{cases} I_{aref} = I_m \\ I_{bref} = -I_m \\ I_{cref} = 0 \end{cases} \tag{3.22}$$

$$\frac{\pi}{2} < \theta < \frac{5\pi}{6} \begin{cases} I_{aref} = I_m \\ I_{bref} = 0 \\ I_{cref} = -I_m \end{cases} \tag{3.23}$$

$$\frac{5\pi}{6} < \theta < \frac{7\pi}{6} \begin{cases} I_{aref} = 0 \\ I_{bref} = I_m \\ I_{cref} = -I_m \end{cases} \tag{3.24}$$

$$\frac{7\pi}{6} < \theta < \frac{9\pi}{6} \begin{cases} I_{aref} = -I_m \\ I_{bref} = I_m \\ I_{cref} = 0 \end{cases} \tag{3.25}$$

$$\frac{9\pi}{6} < \theta < \frac{11\pi}{6} \begin{cases} I_{aref} = -I_m \\ I_{bref} = 0 \\ I_{cref} = I_m \end{cases} \tag{3.26}$$

$$\frac{11\pi}{6} < \theta < \frac{12\pi}{6} \begin{cases} I_{aref} = 0 \\ I_{bref} = -I_m \\ I_{cref} = I_m \end{cases} \tag{3.27}$$

Simulation Result:

A C++ program code is written for Square Wave Current Regulated PWM Control of BLDC Motor for computer simulation. Effectiveness of the drive system is studied. Speed and phase currents of the motor during starting are shown in Figure (3.14) and Figure (3.15). Motor parameters are given in Appendix A.

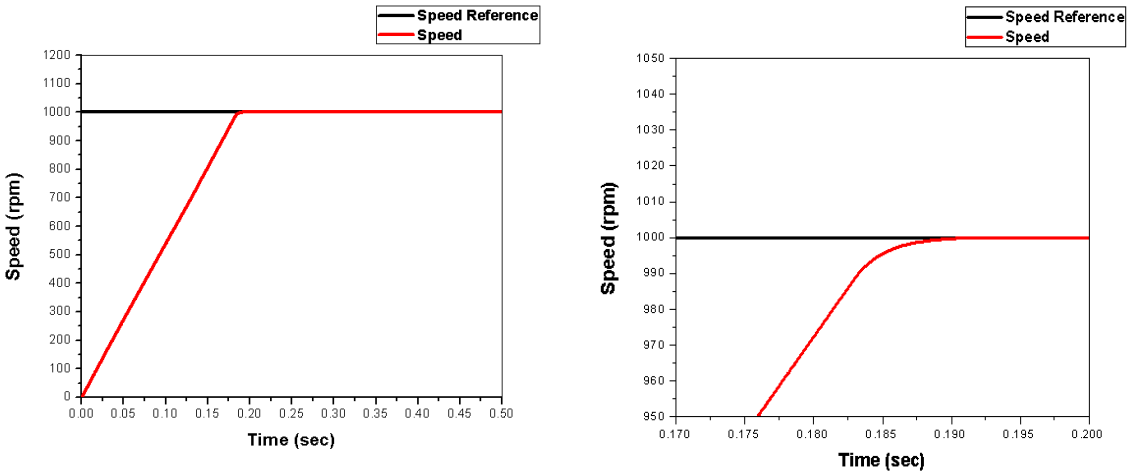

Fig 3.14: Speed characteristic for Square Wave Current Regulated PWM Control.

In Figure (3.14) shows that the motor gain its desired full speed in 0.19 second for speed of 104.72 radian/second or 1000 rpm without any overshoot and the current waves are square shape as shown in Figure (3.15), Figure (3.16). During transient time when speed is rising a very high current flows as shown in Figure (3.15)(a). We can see that Square Wave Current Regulated PWM Control takes less time to reach desired speed than Sinusoidal Current Regulated PWM Control with same PI constants.

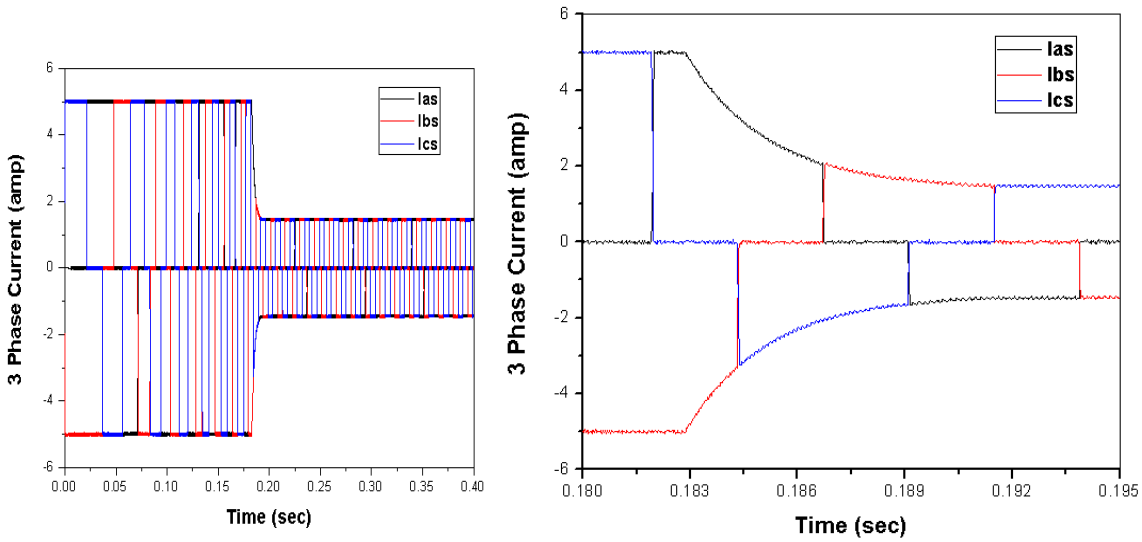

Fig 3.15: Current characteristic during transient period in Square Wave CRPWM Control.

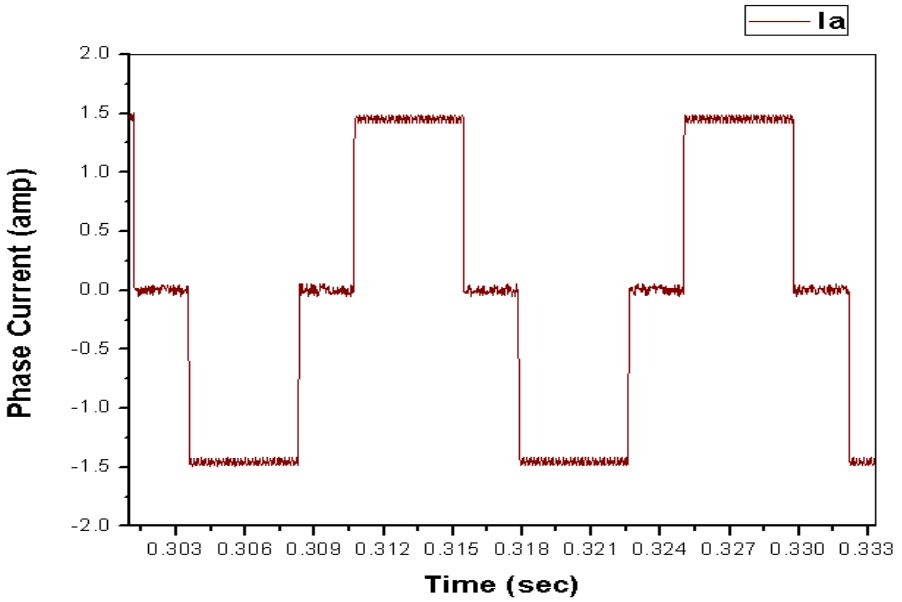

Fig 3.16: Steady state phase current for Square Wave Current Regulated PWM Control.

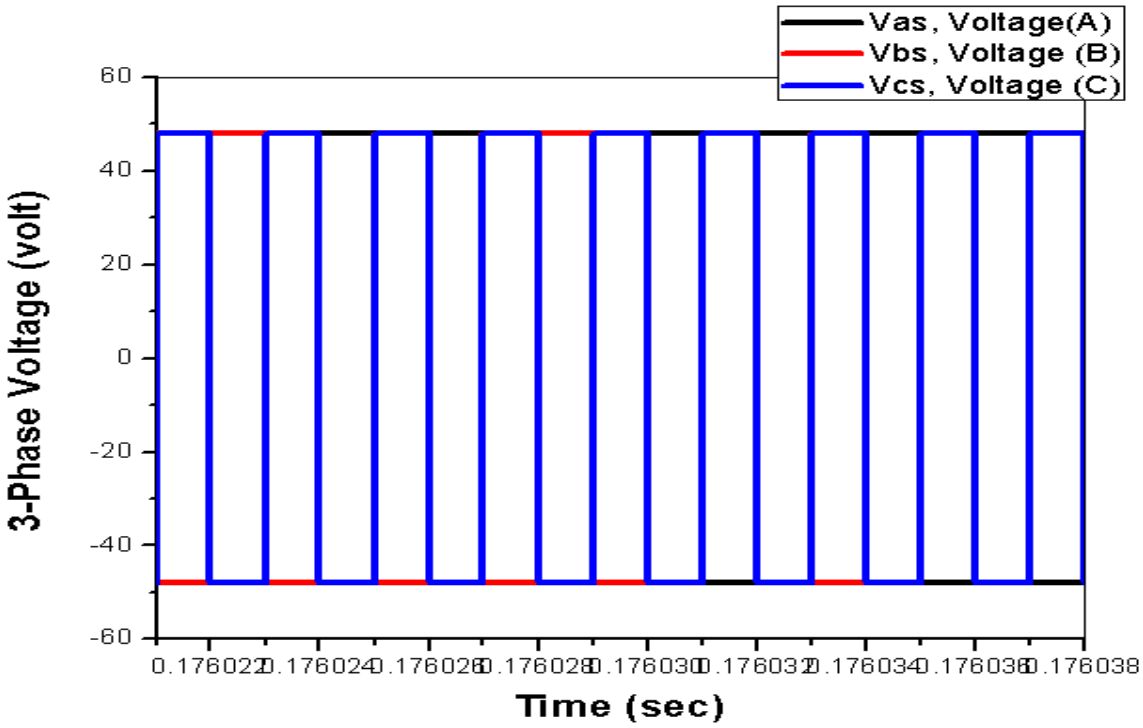

Fig.3.17: Phase voltages for Square Wave CRPWM Control.

Inverter output 3-phase voltages are put into 3 phase windings of PMBLDC Motor. As we can see in Figure (3.17) voltages are rectangular shape.

The fluctuation of two axis (α-β) flux is shown in Figure (3.18). The developed torque is shown Figure (3.19). During starting very high torque is generated as speed reaches its desired speed torque decreases. Load torque is considered 0.8 N-m.

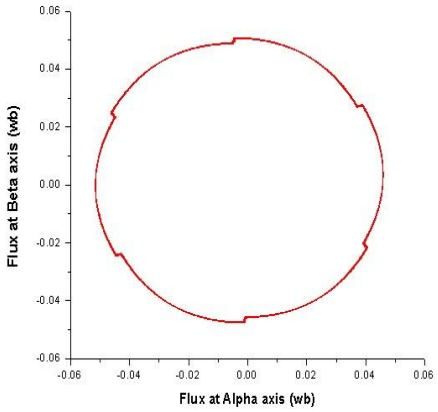

Fig 3.18: Two axis(α-β) flux.

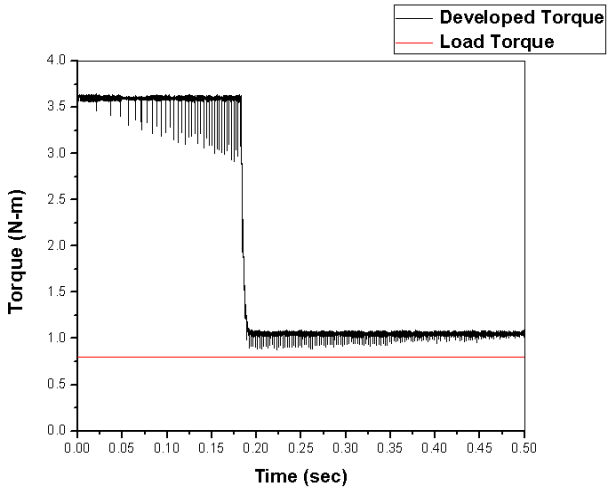

Fig 3.19: Developed torque.

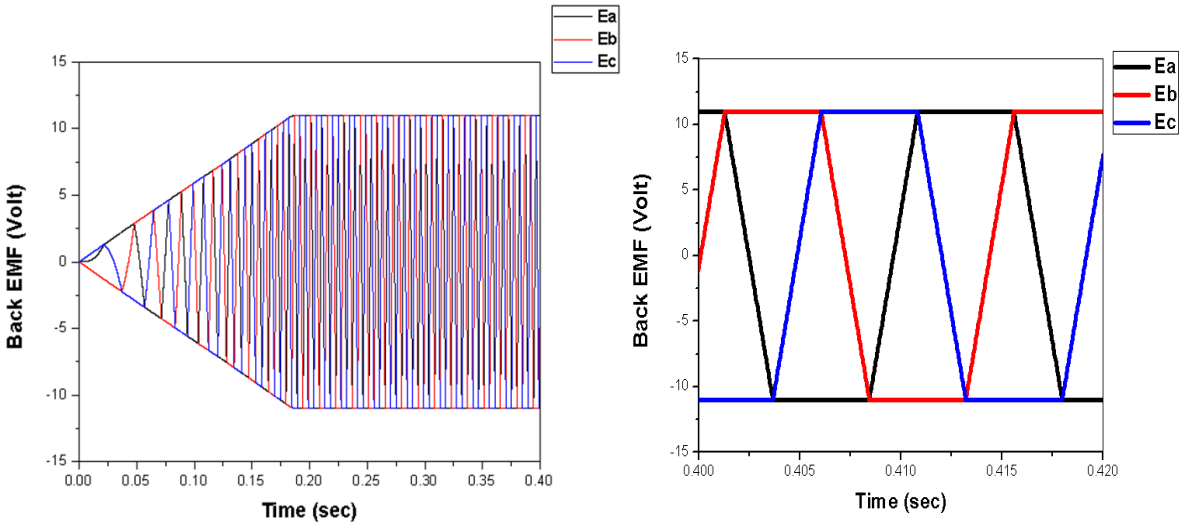

(a) (b)

Fig 3.20: Back EMF with (a) transient condition, (b) steay state condition.

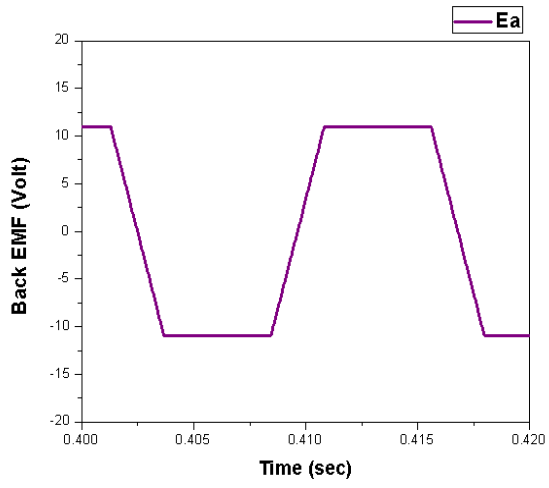

Fig.3.20: (c) Steady state single phase back EMF.

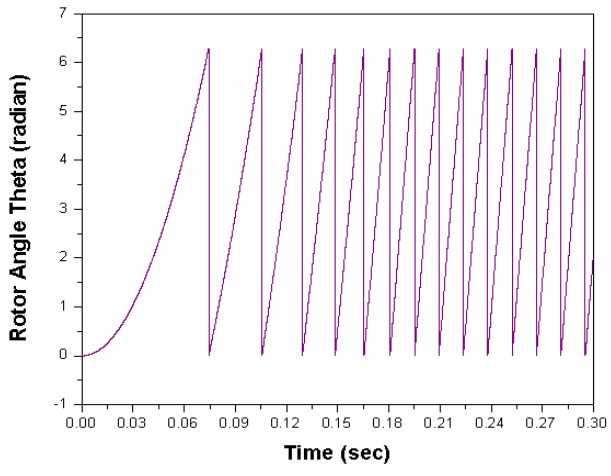

Fig 3.21: Rotor angle variation plot.

Figure (3.20)(a) shows trapezoidal back EMF with transient period. Steady state back EMF plot is shown in Figure (3.20)(b,c). Back EMF starts from zero and when motor reach the desire speed, then back EMF is a constant trapezoidal shape voltage.

Rotor angle plot in Figure (3.21) is showing unidirectional 360 degree rotation of the rotor.

3.6 Conclusion

Two field oriented based current control techniques of PMBLDC Motor are shown in this chapter. It is observed that the PMBLDC Motor performs fine in both cases for starting condition. The performance is better in the case of Square wave CRPWM Control as it can reach desired speed and stability in lesser time, in comparison to Sinusoidal Current Regulated PWM Control considering same PI controller constants. So, the Square wave Current Regulated PWM Control has better speed response.

Chapter IV

SPACE VECTOR PULSE WIDTH MODULATION CONTROL

Chapter at a Glance

4.1 Introduction

Space Vector Modulation (SVM) technique has become the most popular and important PWM technique for Voltage Source Inverter for the control of Brushless DC Motor. The Space Vector Pulse Width Modulation (SVPWM) technique is better than conventional technique because of following excellent features: it has wide linear modulation range, it has lower base band harmonics than conventional Pulse Width Modulation or other sine based modulation methods, 15% more output voltage then conventional Pulse Width Modulation, i.e. better DC-link utilization, more efficient use of DC supply voltage, prevent un-necessary switching, hence commutation loss is decreased and higher efficiency [8].

Space Vector Modulation (SVM) technique is originally developed as a voltage vector approach to Pulse Width Modulation (PWM) for three-phase inverters. SVPWM approximates the 3 phase reference voltages by a combination of eight switching patterns. It confines space vector in six voltage sector in αβ voltage space. Switching sequence is applied according to the region where the output voltage vector is located. The α, β components are found by Clarke and Park transformations and inverse transformations. The determination of switching instant is done by using Space Vector Modulation technique based on the representation of switching vectors in α, β plane. In SVPWM methods, the voltage reference is provided using a revolving reference vector.

The purpose of this chapter is to present the proposed Current Fed Space Vector Pulse Width Modulation Control for PMBLDC Motor. The effectiveness of the control scheme is tested in a C++ simulation environment.

4.2 Space Vector Pulse Width Modulation Control

The block diagram of the proposed Current Fed Space Vector Pulse Width Modulation Control system of PMBLDC Motor is given in Figure (4.1). The proposed PMBLDC Motor drive mainly consists of (1) three adaptive PI controllers, (2) reference voltage generator, (3) micro-controller, (4) IGBT Voltage Source Inverter, (5) optical position sensor, (6) current sensor, (7) SVPWM Controller and (8) a PMBLDC Motor.

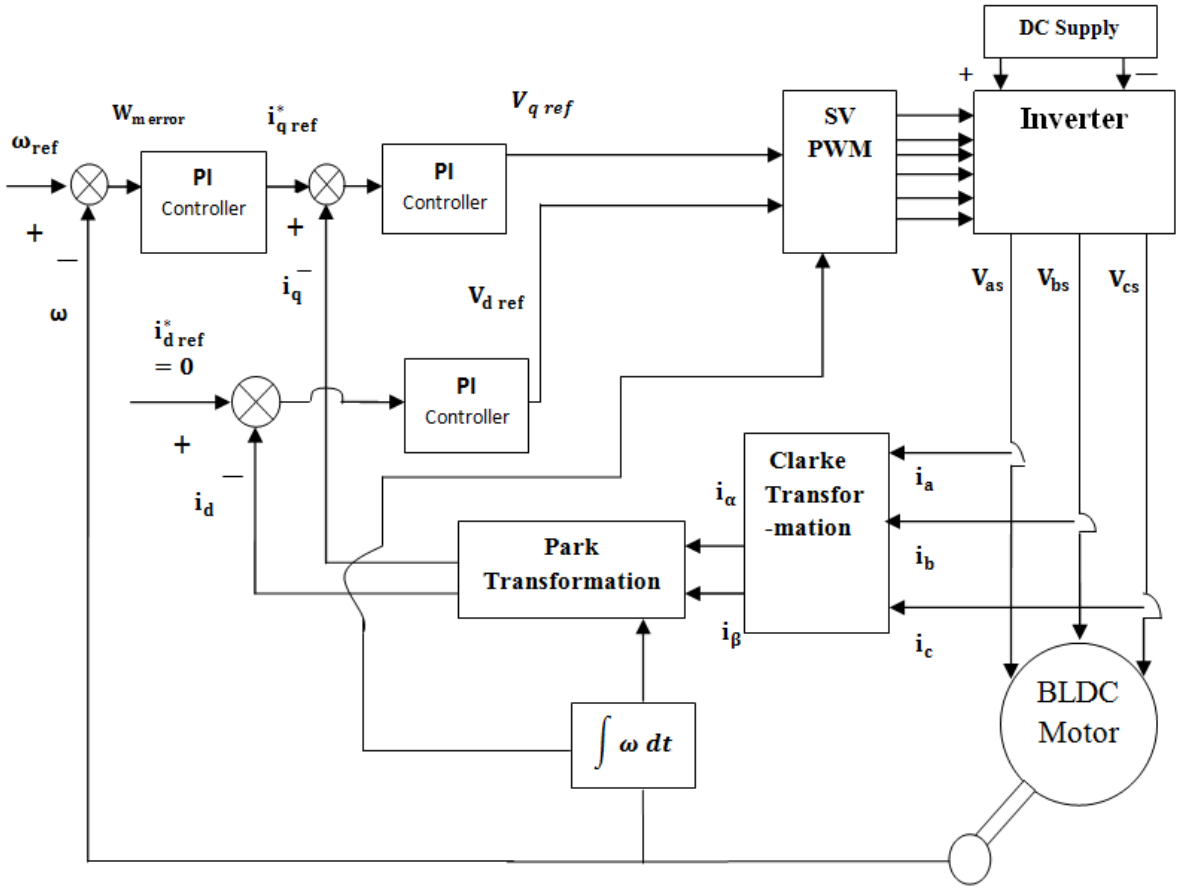

Fig.4.1: Block diagram of the proposed current fed Space Vector Pulse Width Modulation Control method for BLDC Motor.

The proposed control system uses field oriented technique with current and speed feedback to generate quadrature reference voltage and direct axis reference voltage. Then Space Vector Pulse Width Modulation method is applied in SVPWM controller to generate sequential six gate pulses. They are fed into the inverter transistor gates for controlled voltage generation. The controlled voltages are applied to PMBLDC Motor to produce required speed.

In this proposed Voltage Regulated Space Vector Pulse Width Modulation Control system, transformation to different frame is necessary. The required transformations for the proposed system are given below [7],

1. Clarke Transformation :

$$I_\alpha = I_a$$

$$I_\beta = \frac{1}{\sqrt{3}} I_a + \frac{2}{\sqrt{3}} I_b \qquad (4.1)$$

2. Park Transformation :

$$I_d = I_\alpha \cos\theta + I_\beta \sin\theta$$
$$I_q = I_\beta \cos\theta - I_\alpha \sin\theta \quad (4.2)$$

3. Inverse Park Transformation :

$$V_\alpha = V_d \cos\theta - V_q \sin\theta$$
$$V_\beta = V_q \cos\theta + V_d \sin\theta \quad (4.3)$$

4. Inverse Clarke Transformation :

$$V_a = V_\alpha$$
$$V_b = [-V_\alpha + \sqrt{3}.V_\beta]/2$$
$$V_c = [-V_\alpha - \sqrt{3}.V_\beta]/2 \quad (4.4)$$

The reference direct axis current $i_{d\ ref}$ is considered zero. The reference quadrature axis current $i_{q\ ref}$ is calculated according to the requested load torque through the adaptive PI controller from speed error using Equation (3.8). Three phase output current is converted into direct axis current i_d and quadrature axis current i_q using Clarke Transformation and Park Transformation, Equation (4.1-4.2).

The outputs from the other two PI controllers represent a voltage space vector with respect to the rotor, by mirroring the transformation performed on motor currents. Both reference and generated direct axis current are compared to generate reference V_d through PI controller. Both reference and generated quadrature axis current are compared to generate reference V_q through PI controller.

$$K_P = K_{P0} + K_1 * \omega_{merror}$$
$$K_I = K_{I0} + K_2 * \omega_{merror} \quad (4.5)$$

K_{P1}, K_{I1}, K_{P2} and K_{I2} gain constants are made adjustable with speed error by using Equation (4.5). Where, K_{P0} and K_{I0} are initial gain constants of the system, K_1 and K_2 are the constant of the tuner of the proportional and integral gain constants.

$$i_{derror} = i_{dref} - i_d \quad (4.6)$$
$$V_{d\ ref}(t) = V_{d\ ref}(t-1) + K_{P1}[i_{derror}(t) - i_{derror}(t-1)] + K_{I1}\, i_{derror}(t)\, dt \quad (4.7)$$

$$i_{qerror} = i_{qref} - i_q \quad (4.8)$$
$$V_{q\ ref}(t) = V_{q\ ref}(t-1) + K_{P2}[i_{qerror}(t) - i_{qerror}(t-1)] + K_{I2}\, i_{qerror}(t)\, dt \quad (4.9)$$

These signals are processed by Space Vector Pulse Width Modulation to produce voltage control signals for the output inverter bridge. The six inverter switches are turned on or off sequentially, to generate the required output voltage, needed to get the required speed from PMBLDC Motor using Table (4.2).

For a brief time if phase become unbalanced for a small period there is a current flow in neutral wire for star connected motor drive. For this reason to replace phase voltages by line voltages following conversion of the motor equation is done in SVPWM technique for simplification of the program. From Equation (2.8) by substituting V_{as} by V_{bs} , substituting V_{bs} by V_{cs} , substituting V_{cs} by V_{as} we get –

$$\begin{bmatrix} V_{as}-V_{bs} \\ V_{bs}-V_{cs} \\ V_{cs}-V_{as} \end{bmatrix} = \begin{bmatrix} R_s & 0 & 0 \\ 0 & R_s & 0 \\ 0 & 0 & R_s \end{bmatrix} \begin{bmatrix} i_a-i_b \\ i_b-i_c \\ i_c-i_a \end{bmatrix} + \frac{d}{dt} \begin{bmatrix} L-M & 0 & 0 \\ 0 & L-M & 0 \\ 0 & 0 & L-M \end{bmatrix} \begin{bmatrix} i_a-i_b \\ i_b-i_c \\ i_c-i_a \end{bmatrix} + \begin{bmatrix} e_a-e_b \\ e_b-e_c \\ e_c-e_a \end{bmatrix}$$

.....(4.10)

$$V_{ab} = V_{as} - V_{bs} \quad (4.11)$$

$$V_{bc} = V_{bs} - V_{cs} \quad (4.12)$$

$$V_{ca} = V_{cs} - V_{as} \quad (4.13)$$

So,

$$\begin{bmatrix} V_{ab} \\ V_{bc} \\ V_{ca} \end{bmatrix} = \begin{bmatrix} R_s & 0 & 0 \\ 0 & R_s & 0 \\ 0 & 0 & R_s \end{bmatrix} \begin{bmatrix} i_a-i_b \\ i_b-i_c \\ i_c-i_a \end{bmatrix} + \frac{d}{dt} \begin{bmatrix} L-M & 0 & 0 \\ 0 & L-M & 0 \\ 0 & 0 & L-M \end{bmatrix} \begin{bmatrix} i_a-i_b \\ i_b-i_c \\ i_c-i_a \end{bmatrix} + \begin{bmatrix} e_a-e_b \\ e_b-e_c \\ e_c-e_a \end{bmatrix}$$

.....(4.14)

From Equation (2.8) by substituting V_{ab} by V_{bc} , substituting V_{bc} by V_{ca} , substituting V_{ca} by V_{ab} we get,

$$\begin{bmatrix} V_{ab}-V_{bc} \\ V_{bc}-V_{ca} \\ V_{ca}-V_{ab} \end{bmatrix} = \begin{bmatrix} R_s & 0 & 0 \\ 0 & R_s & 0 \\ 0 & 0 & R_s \end{bmatrix} \begin{bmatrix} i_a-i_b-i_b+i_c \\ i_b-i_c-i_c+i_a \\ i_c-i_a-i_a+i_b \end{bmatrix}$$

$$+ \frac{d}{dt} \begin{bmatrix} L-M & 0 & 0 \\ 0 & L-M & 0 \\ 0 & 0 & L-M \end{bmatrix} \begin{bmatrix} i_a-i_b-i_b+i_c \\ i_b-i_c-i_c+i_a \\ i_c-i_a-i_a+i_b \end{bmatrix} + \begin{bmatrix} e_a-e_b-e_b+e_c \\ e_b-e_c-e_c+e_a \\ e_c-e_a-e_a+e_b \end{bmatrix}$$

.....(4.15)

From Equation (2.6),

$$i_a - i_b - i_b + i_c = -3i_b \quad (4.16)$$

$$i_b - i_c - i_c + i_a = -3i_c \quad (4.17)$$

$$i_c - i_a - i_a + i_b = -3i_a \quad (4.18)$$

From Equation (4.15),

$$\begin{bmatrix} V_{ab} - V_{bc} \\ V_{bc} - V_{ca} \\ V_{ca} - V_{ab} \end{bmatrix} = \begin{bmatrix} R_s & 0 & 0 \\ 0 & R_s & 0 \\ 0 & 0 & R_s \end{bmatrix} \begin{bmatrix} -3i_b \\ -3i_c \\ -3i_a \end{bmatrix} + \frac{d}{dt} \begin{bmatrix} L-M & 0 & 0 \\ 0 & L-M & 0 \\ 0 & 0 & L-M \end{bmatrix} \begin{bmatrix} -3i_b \\ -3i_c \\ -3i_a \end{bmatrix} + \begin{bmatrix} e_a - e_b - e_b + e_c \\ e_b - e_c - e_c + e_a \\ e_c - e_a - e_a + e_b \end{bmatrix}$$

.....(4.19)

The new machine model equation is shown in Equation (4.19).

The concept of space vector is derived from the rotating field of AC machine which is used for modulating the inverter output voltage. BLDC Motor can be compared as AC Synchronous Motor. When this 3-phase voltage is applied to the AC machine it produces a rotating flux in the air gap of the AC machine. This rotating flux component can be represented as single rotating voltage vector. From the 2-phase component the reference vector magnitude can be found and used for modulating the inverter output. So, the magnitude and angle of the rotating vector is to be determined.

This SVPWM technique approximates the reference voltage by a combination of the eight switching patterns (V_0 to V_7) as shown in Table (4.2). Switching instant is determined using Space Vector PWM technique based on the representation of switching vectors in α, β plane. The voltage reference is provided using a revolving reference vector shown in Figure (4.2).

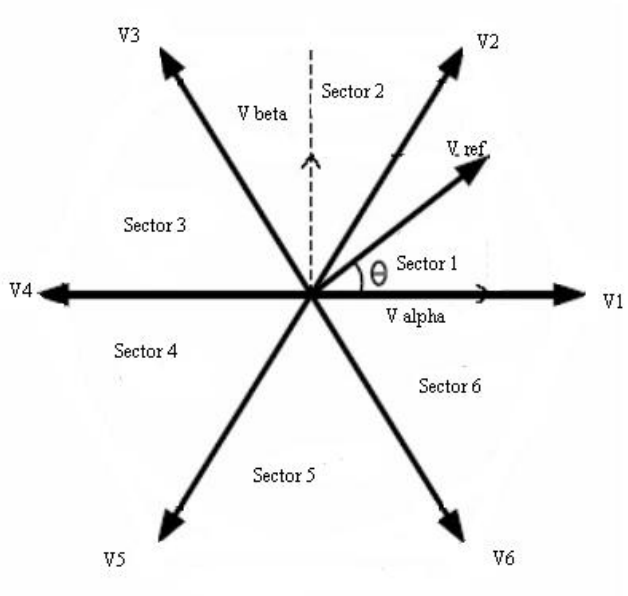

Fig.4.2: Representation of Rotating Vector in Complex Plane.

In Space Vector PWM the sinusoidal voltage is considered as a constant amplitude vector rotating at a constant frequency.

$V_a = \sin(\omega t)$ (4.20)

$V_b = \sin(\omega t - 2\frac{\pi}{3})$ (4.21)

$V_c = \sin(\omega t - 4\frac{\pi}{3})$ (4.22)

Approximation of the reference voltage V_{ref} is done by PWM technique by a combination of the eight switching patterns (V_0 to V_7). Coordinate transformation (abc reference frame to the stationary d-q frame) is done. A three-phase voltage vector is transformed into a vector in the stationary d-q coordinate frame which represents the spatial vector sum of the three-phase voltage as shown in Figure (4.3)[8].

The Space Vector PWM is realized based on the following steps:

1. First calculate V_d, V_q, V_{ref} and angle (α).
2. Then we calculate time duration T_1, T_2 and T_0.
3. Finally, the switching time of each transistor (S1 to S6) is determined.

Determination of V_d, V_q, V_{ref} and angle (α) [8]:

$$V_d = V_{an} - V_{bn}\cos 60° - V_{cn}\cos 60°$$
$$= V_{an} - {}^1\!/_2\, V_{bn} - {}^1\!/_2\, V_{cn} \quad (4.23)$$

$$V_q = V_{an} + V_{bn}\cos 30° - V_{cn}\cos 30°$$
$$= V_{an} - {}^{\sqrt{3}}\!/_2\, V_{bn} - {}^{\sqrt{3}}\!/_2\, V_{cn} \quad (4.24)$$

The reference voltage equations is [6,8],

$$|V_{ref}| = \sqrt{V_d^{\,2} + V_q^{\,2}} = \sqrt{V_\alpha^{\,2} + V_\beta^{\,2}} \quad (4.25)$$

$$\alpha = \tan^{-1}\frac{V_q}{V_d} = \omega_s t = 2\pi f_s t = \theta, \quad (4.26)$$

[considered for PMBLDC Motor as its rotor rotates at synchronous speed]

Where, f_s = Fundamental frequency.

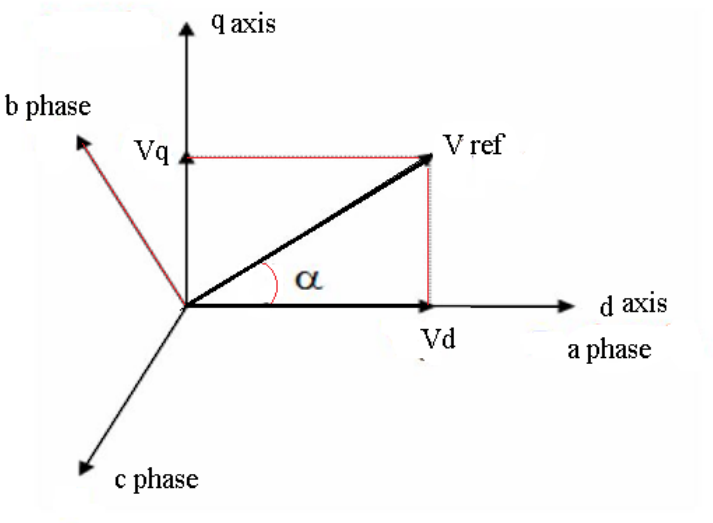

Fig.4.3: Voltage Space Vector and its components.

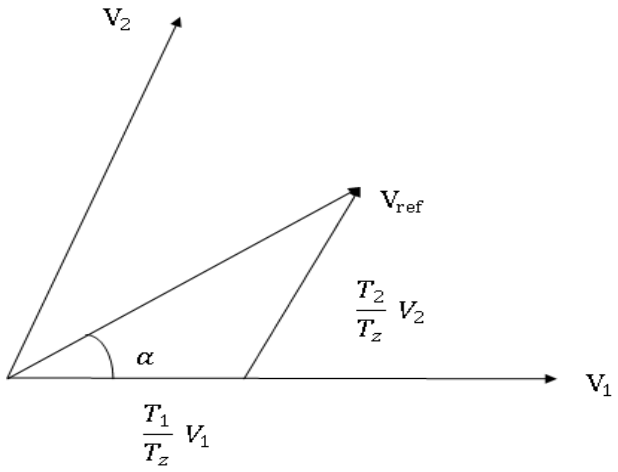

Fig.4.4: Reference vector as a combination of adjacent vectors (sector 1).

Determination of time duration T_1, T_2 and T_0 [8]:

$$\int_0^{T_z} V_{ref} = \int_0^{T_1} V_1\,dt + \int_{T_1}^{T_1+T_2} V_2\,dt + \int_{T_1+T_2}^{T_z} V_0 \tag{4.27}$$

$$\therefore T_z.V_{ref} = T_1.V_1 + T_2.V_2 \tag{4.28}$$

$$\therefore T_z.|V_{ref}|.\begin{bmatrix}\cos\alpha\\ \sin\alpha\end{bmatrix} = T_1.\frac{2}{3}.V_{dc}\begin{bmatrix}1\\0\end{bmatrix} + T_2.\frac{2}{3}.V_{dc}\begin{bmatrix}\cos(\pi/3)\\ \sin(\pi/3)\end{bmatrix}, \tag{4.29}$$

(Where, $0 \leq \alpha \leq 60°$)

$$\therefore T_1 = T_z.a.\frac{\sin\pi/3-\alpha}{\sin\pi/3} \tag{4.30}$$

$$\therefore T_2 = T_z . a. \frac{\sin \alpha}{\sin \pi/3} \quad (4.31)$$

$$\therefore T_0 = T_z - T_1 - T_2 \quad (4.32)$$

$$\text{Where, } T_z = \frac{1}{f_s} \text{ and } a = \frac{|V_{ref}|}{2/3 V_{dc}} \quad (4.33)$$

Here T_1, T_2 and T_0 represent the time widths for vectors V_1, V_2 and V_0. The T_0 is the period in a sampling period for null vectors should be filled. As each switching period T_z starts and ends with zero vectors. Figure (4.5) gives switching pattern for the sectors.

Switching time duration at any Sector [8]:

If, n =1 to 6, (sector 1 to 6)

$$m = \frac{\sqrt{3}.T_z.V_{ref}}{V_{dc}} \quad (4.34)$$

$$\therefore T_1 = m.\sin(\frac{\pi}{3} - \alpha + \frac{(n-1)\pi}{3})$$

$$= m.\sin(\frac{n\pi}{3} - \alpha) \quad (4.35)$$

$$\therefore T_2 = m.\sin\ (\alpha - \frac{(n-1)\pi}{3}) \quad (4.36)$$

$$\therefore T_0 = T_z - T_1 - T_2 \quad (4.37)$$

The construction shown in Figure (4.5) is a symmetrical pulse pattern for two consecutive T_z intervals are shown. The null time has been distributed between the V_0 and V_7 vectors to describe the symmetrical pulse width pattern. A symmetrical pulse pattern gives minimal output harmonics [8].

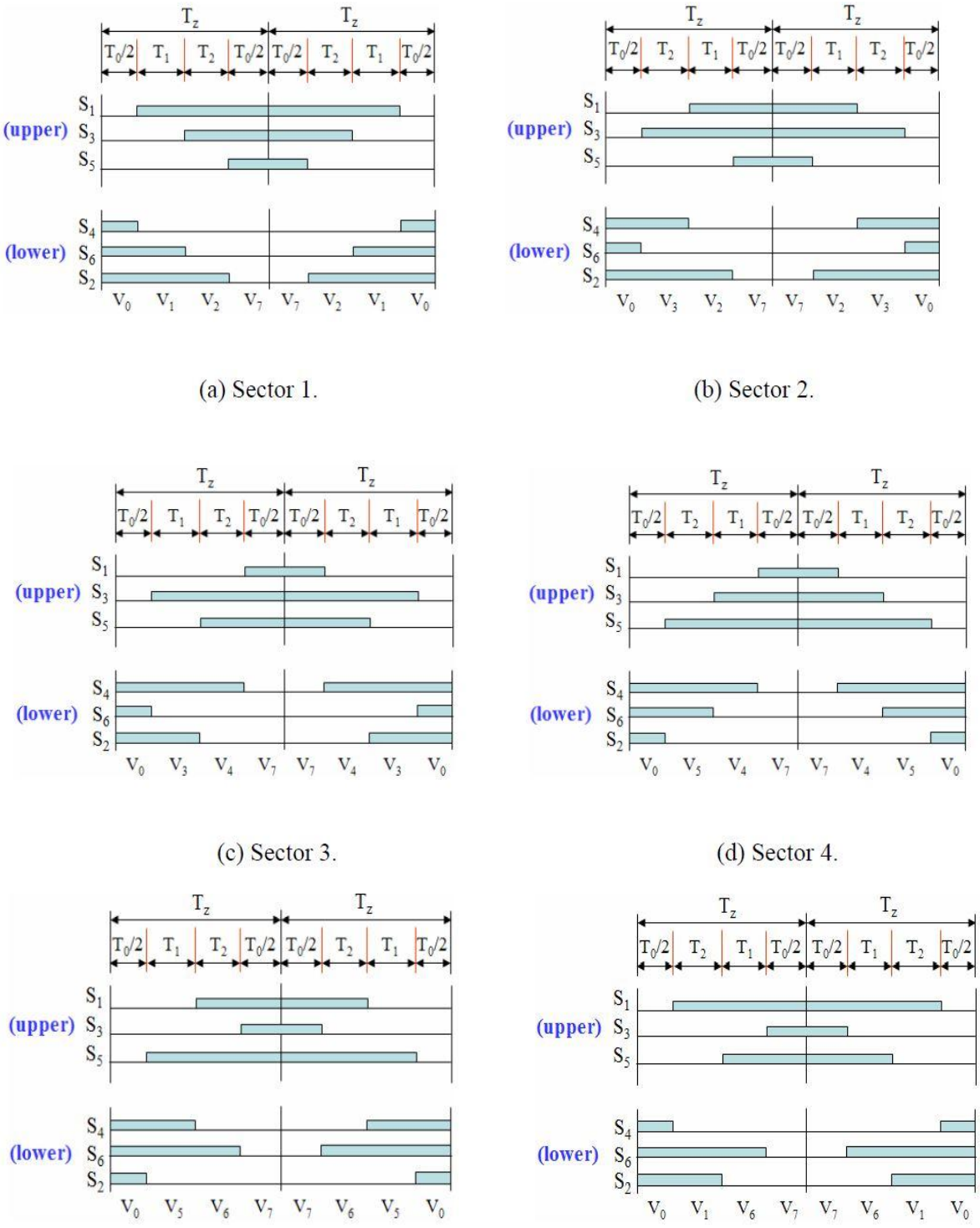

Fig. 4.5: Space Vector PWM switching patterns [8].

Sector	Upper Switches (S_1, S_3, S_5)	Lower Switches (S_4, S_6, S_2)
1	$S_1 = T_1 + T_2 + T_0/2$ $S_3 = T_2 + T_0/2$ $S_5 = T_0/2$	$S_4 = T_0/2$ $S_6 = T_1 + T_0/2$ $S_2 = T_1+T_2+T_0/2$
2	$S_1 = T_1 + T_0/2$ $S_3 = T_1 + T_2 + T_0/2$ $S_5 = T_0/2$	$S_4 = T_2 + T_0/2$ $S_6 = T_0/2$ $S_2 = T_1+T_2+T_0/2$
3	$S_1 = T_0/2$ $S_3 = T_1 + T_2 + T_0/2$ $S_5 = T_2 + T_0/2$	$S_4 = T_1+T_2+T_0/2$ $S_6 = T_0/2$ $S_2 = T_1 + T_0/2$
4	$S_1 = T_0/2$ $S_3 = T_1 + T_0/2$ $S_5 = T_1 + T_2 + T_0/2$	$S_4 = T_1+T_2+T_0/2$ $S_6 = T_2 + T_0/2$ $S_2 = T_0/2$
5	$S_1 = T_2 + T_0/2$ $S_3 = T_0/2$ $S_5 = T_1 + T_2 + T_0/2$	$S_4 = T_1 + T_0/2$ $S_6 = T_1+T_2+T_0/2$ $S_2 = T_0/2$
6	$S_1 = T_1 + T_2 + T_0/2$ $S_3 = T_0/2$ $S_5 = T_1 + T_0/2$	$S_4 = T_0/2$ $S_6 = T_1+T_2+T_0/2$ $S_2 = T_2 + T_0/2$

Table 4.1: Switching Time Calculation at Each Sector [8].

S_{a+}	S_{b+}	S_{c+}	S_i	V_{ab}	V_{bc}	V_{ca}	V_{an}	V_{bn}	V_{cn}	V_α	V_β	V_i
0	0	0	S_0	0	0	0	0	0	0	0	0	V_0
0	0	1	S_1	0	-E	E	-E/3	-E/3	2E/3	-E/2	$-\sqrt{3}E/2$	V_5
0	1	0	S_2	-E	E	0	-E/3	2E/3	-E/3	-E/2	$\sqrt{3}E/2$	V_3
0	1	1	S_3	-E	0	E	-2E/3	-E/3	-E/3	-E	0	V_4
1	0	0	S_4	E	0	-E	2E/3	-E/3	-E/3	E	0	V_1
1	0	1	S_5	E	-E	0	E/3	-2E/3	E/3	E/2	$-\sqrt{3}E/2$	V_6
1	1	0	S_6	0	E	-E	E/3	E/3	-2E/3	E/2	$\sqrt{3}E/2$	V_2
1	1	1	S_7	0	0	0	0	0	0	0	0	V_7

Table 4.2: Switching configuration with output voltages of a three phase inverter [9,10].

S_{a+}, S_{b+} and S_{c+} are the three upper switches of the inverter. The switching configurations and output voltages of a three phase inverter are given in Table (4.2). The controller switches are turned on or off sequentially for six inverter switches, to generate the required output voltage needed to get the required speed from PMBLDC Motor in Space Vector Pulse Width Modulation Control.

Simulation result:

A C++ program code is written for SVPWM Control program of BLDC Motor. The effectiveness of the drive system is studied through simulation. The parameters of the motor for simulation is given in Appendix A.

The motor is run in constant speed of 104.72 radian/second or 1000 rpm. Plots are taken showing initial and running conditions. The speed curve in Figure (4.6) indicates that the motor reaches full speed in 0.16 second for 1000 rpm with no overshoot. So, this control method has fast speed response compared to other two methods.

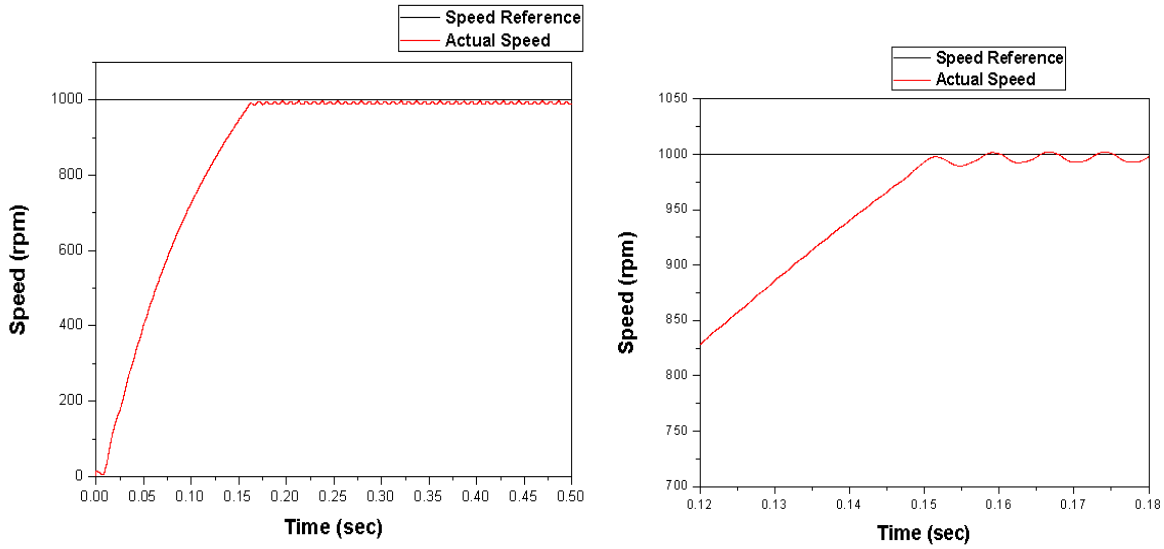

Fig.4.6: Speed characteristic of PMBLDC Motor for SVPWM Control.

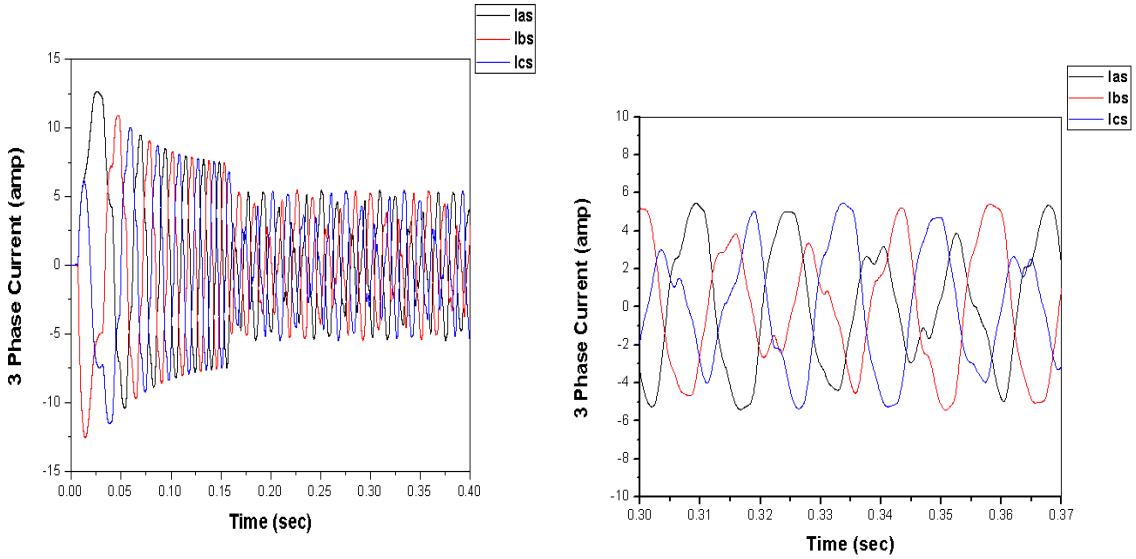

(a) (b)

Fig.4.7: Three phase current with transient condition for SVPWM Control.

During transient time when speed is rising, a high current flows as shown in Figure (4.7)(a). But after 0.16 second when motor reaches desired speed, level of current decreases and stabilizes like shown in Figure (4.7)(b).

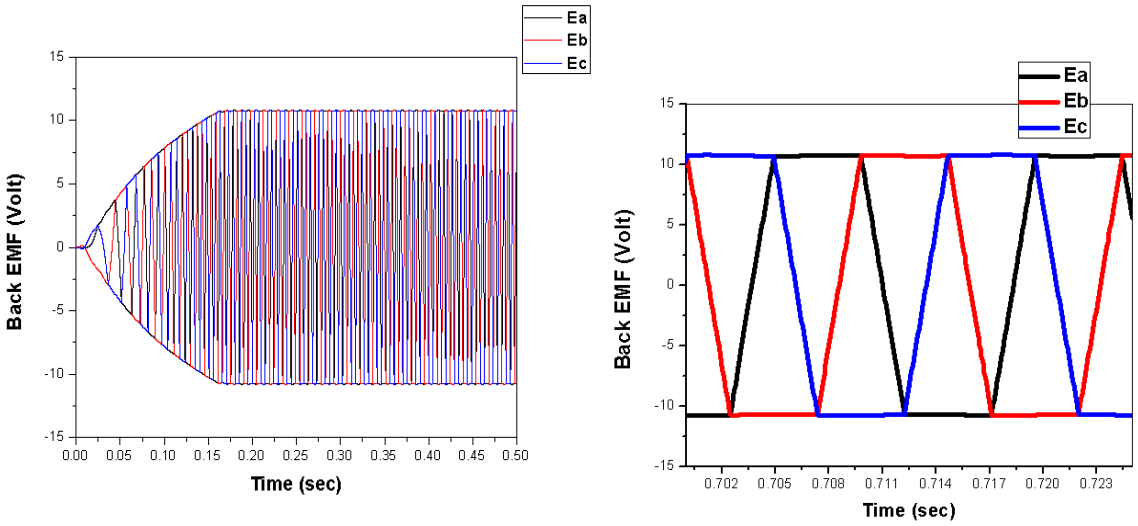

(a) (b)

Fig.4.8: Three-phase back EMF with transient condition for SVPWM Control.

During starting back EMF is zero. But after 0.16 second when motor reaches desired speed, level of current decreases and stabilizes as back EMF becomes trapezoidal shape like shown in Figure (4.8)(b).

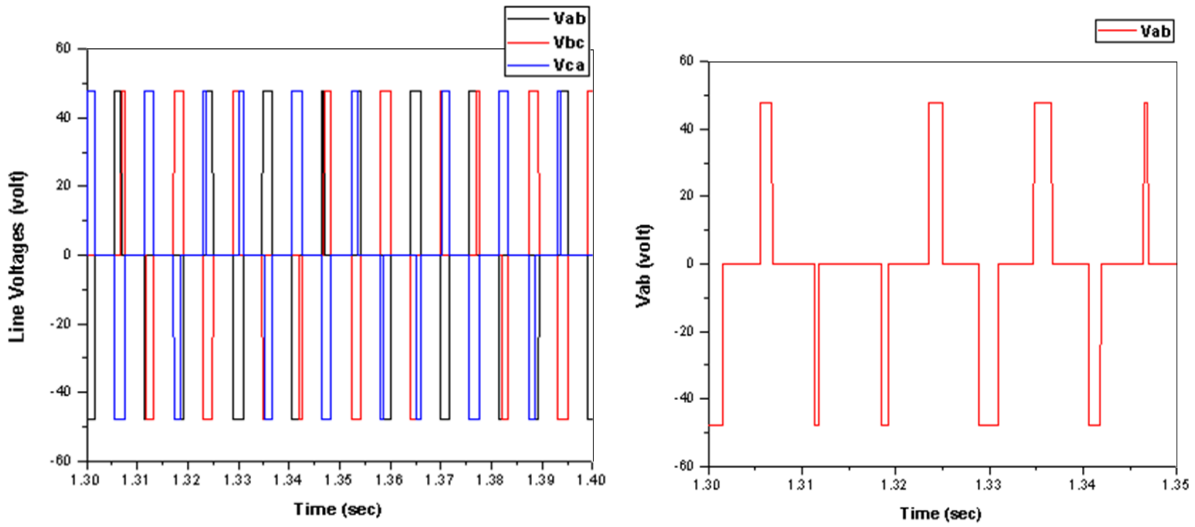

(a) (b)

Fig.4.9: Line voltages in PMBLDC Motor for SVPWM Control.

Inverter output voltages are the input of PMBLDC Motor. As we can see in Figure (4.9) voltages are rectangular shape curve. The width of voltage shape or duty cycle changes according to controller to control speed. As transistor switches are turned ON and

OFF, inverter produces voltage pulses equal to source battery voltage level. Transistor switches are sequentially ON and OFF, according to the V_{ref} 's positioning in a particular voltage sector. There are no voltages at V_0 and V_7 sector. So, SVPWM gives the efficient way of switching and increases the overall efficiency of the system. Hexagonal two axis (α-β) plot of voltages in Figure (4.10) is showing the Space Vector Pulse Width Modulation characteristics.

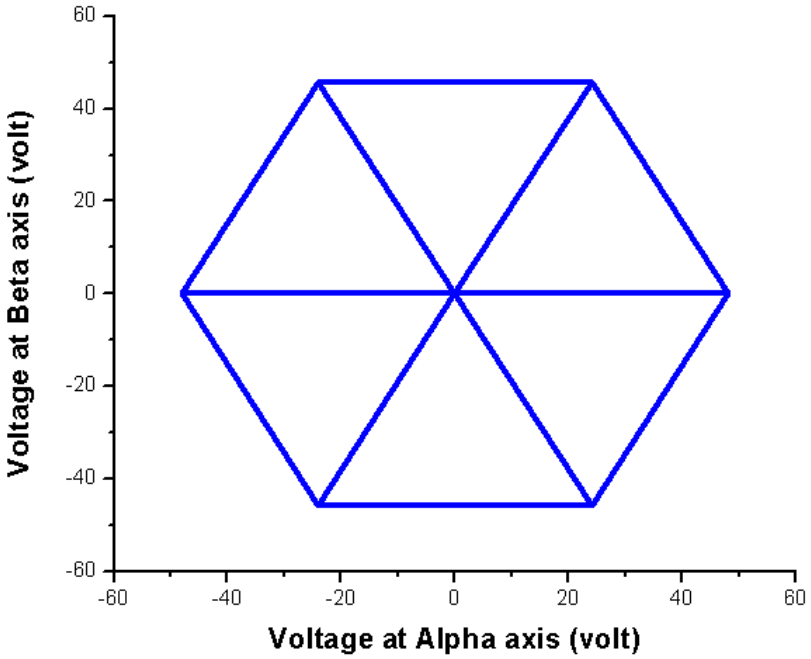

Fig.4.10: Two axis (α-β) plot of Voltages for SVPWM Control.

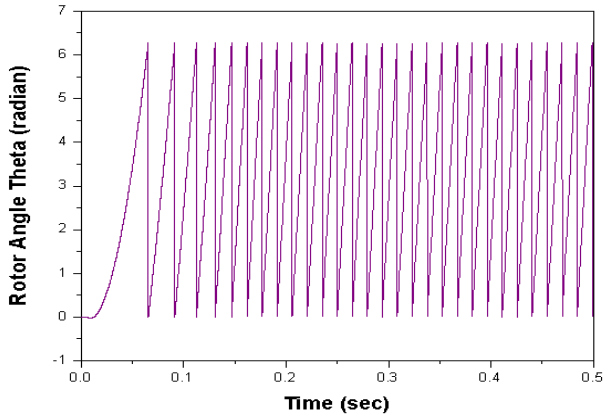

Fig 4.11: Rotor angle plot for SVPWM Control.

Rotor angle plot in Figure (4.11) is showing unidirectional 360 degree rotation of the rotor.

4.3 Conclusion

We have designed the control system of Permanent Magnet Brushless DC Motor on the basis of Space Vector Pulse Width Modulation technique. In this SVPWM Control method current is sensed and it is feedback to the system. The SVPWM Control has shown good speed response.

Chapter V

SIMULATION STUDY AND ANALYSIS OF PMBLDC MOTOR CONTROL METHODS

Chapter at a Glance

5.1 Introduction

In chapter III and IV we see a permanent magnet Brushless DC Motor's control with the Sinusoidal Current Regulated PWM (CRPWM) Control, Square Wave Current Regulated PWM (CRPWM) Control and Space Vector PWM Control. PMBLDC Motor's starting performances and other different operating conditions are analyzed in this chapter. We will consider several dynamic condition for the motor operation for the different control laws as it has been proposed. These are (1) fixed speed (2) variable speed (3) sudden change in load torque (4) change of stator resistance R_s during operation (5) initial rotor angle mismatch ($\theta \neq 0$). The system's simulations are done by C++ program code using Code Block software to run the simulations and plots are taken by Origin software using the "switch.dat" data file, generated from the C++ program's simulation.

5.2 Performance of PMBLDC Motor for Fixed Speed Condition

For a constant 104.72 radian/second or 1000 rpm speed, the characteristics of the control systems are analyzed and plots are given in Chapter III and IV.

Speed characteristics with starting period for Sinusoidal CRPWM Control, Square Wave CRPWM Control and SVPWM Control are shown in Figure (5.1). From these curves we have observed that SVPWM gives faster speed response.

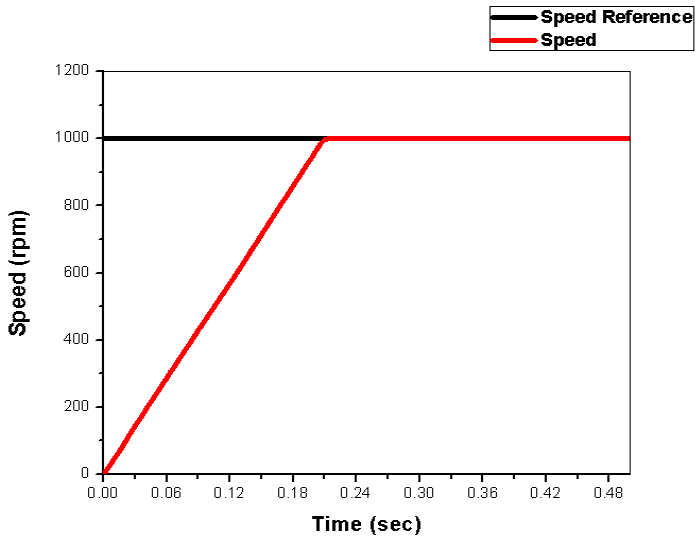

(a)

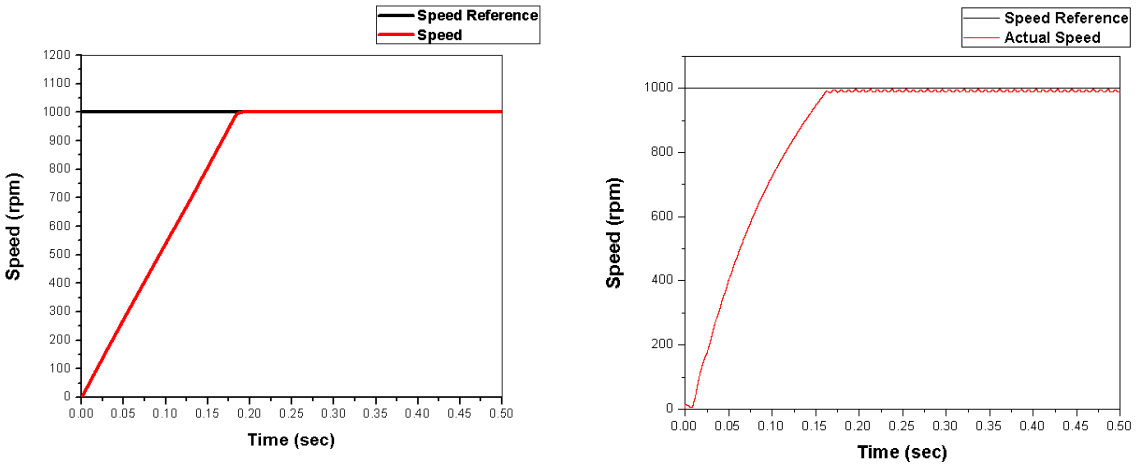

(b) (c)

Fig.5.1: Speed characteristics with starting period (a) for Sinusoidal CRPWM Control, (b) for Square Wave CRPWM Control and (c) for SVPWM Control.

In Figure (5.1)(a), Sinusoidal CRPWM Control motor reaches 1000 rpm speed in 0.22 second without any overshoot and remain stable afterwards and without any pulsation. The motor gain its desired full speed in 0.19 second for speed of 1000 rpm in Square Wave CRPWM Control as shown in Figure (5.1)(b). Furthermore we can see in Figure (5.1)(c), SVPWM Control motor gains full desired speed in just 0.16 second. Speed response in SVPWM Control is faster than the other two methods.

5.3 Operation with Variable Speed Condition

For variable speed condition for Sinusoidal CRPWM Control, we consider initially 104.72 radian/second or 1000 rpm speed, after 0.7 second speed is decreased to 52.36 radian/second or 500 rpm speed and after 1.6 second speed is increased to 146.61 radian/second or 1400 rpm speed as shown in Figure (5.2)(a).

As speed increases back emf increases as more mechanical power is needed to increase speed, because mechanical power is the product of back EMF and armature current. As speed decreases back EMF decreases as shown in Figure (5.2)(b). Figure (5.2)(e) is rotor angle variation frequency, which decreases or increases with rotor speed.

We can see that PMBLDC Motor performs well in variable speed condition for Sinusoidal CRPWM Colntrol.

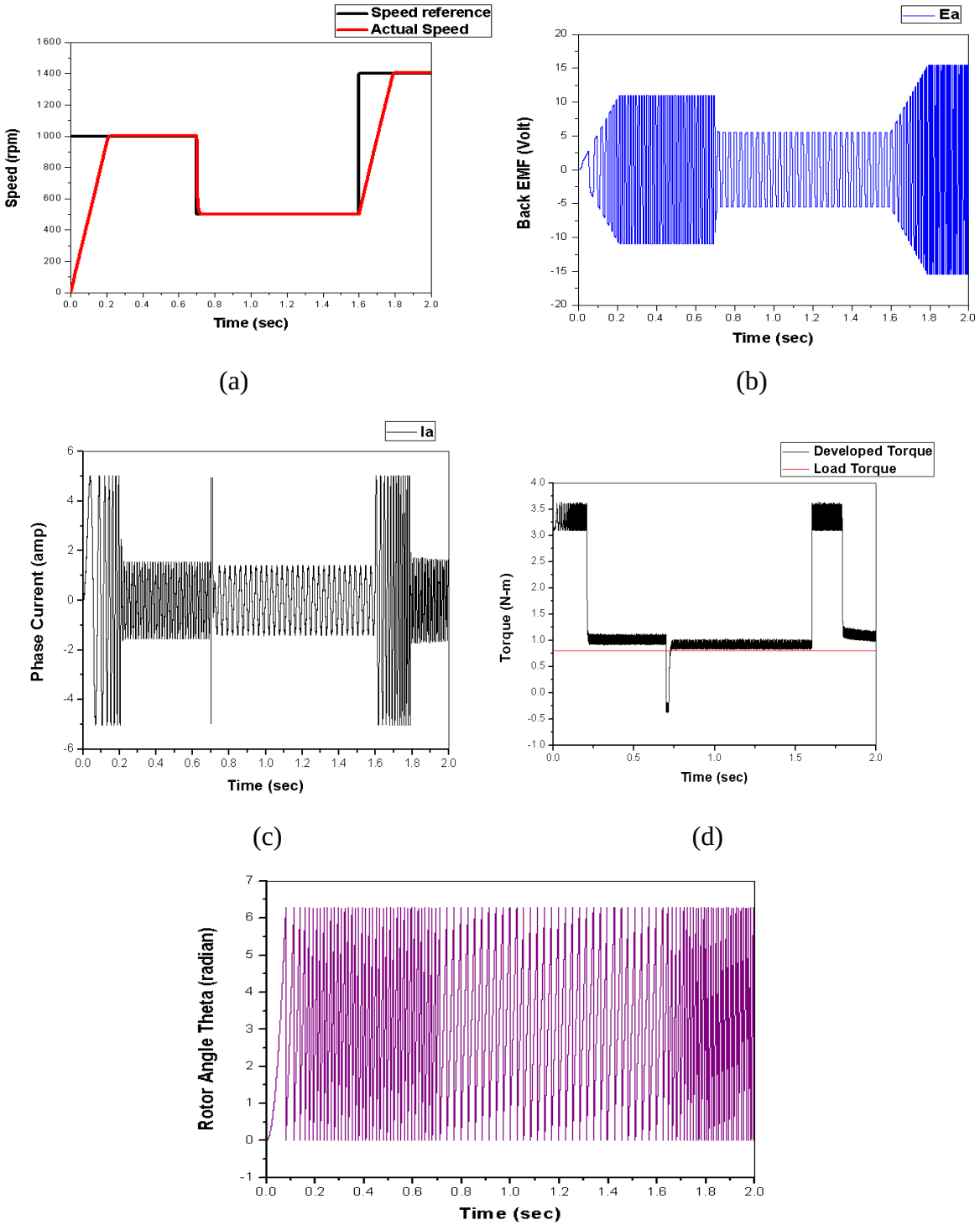

Fig.5.2: Plot for variable speed and its characteristics (a) speed, (b) back EMF, (c) phase current, (d) developed torque, (e) rotor angle theta; for Sinusoidal CRPWM Control.

For Square Wave CRPWM Control, we consider initially 500 rpm speed, after 0.7 second speed is increased to 1000 rpm and after 1.6 second speed is further increased to 1400 rpm speed as shown in Figure (5.3)(a). As speed increases back emf increases as more

mechanical power is needed to increase speed shown in Figure (5.3)(b). Figure (5.3)(e) is showing rotor angle variation frequency, which increases with rotor speed. PMBLDC Motor performs well in variable speed condition for Square Wave CRPWM Control.

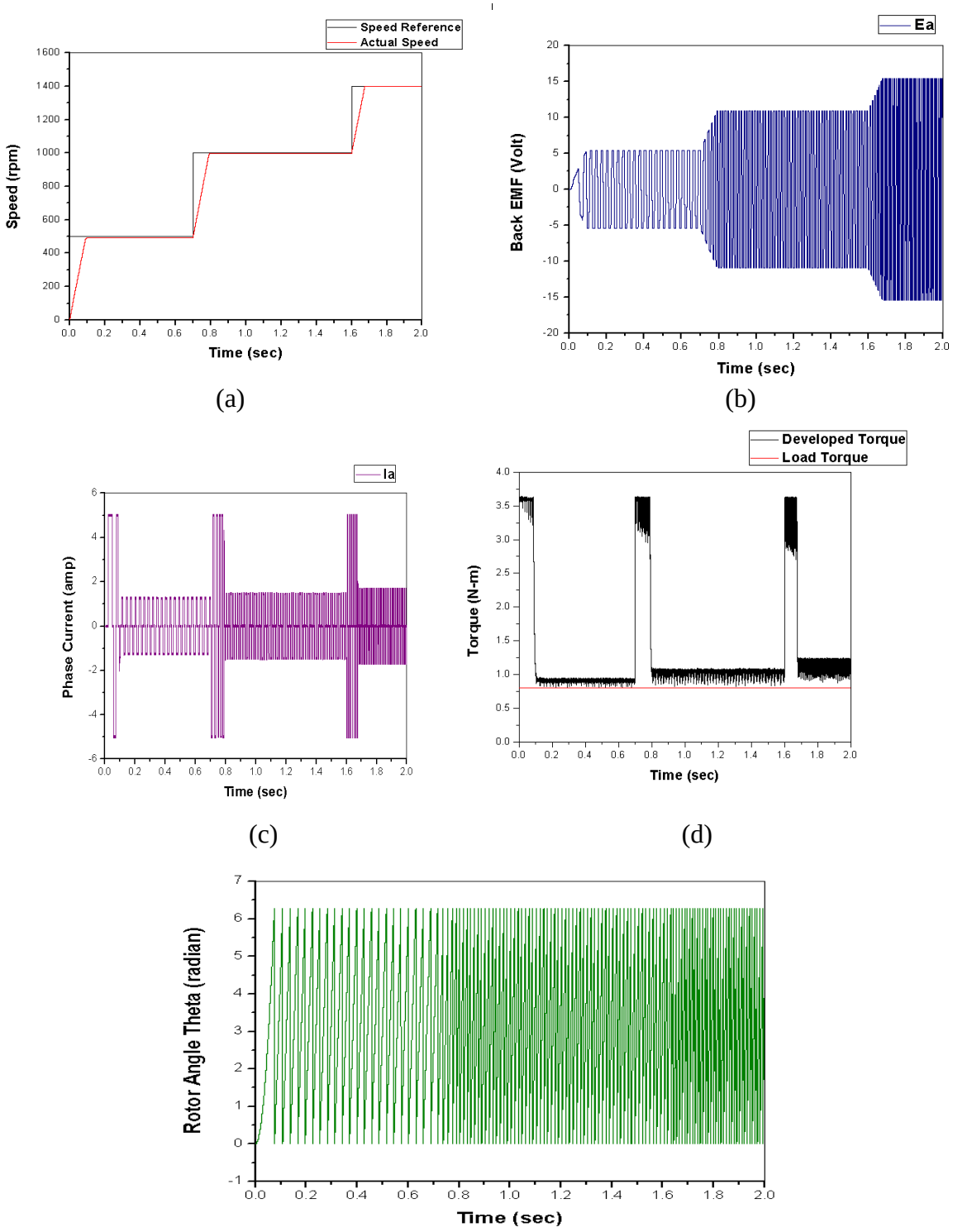

Fig.5.3: Plot for variable speed and its characteristics (a) speed, (b) back EMF, (c) phase current, (d) developed torque, (e) rotor angle theta; for Square wave CRPWM control.

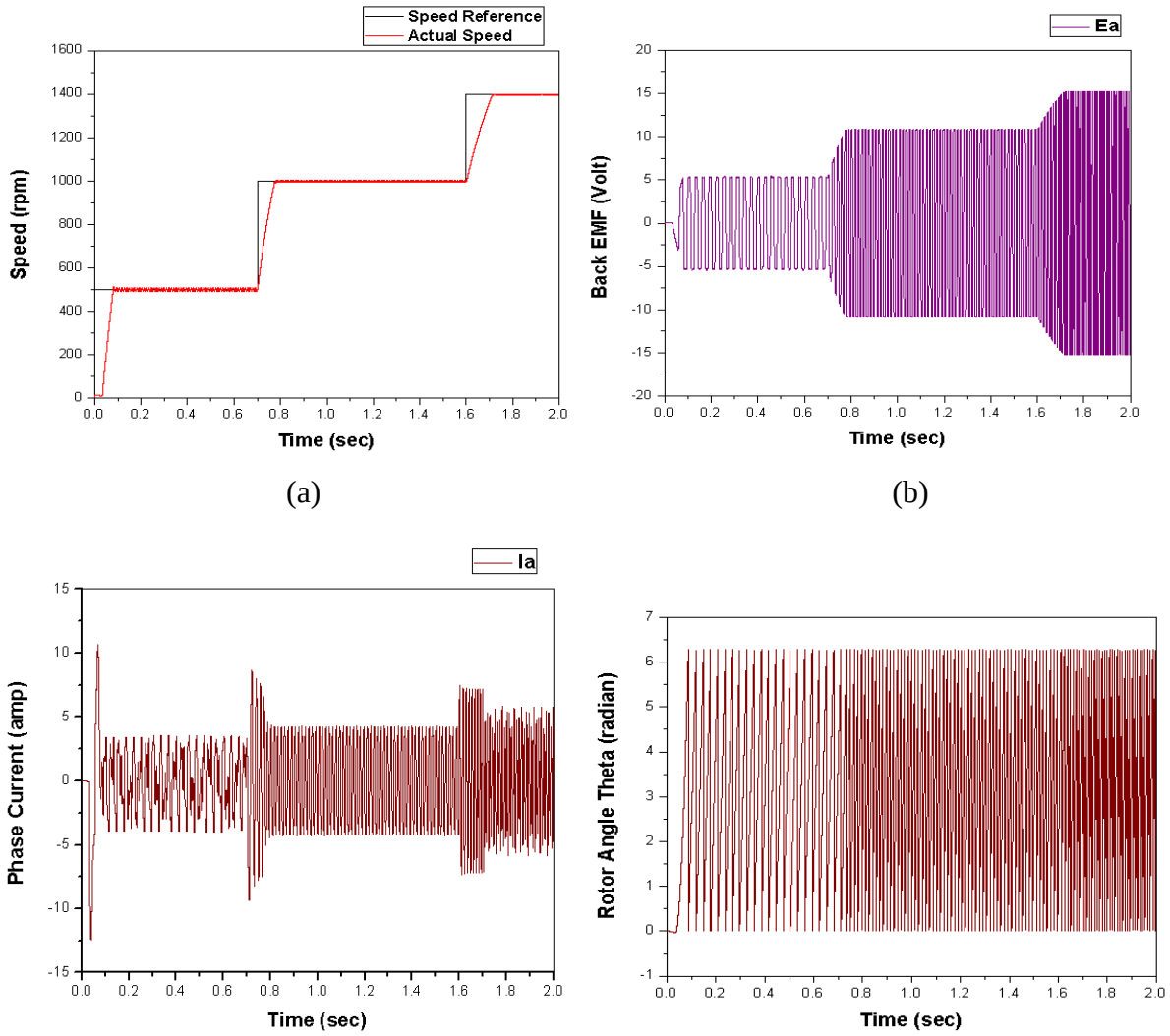

Fig.5.4: Plot for variable speed and its characteristics (a) speed, (b) back EMF, (c) phase current, (d) rotor angle theta; for SVPWM control.

For variable speed condition in SVPWM Control, we consider initial 500 rpm speed, after 0.7 second speed is increased to 1000 rpm and after 1.6 second speed is increased to 1400 rpm speed as shown in Figure (5.4)(a). As speed increases back emf increases as more mechanical power is needed to increase speed shown in Figure (5.4)(b). Figure (5.4)(e) is showing rotor angle variation frequency, which increases with rotor speed. PMBLDC Motor performs well in variable speed condition for SVPWM Control.

5.4 Characteristics of Motor for Sudden Load Torque Change

For sudden change in load torque condition, we consider initially 0.8 N-m load torque, after 1.0 second load torque is increased to 2.0 N-m.

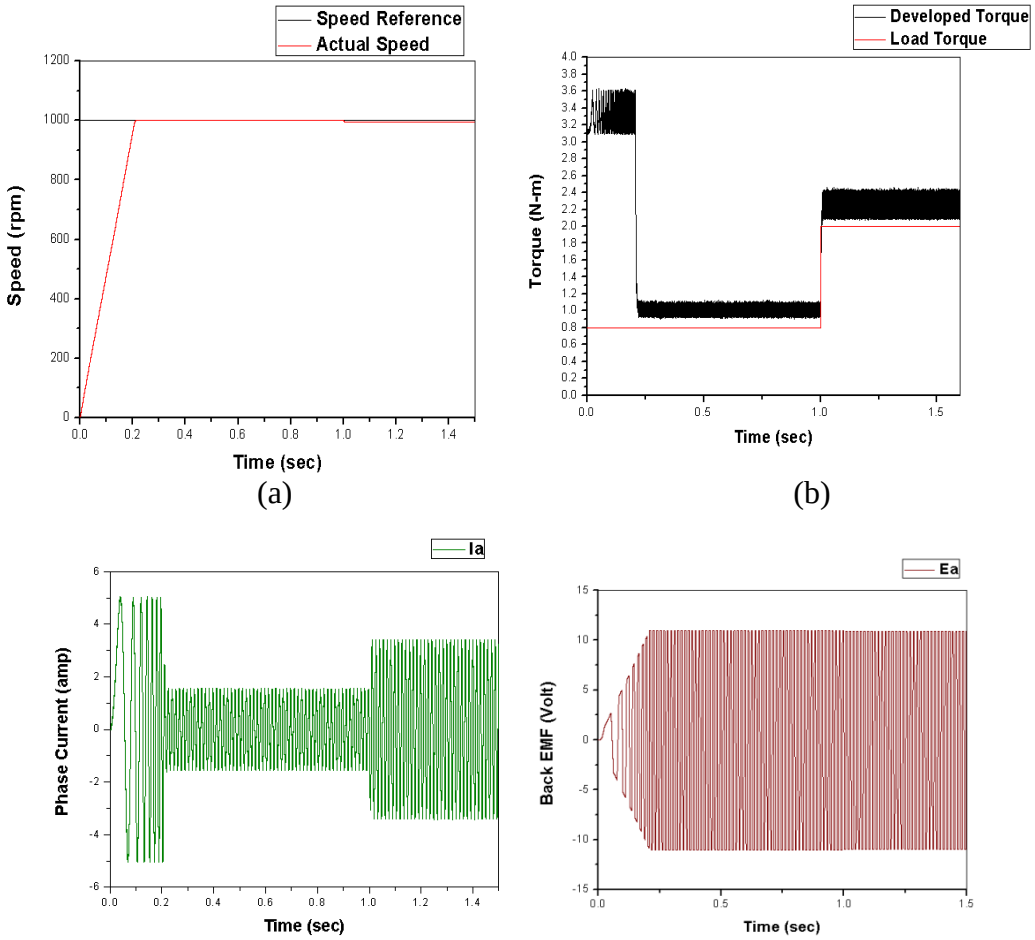

Fig.5.5: (a) Speed, (b) developed torque, (c) current, (d) back EMF characteristic due to step change of load torque from 0.8 N-m to 2.0 N-m for Sinusoidal CRPWM Control.

When the load torque increases, the current increases as well in Figure (5.5)(c). There is no appreciable change in back EMF in Figure (5.5)(d). But for sudden load torque change there is a negligible fall in speed occurs in Sinusoidal CRPWM Control in Figure (5.5)(a).

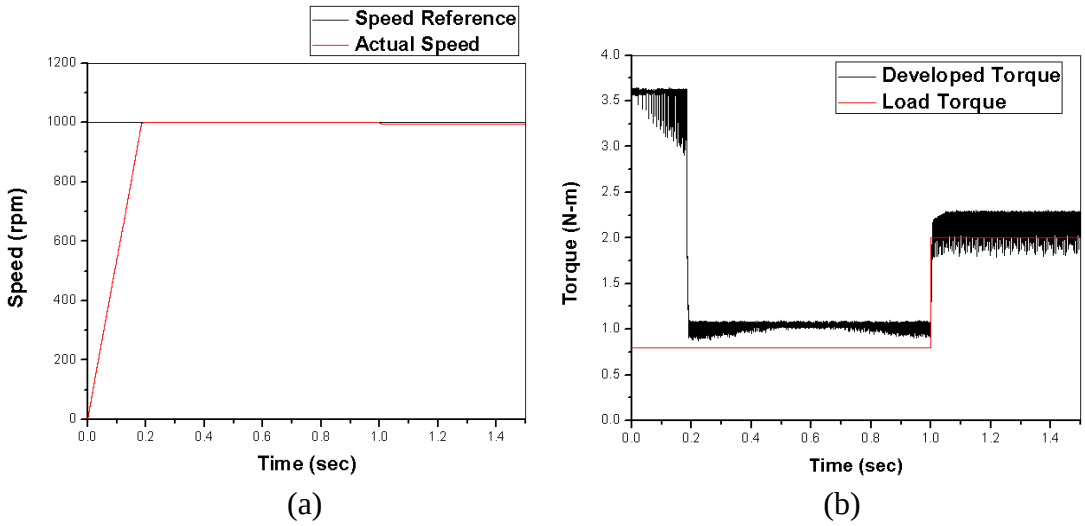

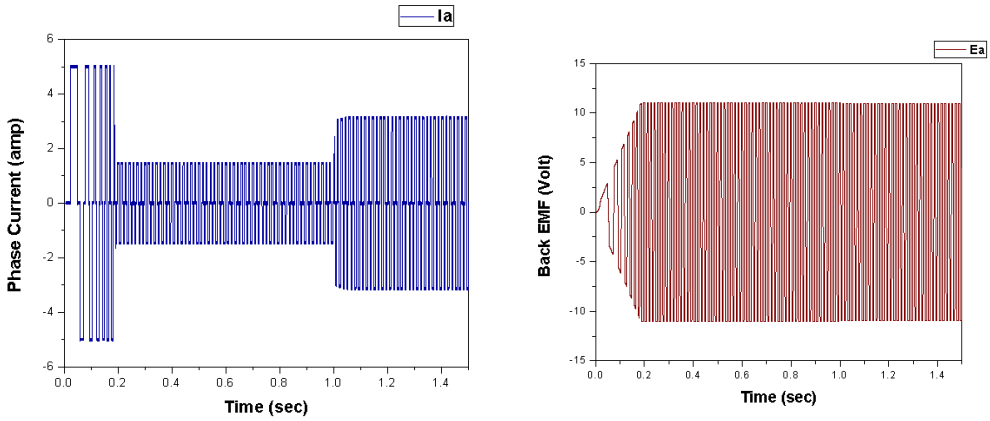

(c) (d)

Fig.5.6: (a) Speed, (b) developed torque, (c) current, (d) back EMF characteristic due to step change of load torque from 0.8 N-m to 2.0 N-m for Square Wave CRPWM Control.

When the load torque increases, the current increases as well in Figure (5.6)(c). There is no appreciable change in back EMF in Figure (5.6)(d). But there is a negligible fall in speed due to change in load torque for Square Wave CRPWM Control in Figure (5.6)(a).

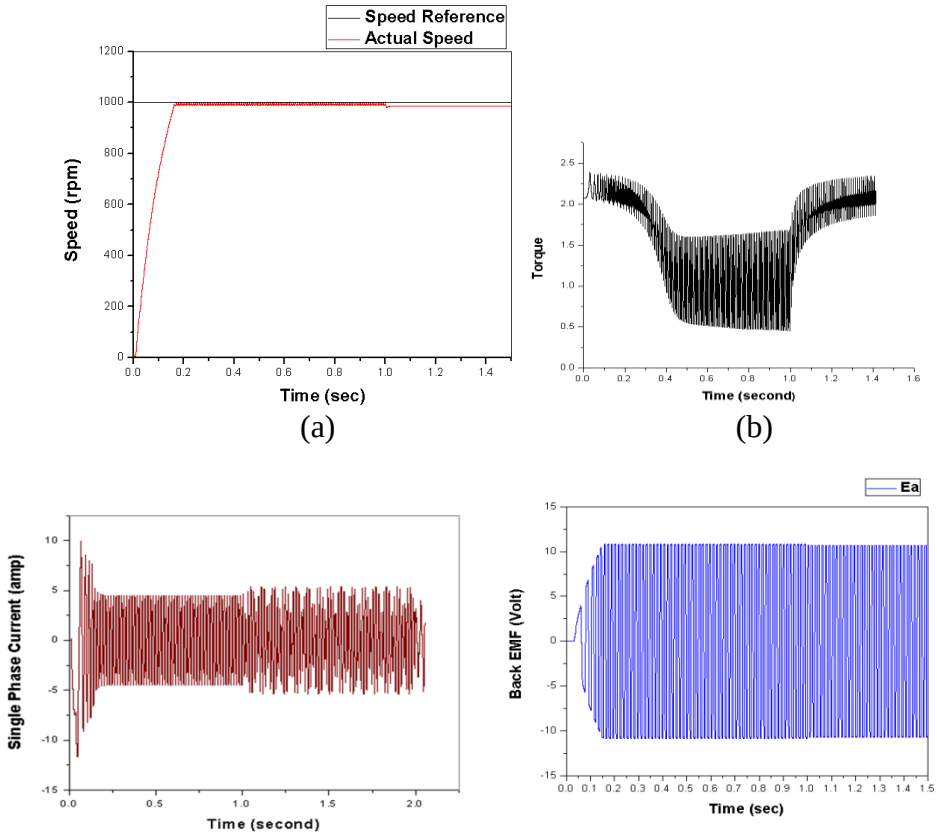

(a) (b)

(c) (d)

Fig.5.7: (a) Speed, (b) developed torque, (c) current, (d) back EMF characteristic due to step change of load torque from 0.8 N-m to 2.0 N-m for SVPWM Control.

When the load torque increases, the current increases as well as shown in Figure (5.7)(c). There is no appreciable change in back EMF in Figure (5.7)(d). But there is a very small fall in speed occurs for load torque change in SVPWM Control as shown in Figure (5.7)(a).

5.5 Effect of Sudden Change in Stator Resistance

Initially the stator resistance, $R_s = 0.36$ ohm and after 1.0 second suddenly stator resistance is increased to $R_s = 2$ ohm.

From the speed plots we see that there is no change in speed occurs due to a small change in stator resistance for Sinusoidal CRPWM Control and Square Wave CRPWM Control as shown in Figure (5.8). But for SVPWM Control there is a negligible fall in speed with a decrease in stator current for this small increase of stator resistance as shown in Figure (5.9).

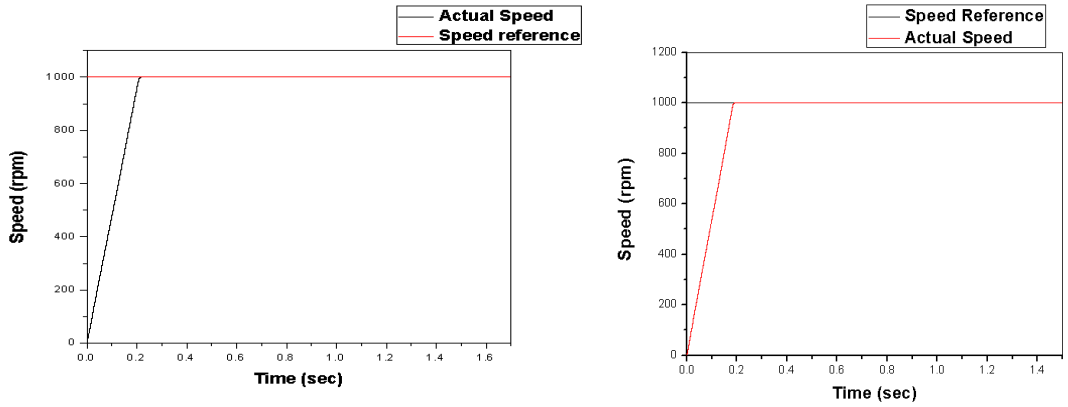

(a) (b)

Fig.5.8: Speed characteristics for a small change in stator resistance, (a) for Sinusoidal CRPWM Control, (b) for Square Wave CRPWM Control.

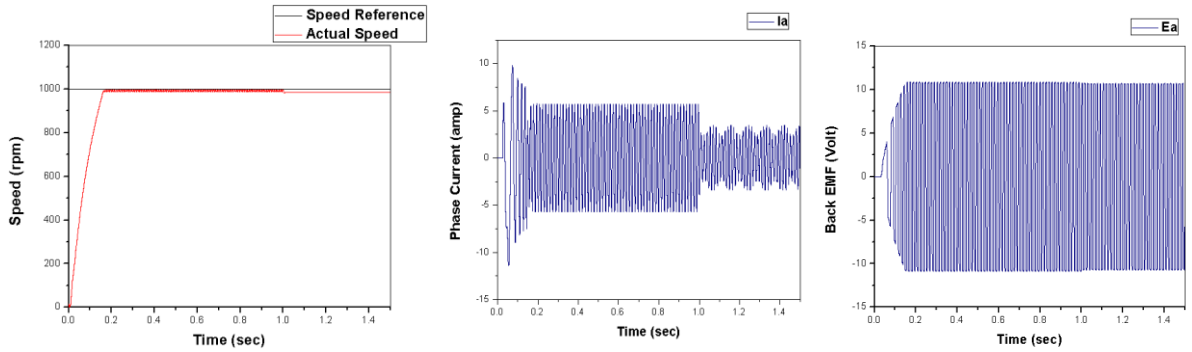

(a) (b) (c)

Fig.5.9: (a) Speed, (b) current, (c) back EMF characteristics for a small change in stator resistance for SVPWM Control.

5.6 Effect of Initial Value of Rotor Angle in the Program

The drive system performance is studied with an initial value of rotor angle = 20°. There is no deviation in performance of the drive system with the change in initial value is observed.

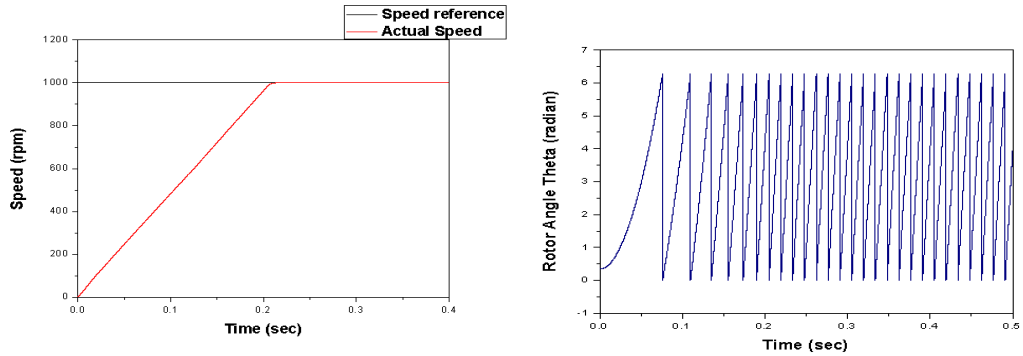

(a)

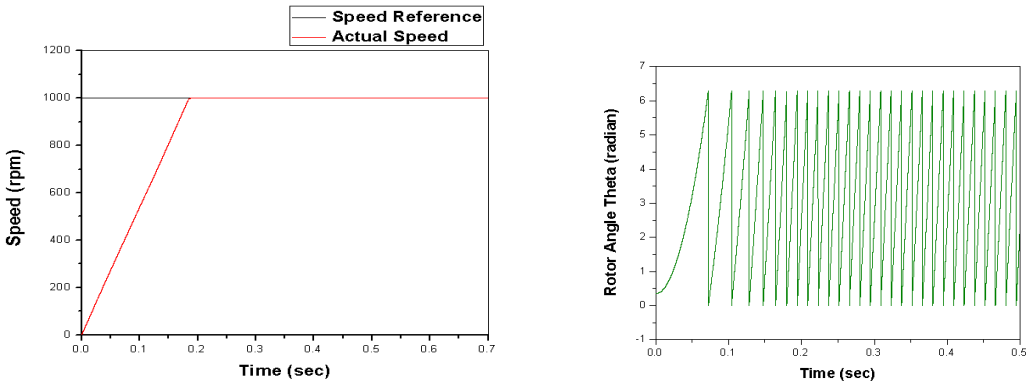

(b)

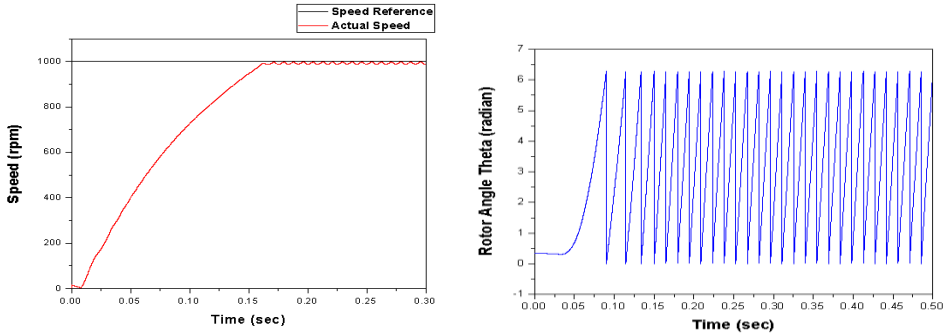

(c)

Fig.5.10: Plot for initial rotor angle mismatch, for (a) Sinusoidal CRPWM Control, (b) Square Wave CRPWM Control, (c) SVPWM Control.

5.7 Conclusion

As we have analyzed the drive system for different control laws, we have found that the motor operation for all the proposed control methods are satisfactory. For the field orientated current control methods the performances are good; but in SVPWM Control the speed response is faster compared to other methods. The motor could be operated at different constant speeds, even if the load torque is changed.

Chapter VI

EXPERIMENTAL STUDY

Chapter at a Glance

6.1 Introduction

In the laboratory an experiment is done using PMBLDC Motor and a prototype is designed. Open loop control system is utilized for speed control of the motor. The motor is run by inverter using a simple program.

6.2 Hardware Components

For experimental setup the following hardware components are used.

1. PMBLDC Motor : Turnigy 500KV
2. Inverter : Hobyking 100A
3. Battery : 5500mA Gens SE
4. Control Board : Arduino UnoR3
5. Battery Charger : IMAX BGAC
6. CT : 20:5
7. Personal Computer : PC for programming
8. Connecting wires : Wires and cables as required

6.3 Control System's Block Diagram

This simple control system for the PMBLDC Motor is developed using hardware components, which are cheap in price. In the market all the components are available. The reference speed and initialization is calibrated in the program. The block diagram of the drive system is shown in Figure (6.1) below:

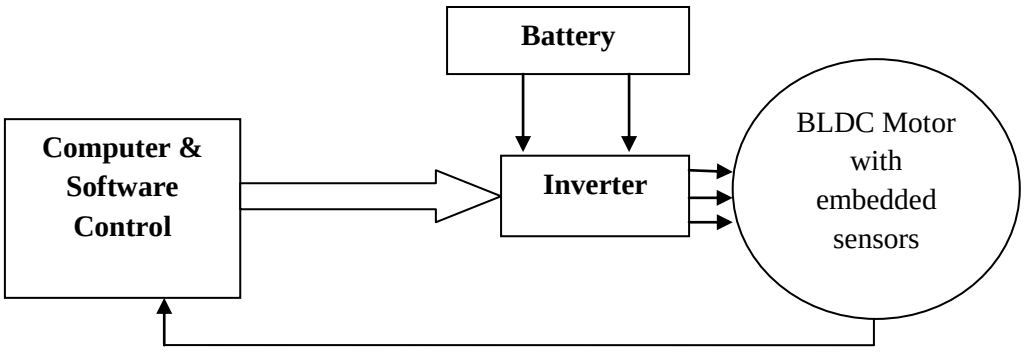

Fig.6.1: Block diagram of experimental setup.

The following picture in Figure (6.2) shows the experimental setup. A Computer is used to generate codes for Arduino Board. CT is used as transducer of the phase current.

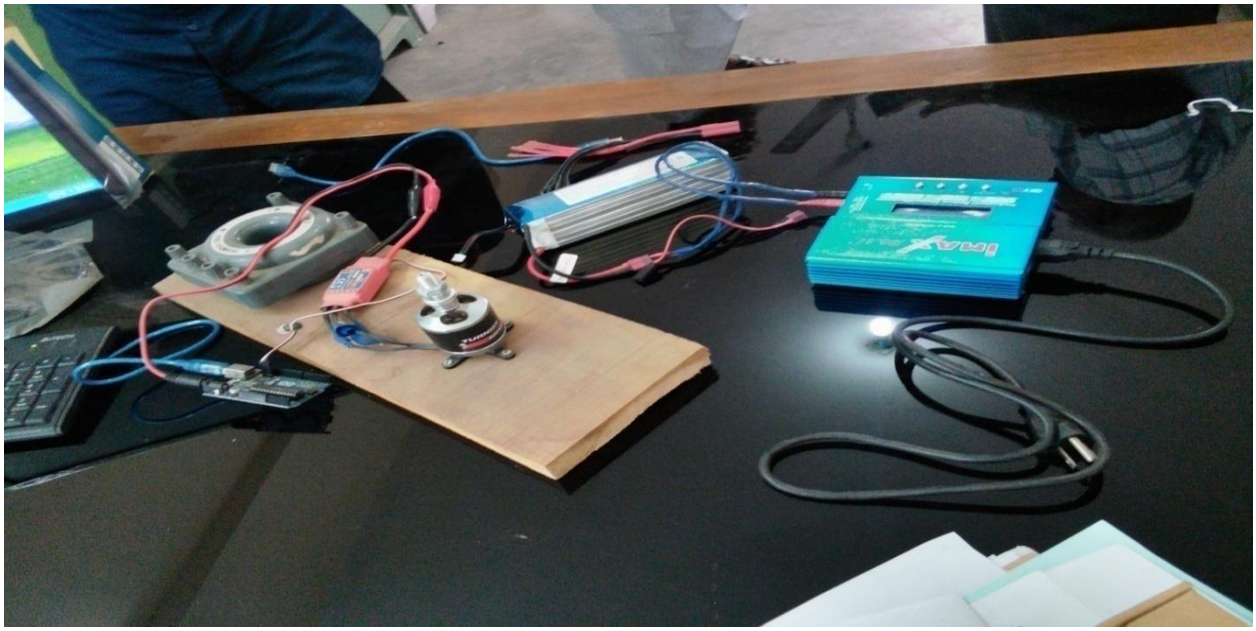

Fig.6.2: Pictorial diagram of experimental setup.

6.4 Experimental Results

PMBLDC Motor is tested for open loop control using a simple program and Arduino board. It is tested for different speeds. Phase current waveform for 2500 rpm is shown in Figure (6.3). Simple filter is used in the CT secondary for eliminating noise and distortion in the current wave.

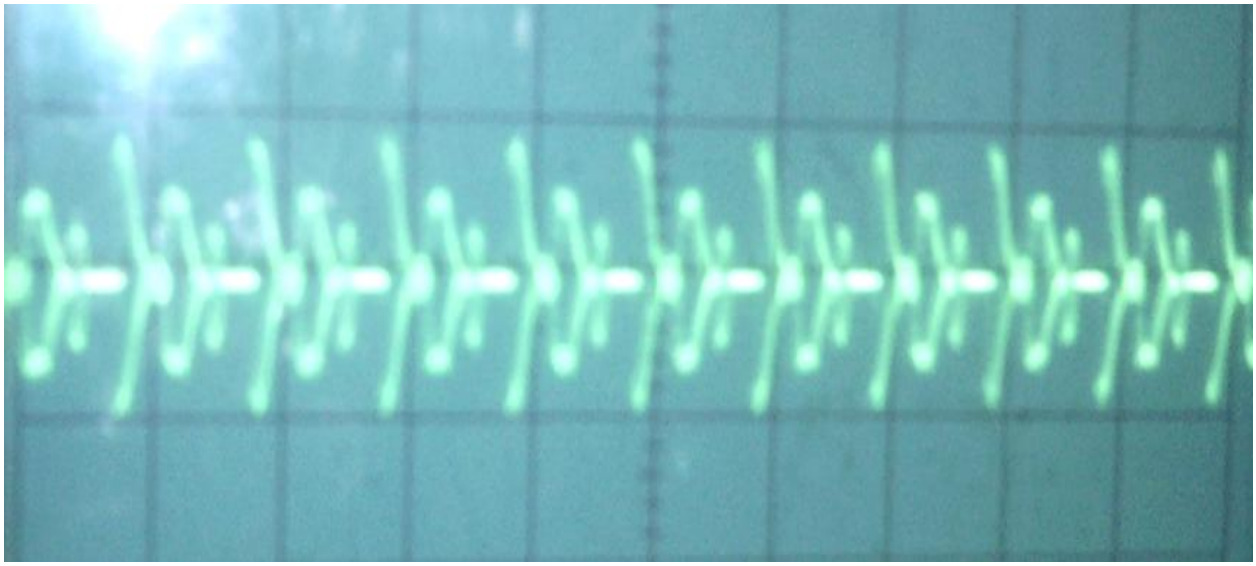

Fig.6.3: Current wave form at high speed.

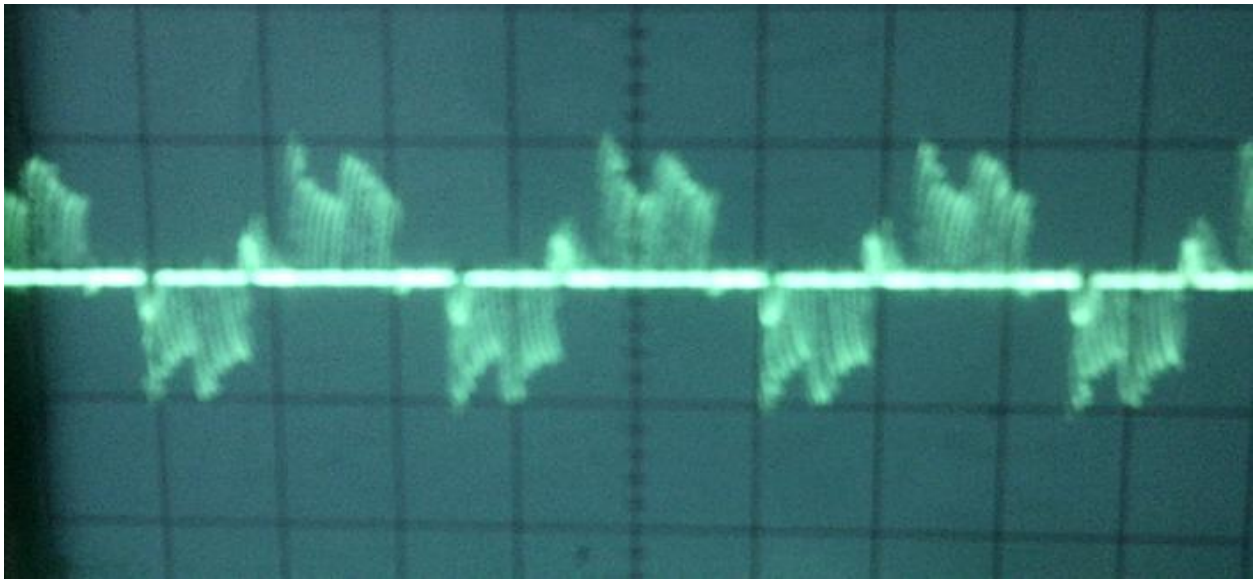

Fig.6.4: Current wave form at lower speed.

The phase current oscillo-graphic waveform at 750 rpm is shown in Figure (6.4).

6.5 Conclusion

The motor runs smoothly at different speed. The experimental motor was run at no load condition and also with loaded condition (connected to a shaft). The acceleration and deceleration was very fast. The motor runs close to its reference speed defined by the system program.

Chapter VII

CONCLUSION AND DISCUSSION

Chapter at a Glance

7.1 Conclusion

We design and test control systems of Permanent Magnet Brushless DC Motor on the basis of Field Oriented Control (FOC). We have designed a Sinusoidal Current Regulated Pulse Width Modulation (CRPWM) technique, a Voltage Controlled Space Vector Pulse Width Modulation (SVPWM) technique and a Square Wave Current Regulated Pulse Width Modulation (CRPWM) technique.

Both sinusoidal reference current and square wave reference current generation are done from speed error through adaptive PI controller in a closed loop control system. The performances of Square Wave CRPWM Control are faster with same controller constants. In SVPWM control, the current is sensed and it is feedback to the system; and from speed error and d-q transformation through PI controllers the direct and quadrature axis reference voltages are generated; the switching sequence of voltage vector are obtained from them.

Several transient conditions are created such as speed variation, load torque change, stator resistance change etc. All the control methods are found to follow the command input without much changing its dynamics. The Field Oriented Control systems have good performance, torque handling capacity and speed response for both normal and parametric perturbed situation. However the SVPWM Control has better speed response than the other two methods.

7.2 Limitations of the Study

We have some limitations in this study. These are that we don't have a lab type motor for experimental part and insufficient loading facilities. Also there are lack of speed, position and suitable current sensors for the experimental setup. But we have showed the motor dynamic performances for different control techniques and there comparison in C++ simulation environment.

7.3. Scope for Further Research

Due to introduction of permanent magnet materials with rare earth materials the importance of PMBLDC Motor has been enhanced. Due to low inertia, the mechanical response of PMBLDC Motor is very fast. To develop the control model further research can be done on the following topics:

a) FOC with other form of current shape like trapezoidal shape CRPWM control, rectangular shape CRPWM control can designed.

b) DTC with sinusoidal CRPWM, trapezoidal shape CRPWM control, rectangular shape CRPWM control can designed.

c) Applying FUZZY-Neuro control technique with the proposed systems.

d) Increasing the efficiency the proposed systems, specially field oriented SVPWM Control can be further improved, by improving the current wave shape by reducing pulsation of current and magnitude.

e) Practical implementation the proposed systems using microcontroller.

f) Speed sensorless field oriented control systems or direct torque control systems can be designed.

g) Using multi-level inverter in SVPWM method for any AC machine drive.

REFERENCES

[1] Gopal K. Dubey, “Fundamentals of Electrical Drives,” Narosa Publishing House's book, 1995.

[2] R. Giridhar Balakrishna, P. Yogananda Reddy, “Speed Control of Brushless DC Motor Using Microcontroller,” International Journal of Engineering Technology, Management and Applied Sciences, volume 3, Issue 6, ISSN 2349-4476, June 2015.

[3] Tony Mathew, Caroline Ann Sam, “Modeling and Closed Loop Control of BLDC Motor using a Single Current Sensor,” International Journal of Advanced Research in Electrical, Electronics and Instrumentation Engineering, vol. 2, Issue 6, pp.2525-2530, June 2013.

[4] José Carlos Gamazo-Real, Ernesto Vázquez-Sánchez and Jaime Gómez-Gil, “Position and Speed Control of Brushless DC Motors Using Sensorless Techniques and Application Trends,” Sensors-2010, vol.10, PP.6901-6947.

[5] S. Rambabu, “Modeling and Control of a Brushless DC Motor,” M. Tech. Thesis, Department of Electrical Engineering National Institute of Technology Rourkela, 2007.

[6] M.V. Ramesh, J. Amarnath, S. Kamakshaiah and M. Balakrishna, “Field Oriented Control for Space Vector Modulation Based Brushless DC Motor Drive,” International Journal of Advanced Research in Electrical, Electronics and Instrumentation Engineering, vol.2, Issue 9, pp.4231-4238, September 2013.

[7] Microsemi, “Field Oriented Control of Permanent Magnet Synchronous Motors User’s Guide,” 2012.

[8] D. Rathnakumar, J. Lakshmana Perumal and T. Srinivasan, “A New Software Implementation of Space Vector PWM,” Conference: SoutheastCon, 2005 (IEEE).

[9] V. Viswanathan and Dr. S. Jeevananthan, “Novel Space-Vector Current-Control Method for Torque Ripple Reduction of Brushless DC Motor Based on Three-level Neutral-Point-Clamped Inverter,” Arabian Journal For Science And Engineering, vol.38, Page 10, October 2012.

[10] Vinayaka K U, Priya.S, “Analysis of BLDC Motor performance Using Space Vector Pulse Width Modulation,” 2016 International Conference on Computation of Power, Energy Information and Communication (lCCPEIC).

[11] Pragasen Pillay and Ramu Krishnan, "Modeling, Simulation and Analysis of a Permanent Magnet Brushless DC Motor Drive Part II: The Brushless DC Motor Drive," IEEE Transactions on Industry application, vol.25, May/Apr 1989.

[12] Marek Lazor, Marek Stulrajter, "Modified Field Oriented Control for Smooth Torque Operation of a BLDC Motor," Technically IEEE sponsored ELEKTRO conference, Rajecke Teplice, 19-20 May, 2014.

[13] B. Pavan Kumar, Krishnan C.M.C, "Comparative Study of Different Control Algorithms on Brushless DC Motors," Biennial International Conference on Power and Energy Systems: Towards Sustainable Energy (PESTSE), Bangalore, 21-23 Jan, 2016.

[14] Siva Gangadhara Rao Venna, Sneha Vattikonda and Sravani Mandarapu, "Mathematical Modeling and Simulation of Permanent Magnet Synchronous Motor," International Journal of Advanced Research in Electrical, Electronics and Instrumentation Engineering, vol. 2, Issue 8, pp.3720-3726, August 2013.

[15] Shiyoung Lee, Tom Lemley and Gene Keohane, "A Comparison Study of the Commutation Methods for the Three-Phase Permanent Magnet Brushless DC Motor," A technical report on BLDC Motor, September 19, 2014.

[16] C.Y. Chen, W.C. Chan, T.C. Ou, S.H. Yu and T.W. Liu, "Sliding Mode Speed Control of Brushless DC Motor Using Pulse-Width-Modulated Current Regulator," 2009 IEEE/ASME International Conference on Advanced Intelligent Mechatronics Suntec Convention and Exhibition Center Singapore, July 14-17, 2009.

[17] Shucheng Wang, "BLDC Ripple Torque Reduction Via Modified Sinusoidal PWM," FAIRCHILD SEMICONDUCTOR POWER SEMINAR 2008 – 2009, pp.1-10.

[18] P.Sarala, Dr. S. F. Kodad and Dr. B. Sarvesh, "Analysis of Closed loop Current Controlled BLDC Motor Drive," International Conference on Electrical, Electronics, and Optimization Techniques (ICEEOT) – 2016.

[19] Protik Chandra Biswas, Bashudeb Chandra Ghosh and Md. Ashraful Islam, "Field Oriented Control of a Current Fed PMBLDC Motor and Its Comparison to Scalar Control Drive," The AIUB Journal of Science and Engineering (AJSE), vol. 15, no. 1, August 2016.

[20] Devisree Sasi and Jisa Kuruvilla, "Modeling and Simulation of SVPWM Inverter Fed Permanent Magnet Brushless DC Motor Drive," International Journal of Advanced Research in Electrical, Electronics and Instrumentation Engineering, vol. 2, Issue 5, pp.1947-1955, May 2013.

[21] Sudhanshu Mitra, Amit Ojha, "Performance Analysis of BLDC Motor Drive using PI and Fuzzy Logic Control Scheme," International Research Journal of Engineering and Technology (IRJET) vol. 02 Issue 06, pp.916-922, September 2015.

[22] Mr. Sudhir G. Mane, Dr. Iranna Korachagaon, "Design of Three Phase Inverter Using Space Vector Pulse Width Modulation Technique (SVPWM)," International Journal of Enhanced Research in Science Technology & Engineering, vol. 3, Issue 7, pp.(251-259), July 2014.

[23] Jianwen Shao, "Direct Back EMF Detection Method for Sensorless Brushless DC (BLDC) Motor Drives," M.Sc. Thesis submitted to the Faculty of the Virginia Polytechnic Institute and the State University, September 2003.

[24] P. Sreekala, A. Sivasubramanian, "Speed Control of Brushless DC Motor with PI and FUZZY Logic Controller Using Resonant Pole Inverter," IEEE PES Innovative Smart Grid Technologies-India, 2011.

[25] N.Senthil Kumar and C.Senthil Kumar, "Design and Implementation of Adaptive Fuzzy Controller for Speed Control of Brushless DC Motors," International Journal of Computer Applications (0975 - 8887) volume 1, no. 27, 2010.

[26] M. V. Ramesh, J. Amarnath, S. Kamakshaiah and G.S. Rao, "Speed Control of Brushless DC Motor by Using Fuzzy Logic PI Controller," ARPN Journal of Engineering and Applied Sciences vol.6, no.9, pp 55-62, September 2011.

[27] C. Subba Rami Reddy and M. Surya Kalavathi, "Performance Studies of Integrated Fuzzy Logic Controller for Brushless DC Motor Drives Using Advanced Simulation Model," ICTACT Journal on Soft Computing: Special Issue on Fuzzy in Industrial and Process Automation, vol. 02, Issue 01, July 2011.

[28] Tan Chee Siong, Baharuddin Ismail, Siti Fatimah Siraj, Mohd Fayzul Mohammed, "Fuzzy Logic Controller for BLDC Permanent Magnet Motor Drives," International Journal of Electrical & Computer Sciences IJECS-IJENS, vol.11, no.02, pp12-18.

[29] Mehmet Çunkaş, Omer Aydoğdu, "Realization of Fuzzy Logic Controlled Brushless DC Motor Drives Using MATLAB/SIMULINK," Mathematical and Computational Applications, vol.15, no.2, pp.218-229, 2010.

[30] Salih Baris Ozturk, Hamid A. Toliyat, "Direct Torque Control of Brushless DC Motor with Non-sinusoidal Back-EMF," Advanced Electric Machines & Power Electronics Laboratory Department of Electrical & Computer Engineering Texas A&M University College Station, TX. 77843-3128, 2007.

[31] Sajana Kunjumon and Johnson Mathew, "Direct Torque Controlled Brushless DC Motor Drive with Rotor Position Estimation Using LabVIEW," International Journal of Advanced Research in Electrical, Electronics and Instrumentation Engineering, vol.2, Special Issue 1, pp.148-156, December 2013.

[32] Yong Liu, Z. Q. Zhu, and David Howe, "Direct Torque Control of Brushless DC Drives With Reduced Torque Ripple," IEEE Trans. on Industry Application,vol.41, no.2, pp.599-606, Mar/Apr 2005.

[33] G.R.Puttalakshmi and S.Paramasivam, "Electromagnetic Flux Analysis of Permanent Magnet Brushless DC Motor Using Magnet Software," International Journal of Engineering and Technology (IJET), vol.4, no.5, pp.3215-3222, 2013.

[34] Abhisek Jain, P R Sarkar and Mohd. Kursheed Siddique, "Modeling and Performance Analysis of a Permanent Magnet Brushless DC Motor Using Instrumentation Technique," International Journal of Engineering Research and Control Science, vol.5, Issue 1, pp.814-820, Jan/Feb 2015.

[35] Rabikiran H.Rushiya, Renish M. George, Prateck R. Dongre, Swapnil B. Borkar, Shankar S. Sonekar and S. W. Khubalkar, "A Review: Modelling of Permanent Magnet Brushless DC Motor Drive," International Journal of Application or Innovation in Engineering & Management (IJAIEM) ISSN-2319, 2013.

[36] A. Tashakori, M. Ektesabi and N. Hosseinzadeh, "Modeling of BLDC Motor with Ideal Back-EMF for Automotive Applications," Proceedings of the World Congress on Engineering 2011, vol. II, WCE 2011, London, U.K, July 6-8, 2011.

[37] Bilal Akin and Manish Bhardwaj, "Sensorless Trapezoidal Control of BLDC Motors," Application Report Texas Instruments, July 2013.

[38] Ward Brown, "Brushless DC Motor Control Made Easy," Microchip Technology Inc., AN857, 2002.

[39] Libor Prokop and Leos Chalupa, "3-Phase BLDC Motor Control with Sensorless Back EMF Zero Crossing Detection Using 56F80x Freescale Semiconductor Application Note," AN1914, Rev.1, November, 2005.

[40] Jian Zhao and Yangwei Yu, “Brushless DC Motor Fundamentals Application Note,” AN047, July 2011.

[41] AVR194: “Brushless DC Motor Control Using ATmega32M1 8-bit Microcontroller Application Note,” April, 2008.

[42] R. A. Gupta, Rajesh Kumar, Ajay Kumar Bansal, “Artificial Intelligence Applications in Permanent Magnet Brushless DC Motor Drives,” Artif. Intell. Rev. (2010) 33:175–186.

[43] Colorado School of Mines CHEN403, “Numerical Method for the Solution of ODE's,” December 11, 2008.

[44] George E. Forsythe, Michael A. Malcolm and Cleve B. Moler, “Computer Methods for Mathematical Computation,” Prentice Hall-1977.

[45] Muhammad H. Rashid, “Power Electronics Circuits, Devices and Applications,” Prentice Hall-2013.

APPENDIX A

Parameters of the PMBLDC Motor:

Sl. No.	Specifications	Quantity
1	No. of Poles	8
2	Rated Voltage	48V
3	Rated Current	5 amp / 10 amp
4	Rated Speed	150 rad/s
5	Rated Torque	1.45 Nm
6	Initial Torque	0.4 Nm
7	Resistance/Phase	0.36 Ω
8	Self-Inductance	2.1 mH
9	Mutual inductance	1.5 mH
10	Flux linkages constant	0.105 V-s/rad
11	Torque constant	0.40 V-s/rad
12	Moment of Inertia	0.0048 kg-m2
13	Damping constant	0.002 N-m/rad/sec